

BRIGHT e-toolkit manual for digital learning in producing medical parts by 3D printing methods in the context of the pandemic

BOOSTING THE SCIENTIFIC EXCELLENCE AND INNOVATION
CAPACITY OF 3D PRINTING METHODS IN PANDEMIC PERIOD



*Răzvan Păcurar, Cristina Borzan, Eugen Guțiu, Cătalin Moldovan, Cristian Vilău,
Sorin Comșa, Cosmin Cosma, Petru Berce, Nicolae Balc, Miloš Simonović,
Aleksandar Miltenović, Milan Banić, Nikola Vitković, Remigiusz Łabudzki,
Filip Górski, Magdalena Żukowska, Filip Sarbinowski, Sven Maričić,
Mate Babic, Branislav Rabara, Peter Košťál, Erika Hrušková*

Toate drepturile rezervate autorilor & Editurii Risoprint

Editura RISOPRINT este recunoscută de C.N.C.S.

(Consiliul Național al Cercetării Științifice).

www.risoprint.ro

www.cncs-uefiscdi.ro



Opiniile exprimate în această carte aparțin autorilor și nu reprezintă punctul de vedere al Editurii Risoprint. Autorii își asumă întreaga responsabilitate pentru forma și conținutul cărții și se obligă să respecte toate legile privind drepturile de autor.

Toate drepturile rezervate. Tipărit în România. Nicio parte din această lucrare nu poate fi reprodusă sub nicio formă, prin niciun mijloc mecanic sau electronic, sau stocată într-o bază de date fără acordul prealabil, în scris, al autorilor.

All rights reserved. Printed in Romania. No part of this publication may be reproduced or distributed in any form or by any means, or stored in a data base or retrieval system, without the prior written permission of the author.

ISBN 978-973-53-3028-6

**BRIGHT e-toolkit manual
for digital learning in producing medical parts by 3D printing
methods in the context of the pandemic**

AUTHORS

Răzvan Păcurar, Cristina Borzan, Eugen Guțiu, Cătălin Moldovan,
Cristian Vilău, Sorin Comșa, Cosmin Cosma, Petru Berce,
Nicolae Balc, Miloš Simonović, Aleksandar Miltenović,
Milan Banić, Nikola Vitković, Remigiusz Łabudzki, Filip Górski,
Magdalena Żukowska, Filip Sarbinowski, Sven Maričić,
Mate Babic, Branislav Rabara, Peter Košťál, Erika Hrušková

Director editură: GHEORGHE POP

The publishing of this project guidebook has been financially supported by the ERASMUS KA 226 project entitled “Boosting the scientific excellence and innovation capacity of 3D printing methods in pandemic period”, the implementation of the project being supervised by the National Agency for Community Programmes in the Fields of Education and Vocational Training (project reference: 2020-1-RO01-KA226-HE-095517).

BRIGHT e-toolkit manual for digital learning in producing medical parts by 3D printing methods in the context of the pandemic

CONTENT

Introduction	2
Toolkit 1 - Skull implants made by Selective Laser Sintering and Vacuum Casting technologies..	4
Toolkit 2 - Design and SLM manufacturing of custom facial implant used to reconstruct the supraorbital margin and Zygomatic bone.....	36
Toolkit 3 - Fixator made by Stereolithography (Digital light processing method).....	64
Toolkit 4 - Methodology of design and rapid manufacturing of mid-surgery supplies in otolaryngology (Fused Filament Fabrication and Vacuum Casting).....	99
Toolkit 5 - Production of medical parts with use of Fused Deposition Modelling and Reprap technologies.....	137
Toolkit 6 - Rapid tooling.....	157
Final Conclusions	182

INTRODUCTION

Aspects related to 3D printing technologies / working principles of these types of modern technologies are easy to be understood in theory, but very hard to be applied in practice. When it comes to practice, the way the parts are being designed and prepared to be printed differs from one product to another in accordance with the shape of the part to be printed out, the type of material, parameter settings, part orientation, type of method used for printing, etc. In this context, the BRIGHT toolkit manual which has been prepared by the BRIGHT consortium in relation with 3D printing technologies for producing specific parts (applications) made for the medical sector consisting in 6 laboratory toolkit modules have been related not just to the basics knowledge about 3D printing processes that could be used for certain application in close correlation to the CAD particularities of the parts and specific technology of 3D printing selected for the realizing of these applications, and also to the other preliminary steps that are required to be followed for pre-validation steps of the needed to be performed for the setup of the 3D printing equipment (pre-processing steps), setup of the 3D printing orienting and parameters specific that are used for 3D printing process itself and post-processing steps that are needed to be realized in the end. The toolkit laboratory modules that have been comprising the e-toolkit manual that has been realized in the frame of O2 were shared and are available on the BRIGHT project website.

Examples provided in the toolkit laboratory modules have been selected in concordance with the existing infrastructure, logistics and 3D printing equipment items (3D printing technological methods) that are available within different Higher institutions of BRIGHT consortium in close correlation to the type of applications (parts) on which the BRIGHT consortium partners have been working on for medical case studies / specific patients.

Therefore, first toolkit module has been related to the realizing of skull implants that were made at Technical University of Cluj-Napoca using the Selective Laser Sintering (SLS) 3D printing technology and Rapid Tooling (Vacuum Casting) technologies for producing real implants of the patients that were surgically operated on Medical Clinics in Cluj-Napoca.

The 2nd toolkit module is oriented on a second case study that has been realized at TUCN for manufacturing of a customized facial implant that was used to reconstruct the supraorbital margin and zygomatic bone, this part being produced by using the Selective Laser Melting (SLM) 3D printing technology.

The 3rd toolkit module has been realized by the University of Nis (Serbia) partner, being focused on the realizing of one medical fixator that has been produced using the Stereolithography (SLA) 3D printing process.

The 4th toolkit module has been realized by Poznan University Technology (PUT) partner in Poznan in collaboration with BM Plast company of Opatija (Croatia), being focused on the realizing of mid-surgery supplies in otolaryngology using Fused Filament Fabrication 3D printing technology and Rapid Tooling (Vacuum Casting).

The 5th toolkit module that has been related to the producing of an orthosis made by Fused Deposition Modelling 3D printing and Reprap technologies has been produced by PUT partner in collaboration with Juraj Dobrila University of Pula (Croatia).

The 6th toolkit module that was focused on the realizing of an orthosis reinforcement aimed to replace metallic components with resin ones has been realized jointly by STU Trnava and BIZZCOM partners, using casting of different types of resins into silicone rubber molds that have been produced by Rapid Tooling (Vacuum casting) technology.

BRIGHT

Erasmus+ strategic partnership for Higher Education

BOOSTING THE SCIENTIFIC EXCELLENCE AND INNOVATION
CAPACITY OF 3D PRINTING METHODS IN PANDEMIC PERIOD

TOOLKIT 1

SKULL IMPLANTS MADE BY SELECTIVE LASER SINTERING AND VACUUM CASTING TECHNOLOGIES

Project Title	Boosting the scientific excellence and innovation capacity of 3D printing methods in pandemic period 2020-1-RO01-KA226-HE-095517
Output	IO2 – BRIGHT e-toolkit manual for digital learning in producing medical parts by 3D printing methods in the context of the pandemic
Toolkit	Toolkit 1 Skull implants made by Selective Laser Sintering and Vacuum Casting technologies
Date of Delivery	2021
Authors	Răzvan Pacurar, Cristina Borzan, Eugen Guțiu, Cătălin Moldovan, Cristian Vilău, Sorin Comșa
Version	Final variant

This project has been funded with support from the European Commission. This publication [communication] reflects the views only of the author, and the Commission cannot be held responsible for any use which may be made of the information contained therein.

Contents

1	Introduction. Presenting of the medical case study.....	6
2	Medical imaging and data collection for CAD modelling	9
2.1	The image processing stages	9
2.2	Obtaining the medical models.....	12
2.3	Data acquisition and image processing for the case study.....	14
3	CAD modelling preparation of the skull using specific software (Mimics)	15
3.1	Construction of the physical model of the destroyed (damaged) area.....	16
4	Realizing of the part used as master model by Selective Laser Sintering technology.....	17
4.1	Possibilities of RP technologies to make models starting from CT (Computer Tomograph) and MRI (Magnetic Resonance Imaging) images.....	17
4.2	The manufacturing technology of customized implants	18
4.3	Manufacturing of Parts by Selective Laser Sintering (SLS)	21
5	Realizing of silicone rubber moulds by Vacuum Casting method	28
6	Realizing of the real implant made of PMMA material using silicone rubber moulds.....	29
7	Conclusions.....	34
8	References.....	35

This project has been funded with support from the European Commission. This publication [communication] reflects the views only of the author, and the Commission cannot be held responsible for any use which may be made of the information contained therein.

1 Introduction. Presenting of the medical case study

The scientific literature refers to various cases in which customized implants are used. In general, all cases have the following layout:

- initial clinical condition containing images of the patient accompanied by a brief presentation of the defect cause (medical cause or accident)
- images with the virtual reconstruction and the physical model of the destroyed area, sometimes accompanied by short explanations regarding the manufacturing technology of the physical model (Additive Manufacturing technologies or conventional cutting technologies) and the location where this model was made
- in some cases, images of the implant without technical details of its realization sometimes mentioning a generic technology through which the implant can be made
- the post-operative image of the subject without complete details regarding the surgery technique used or the time necessary to obtain the presented result.

Recently, applications of medical models that are not intended for customized implants have been published more and more frequently. In this sense, there are cases of using medical models for planning very complex surgeries.

Accidents, tumours of the skull bones and certain infections are the main causes of large cranial defects. The main reasons for the reconstruction of these defects are both aesthetic and the need to protect the intracranial structures against mechanical impacts.

The patient, presented in Figure 1.1, due to an ischemic cerebral vascular accident in the right sylvian area, and with a history of persistent obliterative arteriopathy of the inferiorlimbs, was hospitalized. He was in a mild coma and had left hemiparesis at the time of his arrival. To treat the cerebral oedema, the patient received rigorous pharmacological therapy. The symptoms, on the other hand, did not go away. A growing cerebral oedema was discovered on repeated cranial CT examinations. The neurological state improved after a decompressive hemicraniectomy, which left a large bone defect in the right cranial vault. An infection forced the removal of a piece of the cranial vault that had been implanted within the subcutaneous abdominal tissue. The cranial deformity caused not just a cosmetic problem, but also the disadvantages of a craniectomy.

This project has been funded with support from the European Commission. This publication [communication] reflects the views only of the authors, and the Commission cannot be held responsible for any use which may be made of the information contained therein.

have any speech problems and was completely self-sufficient. A customized cranioplasty was developed and a plate was created as specified to avoid the disadvantages of a craniectomy status.

The bone defect was revealed and prepared utilizing the old scar under general anaesthesia. The custom-made plate was installed, precisely fitting, and requiring no further processing. 2.0 silk sutures were used to close the wound.

There were no difficulties during the procedure, and the patient was discharged on the seventh day following surgery. There were no complications at the 1-month and 6-month follow-ups, and the patient tolerated the cranioplasty plate well.

The cranioplasty plate (Figure 1.2) was made by using a mould. The margins of the final custom-made cranioplasty plate were somewhat manually treated after removal from the mould to remove excess and drill holes for fixation [ROT06].

The result of the intervention is presented in Figure 1.3.

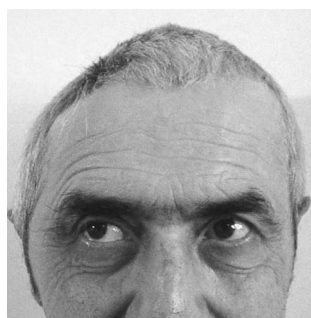


Figure 1.1 The patient's initial condition

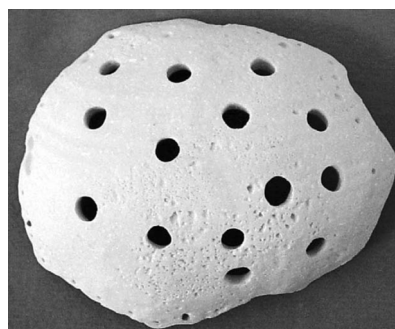


Figure 1.2. The cranioplasty plate

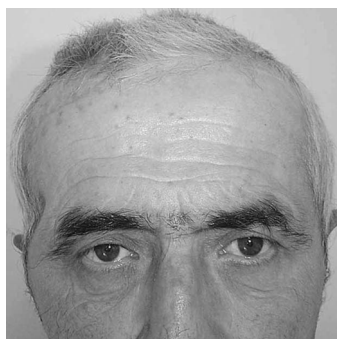


Figure 1.3 The result of the surgery

This project has been funded with support from the European Commission. This publication [communication] reflects the views only of the authors, and the Commission cannot be held responsible for any use which may be made of the information contained therein.

The following steps must be followed in order to create personalized cranial plates:

- A spiral cranial CT scan was performed on the patient, from the Frankfurt horizontal to the vertex with a 01 tilt. The thickness of the axial slices was 2mm (continuous). A virtual 3D model of the vault and defect was generated using 3D reconstruction, and a cranioplasty plate was built using mirroring methods, superimposition, and algebraic Boolean operations.
- Both virtual models (defect and plate) were turned into real polyamide models using selective laser sintering (SLS) for rapid prototyping. The plate fit flawlessly into the defect after minimal manual polishing.
- A silicone rubber mould was created using the pattern of the polyamide cranioplasty plate (via SLS). By combining PEM powder with hydroxyapatite granules and liquid ethylmethacrylate, a thinner paste of PEM mixed with hydroxyapatite was created. This paste was pressed into shape after being cast in a silicone rubber mould (Figure 1.4). Silicone rubber moulds were first utilized in the industrial casting of liquid polymers. The casting procedure used a thin paste of PEM and a mould with larger walls to achieve an accurate model and avoid mould deformations. To drain extra material, large drainage canals were carved into the mould's edges. The mould's cover was forced against its base with manual pressure, and it was kept in place when it was completely closed by placing the mould in a press without applying significant pressure. Following autopolymerization (an exothermic reaction), the entire piece was gently thermopolymerized for 24 hours at 60 degrees Celsius to remove all traces of monomer. The silicone rubber mould was retained in the press in the same position as during autopolymerization during thermopolymerization.
- The margins of the final custom-made cranioplasty plate were somewhat manually treated after removal from the mould to remove excess and drill holes for fixation. To prevent the development of an epidural haematoma, 5–7mm holes were bored in the centre.

This project has been funded with support from the European Commission. This publication [communication] reflects the views only of the authors, and the Commission cannot be held responsible for any use which may be made of the information contained therein.

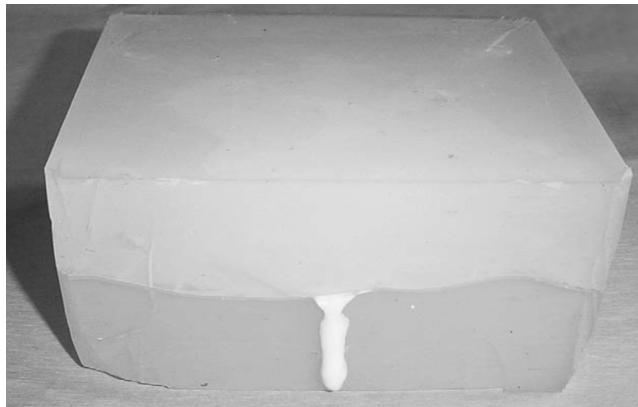


Figure 1.4 The silicone rubber mould

2 *Medical imaging and data collection for CAD modelling*

2.1 The image processing stages

To analyse structures inside the body, medical practitioners utilize computed tomography, generally known as a CT scan. This captures photographs of the bones, muscles, organs, and blood arteries in very tiny "slices" so that healthcare specialists may observe the body in exquisite detail.

X-ray machines that employ a fixed tube to point X-rays at a particular place are known as traditional X-ray machines. X-rays are absorbed in various amounts by different tissues as they pass through the body. Against the black background of the film, higher density tissue produces a whiter image than other tissues [www 02].

As it moves through an arc, a CT scanner emits a series of narrow beams into the human body. An X-ray machine, on the other hand, sends only one radiation beam. Compared to an X-ray image, a CT scan produces a more detailed final image.

The X-ray detector in a CT scanner can detect hundreds of different degrees of density. It has the ability to view tissues within a solid organ. This information is sent to a computer, which creates a 3-D cross-sectional image of the bodily component and presents it on the screen. A contrast dye is occasionally used to assist reveal particular structures more clearly.

If a 3-D imaging of the abdomen is needed, the patient may be required to consume a barium meal. On the scan, the barium appears white as it passes through the digestive system. If images of the lower body, such as the rectum, are needed, the patient may be

This project has been funded with support from the European Commission. This publication [communication] reflects the views only of the authors, and the Commission cannot be held responsible for any use which may be made of the information contained therein.

given a barium enema. A contrast agent will be injected into the veins if blood vessel pictures are the goal.

The use of spiral CT, a relatively recent technique, may increase the accuracy and speed of CT scans. During scanning, the beam follows a spiral route, collecting continuous data with no pauses between images.

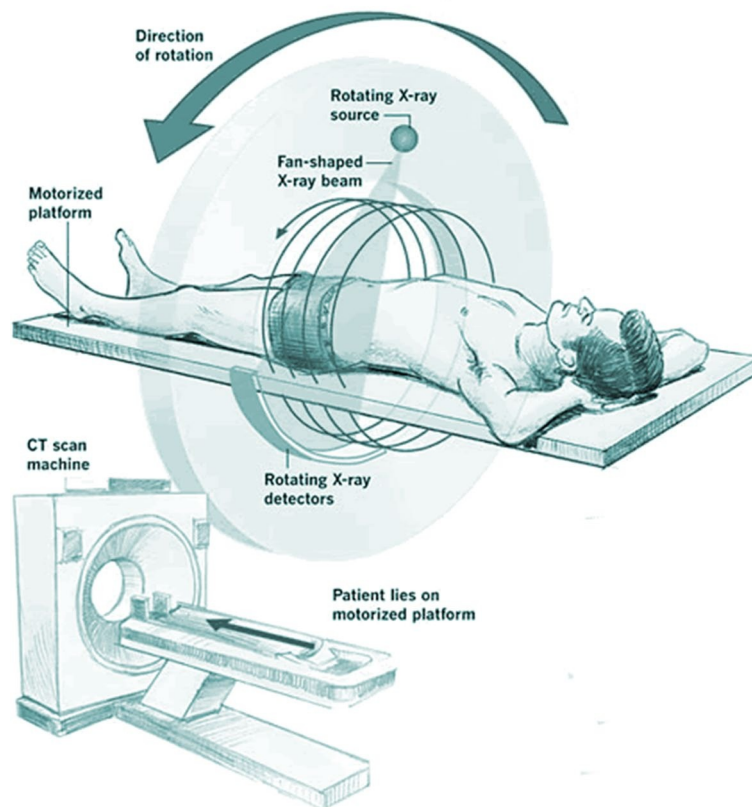


Figure 2.1 The working principle of a CT scan [www 04]

CT is a vital tool for assisting in medical diagnosis, however it emits ionizing radiation that has the potential to cause cancer.

CT scan can be used to get photographs of:

- soft tissues
- the pelvis
- blood vessels
- lungs

This project has been funded with support from the European Commission. This publication [communication] reflects the views only of the authors, and the Commission cannot be held responsible for any use which may be made of the information contained therein.

- brain
- abdomen
- bones

Many cancers, such as liver, lung, and pancreatic tumours, are routinely diagnosed using CT scans. A clinician can use the image to confirm the presence and location of a tumour, as well as its size and the extent to which it has damaged neighbouring tissue.

A head scan can reveal critical information about the brain, such as whether there is any bleeding, artery swelling, or a tumour.

A CT scan of the abdomen can identify a tumour as well as any swelling or inflammation in the internal organs surrounding. It can reveal any spleen, kidney, or liver lacerations.

A CT scan is useful for planning locations for radiotherapy and biopsies because it detects abnormal tissue, and it can also provide significant data on blood flow and other vascular issues. It can aid a physician in determining bone disorders, bone density, and the condition of a patient's spine. It can also provide important information regarding a patient's injuries to their hands, feet, and other skeletal structures. Even little bones, as well as their surrounding tissue, are clearly apparent.

A CT scan exposes you to a little amount of radiation that is precisely focused. Even in persons who have had multiple scans, these levels of radiation have not been shown to be detrimental. The likelihood of developing cancer as a result of a CT scan is estimated to be less than one in 2,000. The level of radiation involved is considered to be similar to what a person might be exposed to in the environment over a period of few months to several years.

A scan is only performed if there is a compelling medical reason. The findings may lead to treatment for diseases that might otherwise be fatal. When deciding whether or not to get a scan, doctors will make sure that the advantages outweigh the risks.

Before the scan, the patient may be required to fast from food and perhaps drink for a period of time.

On that particular day, in most cases, the patient will be required to undress to their underwear and put on a gown provided by the health centre. If a gown is not provided by the hospital, the patient should dress loosely with no metal buttons or zippers. Some patients may be required to consume a contrast dye, which may also be administered through enema or injection. The image of some blood vessels or tissues is improved as a

This project has been funded with support from the European Commission. This publication [communication] reflects the views only of the authors, and the Commission cannot be held responsible for any use which may be made of the information contained therein.

result of this. Any patient who has a reaction to contrast material should inform their doctor ahead of time. Certain drugs can help those who are allergic to contrast materials. Because metal interferes with the CT scanner's operation, the patient must remove all jewellery and metal fastenings.

The patient must lie down on a motorized examination table that glides into a doughnut-shaped CT scanning machine during the scan. The patient will most likely be lying on their back, facing up. They may, however, be required to lie face down or sideways on occasion. The couch will move slightly after one x-ray image, and the machine will take another image, and so on. For the best outcomes, the patient must lie completely still.

Everyone in the room except the patient will leave during the scan. An intercom will allow the radiographer and the patient to communicate in both directions. A parent or adult may be allowed to stand or sit near the patient if the patient is a youngster, but they must wear a lead apron to avoid radiation exposure [www 03].

2.2 Obtaining the medical models

In the early 1980s, models of the internal bone structures of the human body were made using thin sheets of aluminium that were cut out of the bone contours from images obtained by tomography. The three-dimensional model was obtained by assembling these sheets. The same technology has been used in the construction of moulds with the help of prostheses or implants made of biocompatible materials.

Later, numerically controlled milling machines were used to make the models, the complexity of the models increasing with the increase in the number of numerically controlled axes. These machines made the models directly in wax, polystyrene or polyurethane foam. The numerically controlled five-axis milling system developed in Kiel (Germany) produces models that are very close to the original structures. Taken as a whole, the realization of models by milling cannot be considered a complete solution for the realization of medical models due to technical limitations: the resolution of the models is limited, the presence on most models of complicated concave areas, with small dimensions, and with thin walls. In general, models are useful in very complex cases that are difficult to imagine with the help of 3D views, which is impossible to achieve by milling and leads to

This project has been funded with support from the European Commission. This publication [communication] reflects the views only of the authors, and the Commission cannot be held responsible for any use which may be made of the information contained therein.

limited application of the method. Despite its limitations, this technology is still often used to make relatively simple models such as joints and long bones.

Currently, complex medical models are made using rapid prototyping technologies.

As stated before, the principle of operation of a computer-assisted tomograph is as follows: a tube that generates X-rays and a receiving analyser element are rigidly fixed on a rotor that rotates 360° around the patient's axis. This allows to perform several thousand measurements from different angles through the patient. Starting from these measurements, a computer creates an artificial image of a cross section through the patient.

The three-dimensional image is obtained by assembling the sections made by the tomograph and the 2D section package determines the geometric elements of the three-dimensional model. A first problem that arises when generating these images is the amount of radiation used. A high dose of radiation is needed to produce very good quality images. Thus, when performing a three-dimensional scan with the aim of obtaining very fine details, this dose may become critical. Another problem that occurs during a three-dimensional scan is the time the patient is immobilized, and a full scan can take up to 30 minutes.

Spiral scanning or continuous volume scanning can be a solution to the above problems. The procedure consists in the axial movement of the patient synchronized with a multitude of rotations performed by the receiver and the X-ray generator tube. In this case the received data no longer come from discrete sections, parallel to each other, but are presented in the form of a continuous film that consists of normal sections to an imaginary helical trajectory around the patient. Spiral CT scanners allow the user to choose both the pitch of the path and the thickness of the radiation beam that performs the scan. The proper choice of these parameters leads to the realization of helical spirals on spiral which is similar to the complete analysis of a volume.

Spiral CT scanners require special software packages to process data. These programs must be able to perform 3D reconstruction of the analysed models simultaneously with the removal of artifacts due to patient movement. The data must be stored in flat sections, and the model is made by assembling these sections. Due to the spiral scan, the flat sections are made by interpolating the analysed data. When performing a full spiral scan of a volume, the user can choose the distance between the parallel plane sections that will be calculated.

Nuclear magnetic resonance tomography is used to analyse and perform medical models of internal structures that are composed of soft tissues. Magnetic resonance imaging

This project has been funded with support from the European Commission. This publication [communication] reflects the views only of the authors, and the Commission cannot be held responsible for any use which may be made of the information contained therein.

systems are based on the fact that odd-numbered nuclei rotate around their own axis, giving them a magnetic moment. When these nuclei are placed in an external magnetic field over which low-frequency radio waves overlap, the properties of these nuclei allow extremely detailed images of cross-sections to be obtained through the human body. The response frequencies are characteristic of each scanned tissue, which makes it possible to differentiate the analysed internal organs easily visually.

The process of 3D reconstruction of the analysed structures is similar to that of X-ray tomographs, in this case there is no possibility of spiral scanning. Although it seems to be a disadvantage, the absence of this facility does not affect the results of the analysis because exposure to magnetic fields is less harmful than exposure to X-rays.

2.3 Data acquisition and image processing for the case study

Three-dimensional data of the internal and external structures of the human body are obtained by using computed tomography (CT) systems for bone structures. In principle, it is possible to use any system that provides images of flat sections through the human body and that are able to make a mathematical correlation between these sections to make possible the 3D reconstruction of the analysed structure. Spiral scanning tomography was used in this case. The procedure consists in the axial movement of the patient synchronized with a multitude of rotations performed by the receiver and the X-ray generating tube. In this case, the received data no longer come from discrete sections, but are presented as a continuous film consisting of normal sections, to an imaginary helical trajectory around the patient. The image obtained by tomography is shown below, Figure 2.2:

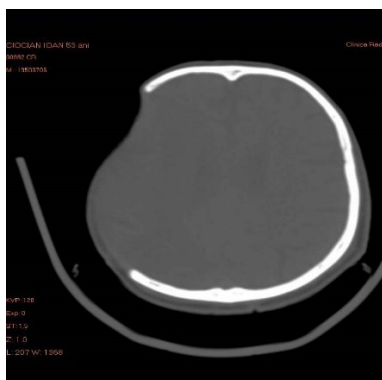


Figure 2.2 Tomography image

This project has been funded with support from the European Commission. This publication [communication] reflects the views only of the authors, and the Commission cannot be held responsible for any use which may be made of the information contained therein.

The three-dimensional image is obtained by "assembling" the sections made by the tomograph, and the 2D section package determines the geometric elements of the three-dimensional model.

Special software packages are used to process the data. This program is able to perform 3D reconstruction of the analysed model simultaneously with the removal of artefacts due to patient movement.

The interpretation of the images is performed by radiologists with the help of a 3D modelling program, namely the MIMICS program. During this stage, doctors determine the shape and size of the areas of interest in each section. The delimitation of the elements present in each section is called segmentation. Once the medical team has made the complete and correct segmentation at the level of each section, it is possible to proceed to the processing of the images provided by the tomograph.

3 CAD modelling preparation of the skull using specific software (Mimics)

The great advantage of using the CT - Modeler model provided by Materialize is that it interpolates the scanned sections without the need for the user to have advanced surface modelling knowledge. Basically CT - Modeler hides a very complex mathematical device, and the effect of processing the images provided by the tomograph can be visualized by displaying the three-dimensional model on the computer monitor, as seen in the figures below.

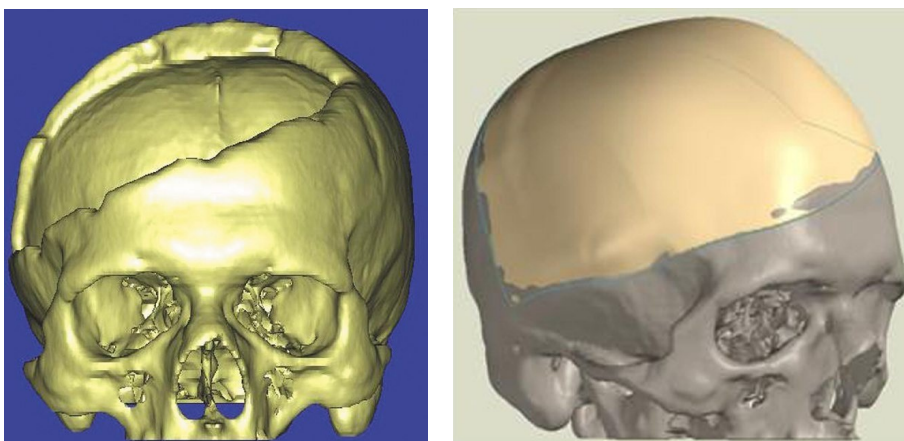


Figure 3.1 Virtual 3D reconstruction model of a patient's skull

This project has been funded with support from the European Commission. This publication [communication] reflects the views only of the authors, and the Commission cannot be held responsible for any use which may be made of the information contained therein.

3.1 Construction of the physical model of the destroyed (damaged) area

With the help of these technologies, objects are made by adding material in successive layers as opposed to classical technologies, where the models are made by removing material (cutting, EDM) or by redistributing material (injection, casting, forging, moulding).

The procedure behind obtaining the implant prototype is:

- starts from a virtual 3D model built on a computer system.
- this model is imported in specialized software packages, specific to each FRP system. In this software, the model is intersected with equidistant parallel planes and the intersection between the model and these planes is determined.
- the FRP system successively materializes these intersections, the piece being built sequentially layer by layer by selective laser sintering.

With this method the medical model is obtained, called the model of the destroyed area.

The model of the destroyed area means that part of a medical model, made on a 1: 1 scale, which includes the area on which the surgery will be performed.

To produce the custom-made cranioplasty implants, a spiral CT scan of the head (Siemens Somatom, Erlangen, Germany) was performed as the first step. A virtual 3D model of the skull was obtained using a 3D reconstruction program (MIMICS, Materialise NV, Leuven, Belgium). The virtual 3D model of the patient-specific implant was designed using FreeForm Modeling Plus 9.0 (Sensable, Wilmington, MA). Using selective laser sintering (Sinter Station 2000, 3D System, Darmstadt, Germany) or 3D printing (Eden 330, Objet Geometries, Rehovot, Israel), the virtual models (of the calvarial defect and the custom-made implant) were transformed into physical models. The designed implant was well suited for the defect, which was not needed for further manual processing [ROT12].

This project has been funded with support from the European Commission. This publication [communication] reflects the views only of the authors, and the Commission cannot be held responsible for any use which may be made of the information contained therein.

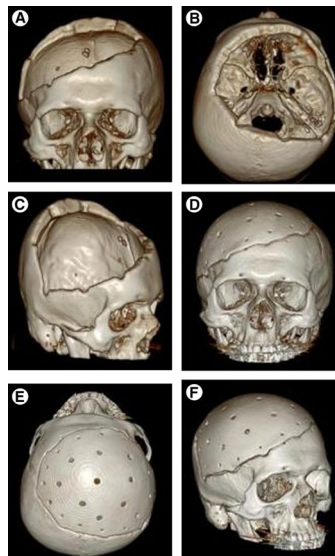


Figure 3.2 Three-dimensional computed tomographic images A-C, before versus D-F, after surgery show that the defect was successfully reconstructed.

4 Realizing of the part used as master model by Selective Laser Sintering technology

4.1 Possibilities of RP technologies to make models starting from CT (Computer Tomograph) and MRI (Magnetic Resonance Imaging) images

For selective laser sintering (SLS), the powders - the raw material must be coated with a thermoplastic polymer. During the laser beam sweeping of the successive layers (that by assembly generates the finished part), the thermoplastic polymer on two particles in contact must be welded to complete the strength of the metal-to-metal welding bridges. From the point of view of the resistance of the direct joint with laser radiation, the optimal shape of the particles is irregular, with marked peaks. This is the situation of titanium powders obtained by the process of hydration - grinding - dehydration. In addition to the metal peaks, the particles must have polymer-coated portions after conditioning. Presintered compacts made by SLS must have sufficient mechanical stability for the final sintering. In addition, the thickness of the metal-metal bridges must ensure sufficient mechanical stability during the

This project has been funded with support from the European Commission. This publication [communication] reflects the views only of the authors, and the Commission cannot be held responsible for any use which may be made of the information contained therein.

removal of the organic binder. A too low sintering of titanium particles can compromise the shape of the final compact if the polymer-polymer welding bridges fail before making stable metal-to-metal "necks". Also, the adhesion of the metal substrate-coating polymer must be sufficient to ensure the mechanical strength of the precompact.

4.2 The manufacturing technology of customized implants

The creation of customized implants required a complex technology that includes six essential steps, namely:

- Acquisition and processing of tomographic images to obtain the virtual model of the destroyed area. The images obtained by tomography were processed on the computer with the help of the Materialize package which includes the 3D Mimics modelling program and the CAD system after which the STL, CT file is generated.
- After obtaining the data, the virtual generation of the implant was attempted using symmetry with the healthy part.
- The third stage in obtaining the customized implant consists in the construction of the physical model of the destroyed area and of the implant from materials specific to Rapid Prototyping (AM) technologies, namely in this case by selective laser sintering.
- After obtaining the implant, an adjustment is made to the physical model of the destroyed area.
- Construction of a silicone rubber mould for the formation of the real implant, made of biocompatible material.
- After a whole technology the real implant will be obtained.

The Sinterstation 2000 machine presented in figure 4.1, from the endowment of the National Centre for Rapid Manufacturing of Prototypes within the Technical University of Cluj-Napoca, works with several types of powder: metal powder, plastic powder (polyamide), polystyrene powders or powders from ceramic material.

This project has been funded with support from the European Commission. This publication [communication] reflects the views only of the authors, and the Commission cannot be held responsible for any use which may be made of the information contained therein.



Figure 4.1 SINTERSTATION 2000 machine from the National Centre for Rapid Prototyping (UTC-N)

If this equipment were described in more detail, we could say that it is a control equipment, equipment that has the appropriate software characteristic of these systems, capable of taking over certain files for execution, files in ".stl" format, which the machine recognizes, as well as to effectively control the entire effective sintering process (through the indicated working parameters). The machine itself includes working chamber, mirrors, laser system, sensors, cartridges, adjusting elements, conveyor roller, etc.

The working space is limited to a 250 mm cylinder, but due to the deformations that occur on the edges due to the variation of the temperature in the enclosure, the working space is further limited to about 230 mm.

The characteristics of the SLS equipment are presented in the following table (Tab. 4.1)

Table 4.1 SLS equipment characteristics

Resolution	0.75 in the x / y plane, 0.005mm minimum layer thickness on Z
Overall dimensions	3937x 1499x 1905
Power supply	208/240VAC, 70A, 60Hz AND 120VAC, 20A
Laser	50W CO2 Laser
Working dimensions	203x254x152

This project has been funded with support from the European Commission. This publication [communication] reflects the views only of the authors, and the Commission cannot be held responsible for any use which may be made of the information contained therein.

The working principle in the manufacture of parts by selective sintering with laser is shown in figure 4.2. As can be seen in this figure, the process of rapid prototyping by selective laser sintering (SLS) is based on the materialization of a virtual 3D model (built into a CAD system) by adding successive layers. It is not necessary to build supports because the previous layer of material (sintered or not) is a support for the current layer of material. The laser system generates laser radiation which is focused by means of lenses and is then directed through a system of mirrors to the surface of the work platform. At the beginning of the work process, the platform is in the upper (top) position. A feeding system deposits a thin layer of powder, of controlled thickness, on the surface of the platform. The laser beam scans the surface of the platform according to a trajectory corresponding to the geometry of the first section through the workpiece. Following the scanning process, the laser radiation sinters the powder layer locally. After the laser radiation has completely scanned the surface of the first layer, the work platform descends a distance equal to the thickness of a layer. The material supply system deposits a new layer of metal powder over the previous layer. Again, the laser radiation will scan the current layer of powder according to the geometry of the new section through the solid model of the workpiece. During the process, there will be a permanent control between the thickness of the powder layer deposited on the work platform, the distance between the sections made by the computer software through the solid part model and the size of the work platform movement after each layer processed. [www 05]

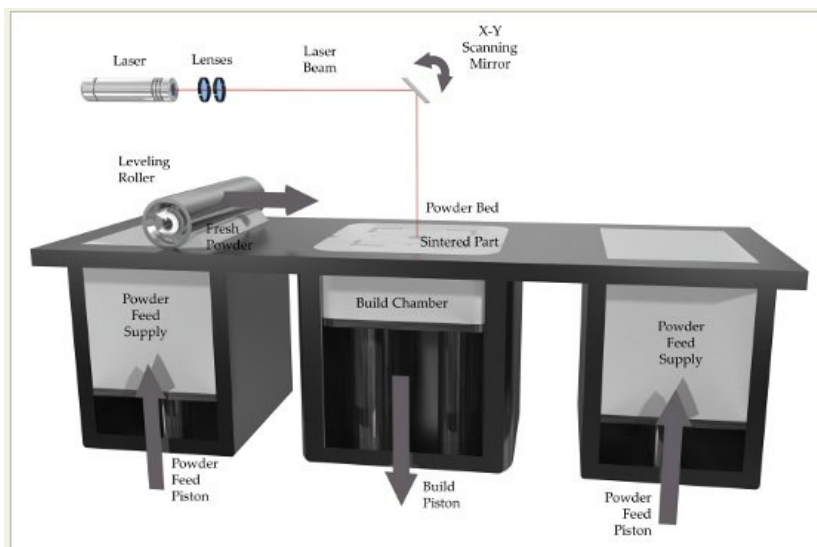


Figure 4.2 Working principle of laser selective sintering technology (SLS) [www 05]

This project has been funded with support from the European Commission. This publication [communication] reflects the views only of the authors, and the Commission cannot be held responsible for any use which may be made of the information contained therein.

The characteristics of the material used to make the prototypes (Duraform Polyamide P6 plastic powder) are shown in Figure 4.3. [www 06]

TECHNICAL DATA		
General Properties		
MEASUREMENT	METHOD/CONDITION	VALUE
Specific Gravity	ASTM D792	1.00 g/cm ³
Moisture Absorption - 24 hours	ASTM D570	0.07 %
Mechanical Properties		
MEASUREMENT	METHOD/CONDITION	VALUE
Tensile Strength, Yield	ASTM D638	N/A*
Tensile Strength, Ultimate	ASTM D638	43 MPa (6237 psi)
Tensile Modulus	ASTM D638	1586 MPa (230 ksi)
Elongation at Yield	ASTM D638	N/A*
Elongation at Break	ASTM D638	14 %
Flexural Strength, Yield	ASTM D790	N/A*
Flexural Strength, Ultimate	ASTM D790	48 MPa (6962 psi)
Flexural Modulus	ASTM D790	1387 MPa (201 ksi)
Hardness, Shore D	ASTM D2240	73
Impact Strength (notched Izod, 23°C)	ASTM D256	32 J/m (0.6 ft-lb/in)
Impact Strength (unnotched Izod, 23°C)	ASTM D256	336 J/m (6.3 ft-lb/in)
Gardner Impact	ASTM D5420	2.7 J (2.0 ft-lb)
Thermal Properties		
MEASUREMENT	METHOD/CONDITION	VALUE
Heat Deflection Temperature (HDT)	ASTM D648 @ 0.45 MPa	180 °C (356 °F)
	@ 1.82 MPa	95 °C (203 °F)
Coefficient of Thermal Expansion	ASTM E831 @ 0 - 50 °C	62.3 µm/m-°C (34.6 µin/in-°F)
	@ 85 - 145 °C	124.6 µm/m-°C (69.2 µin/in-°F)
Specific Heat Capacity	ASTM E1269	1.64 J/g-°C (0.392 BTU/lb-°F)
Thermal Conductivity	ASTM E1225	0.70 W/m-K (4.86 BTU-in/hr-ft ² -°F)
Flammability	UL 94	HB

Figure 4.3 Mechanical and thermal characteristics of Duraform PA6 powder [www 02]

4.3 Manufacturing of Parts by Selective Laser Sintering (SLS)

Models designed with SOLID WORKS software are saved as “.stl” files, which are later recognized by the DTM SINTERSTATION 2000 machine software.

The software of the SLS machine contains two actual packages, one in which the model is prepared, indicating at the same time the working parameters depending on the material used, respectively the scaling factors necessary to compensate the contractions resulting from the manufacturing process, respectively a second package in which the actual manufacture takes place on the sintering machine (the control part of the machine).

This project has been funded with support from the European Commission. This publication [communication] reflects the views only of the authors, and the Commission cannot be held responsible for any use which may be made of the information contained therein.

The preparation of the model is therefore done using a first software package of the SLS machine, namely the BUILD SETUP program.

The interface of this software is very similar to the interface of a design software, being easy to manipulate.

Thus, in a first phase, the saved “.stl” type models are imported into the machine program, thus building the package for the working session, so as to meet the minimum conditions on z, a condition that ultimately influences the cost price of the models, increasing or decreasing the working time, respectively the overall conditions, not exceeding 230 mm (cylinder diameter), otherwise the part suffering seriously from the point of view of precision, as well as qualitatively due to deformations.

Then select from the menu, the type of material from which the models will be made on the sintering machine, which will be the plastic powder type Duraform Poliamyde PA6 in our case.

Next, the parts are positioned for manufacture on the sintering machine, taking into account the shape of the models to be manufactured on this equipment in order to finally have a minimum package height in the direction of the Z axis (on height), which will reflect on the manufacturing time, respectively on the manufacturing costs using this equipment without affecting the quality and dimensional accuracy of the manufactured models (see figure 4.4).

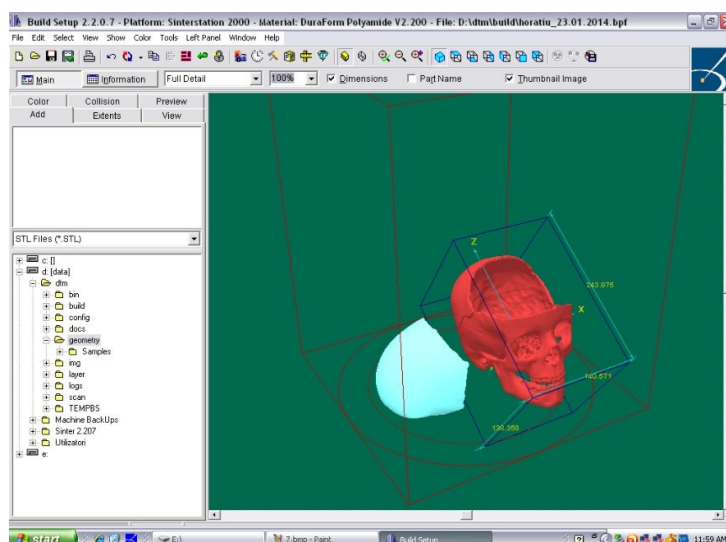


Figure 4.4 3D models imported in the Build Setup software

This project has been funded with support from the European Commission. This publication [communication] reflects the views only of the authors, and the Commission cannot be held responsible for any use which may be made of the information contained therein.

The working parameters are applied according to the chosen plastic powder. Thus, in a first phase, the scaling of the models to be manufactured takes place. These were each scaled in the direction of the X axis by 1.03510 mm, in the direction of the Y axis by 1.03310 mm, and in the direction of the Z axis by 1.01800 mm, in order to compensate for the contractions resulting from the sintering process itself (Figure 4.5).

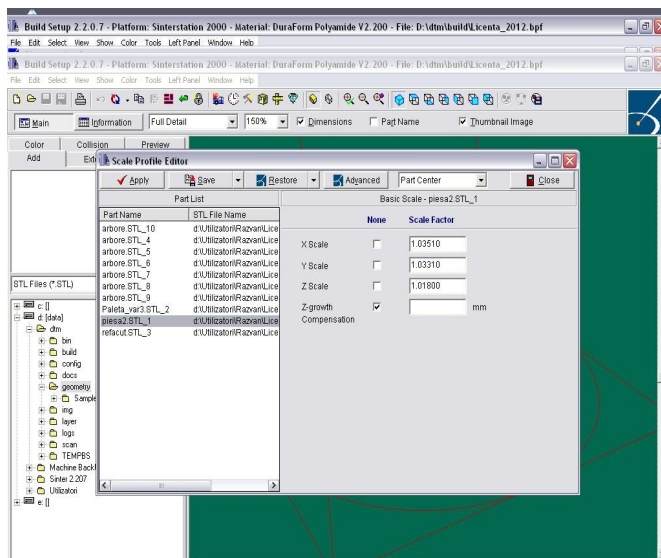


Figure 4.5 The used scaling factors

Next, the power of the laser that was used during the sintering process was set for all manufactured models. A laser power of 4.5 W was used for all the manufactured models, enough power to melt the plastic granules (Figure 4.6).

Also, as can be seen in Figure 4.7, a second parameter that was set was the temperature used during the manufacturing process. As can be seen in Figure 4.7, we have three temperature zones to be set, distinct on the machine, namely, a temperature value required for the area of the heating cycle, when the machine heats up to a set temperature of C, during which time the necessary base for the models to be manufactured is built. This base is necessary to maintain a constant temperature of the package containing the models throughout the manufacture. It is also possible to observe a second zone specific to the actual manufacturing, which comprises a temperature value of C, kept constant throughout the manufacturing process, followed by a third zone, on the cooling phase, when the process

This project has been funded with support from the European Commission. This publication [communication] reflects the views only of the authors, and the Commission cannot be held responsible for any use which may be made of the information contained therein.

temperature drops sharply. controlled, at a value of C, at which point the process of selective laser sintering is considered to be completed.

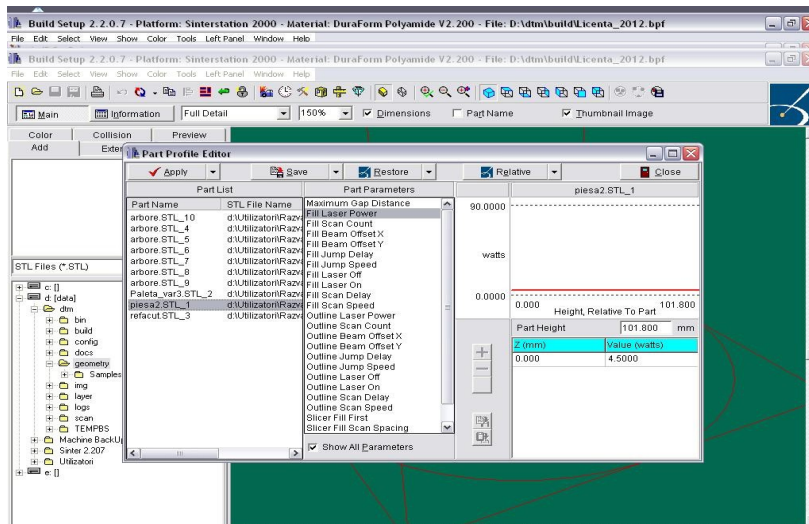


Figure 4.6 The laser power

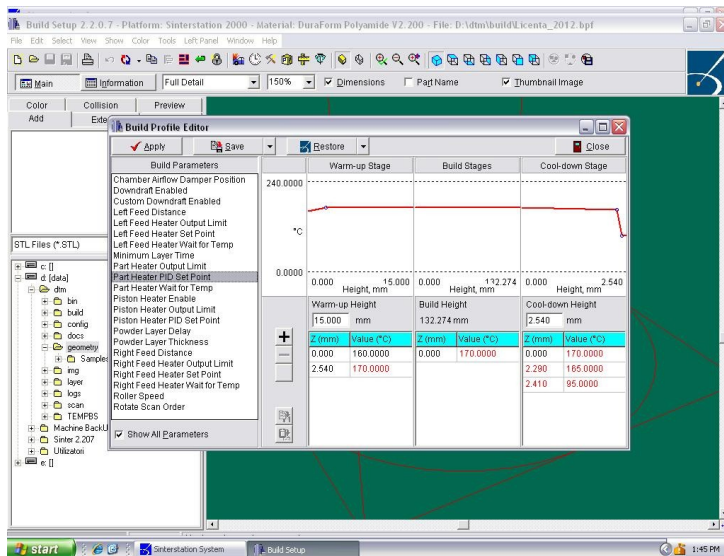


Figure 4.7 Working temperature on the three cycles

The thickness of the layers that was used in the selective sintering process with laser was 0.10 mm on all three areas mentioned above, as can be seen in the image in Figure 4.8.

This project has been funded with support from the European Commission. This publication [communication] reflects the views only of the authors, and the Commission cannot be held responsible for any use which may be made of the information contained therein.

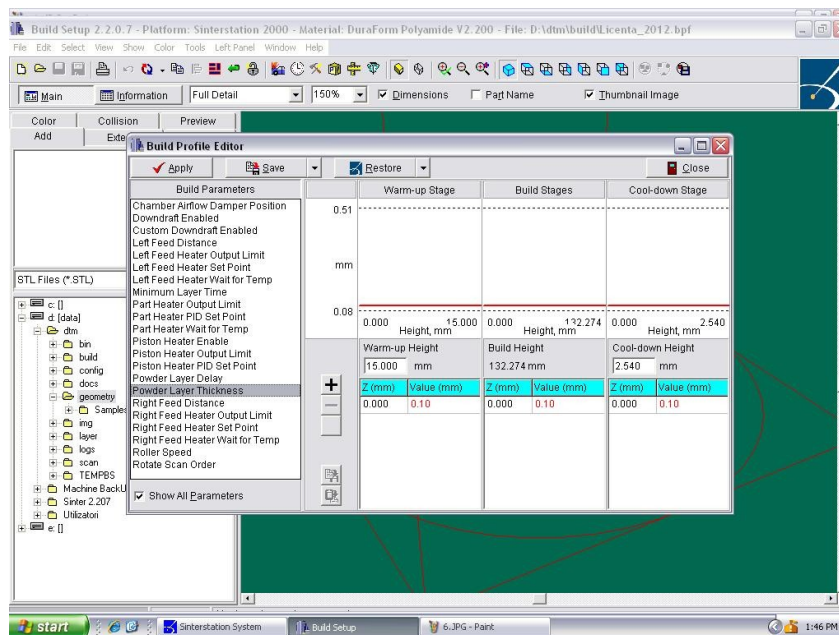


Figure 4.8 The used layer thickness

Finally, a last basic parameter that was set was the laser scanning speed, which has a value of 1257.30 mm / s. This parameter is particularly important, as a change in speed in the direction of its increase or decrease ultimately leads to improper sintering of the plastic powder granules, the parts becoming brittle, their tensile strength being significantly affected in this case (see Fig. 4.9).

Finally, all this information related to the manufacturing models is included in the analysis bulletins within the BUILD SETUP software, the package containing these settings can be accessed and manufactured at any time thereafter.

Thus, in these bulletins you can view information related to the material from which the package is made, the number of pieces of the models in the package, the number of facets of the models, the size in MB per disk drive (file size. * Stl), the required quantity of the material (powder) for the finalization of the package to be manufactured, respectively a particularly useful information regarding the time required for the manufacture of the package, which was estimated in this case of the models presented in Figure 4.4. at a total of 18 hours and 14 minutes (see Figure 4.10).

This project has been funded with support from the European Commission. This publication [communication] reflects the views only of the authors, and the Commission cannot be held responsible for any use which may be made of the information contained therein.

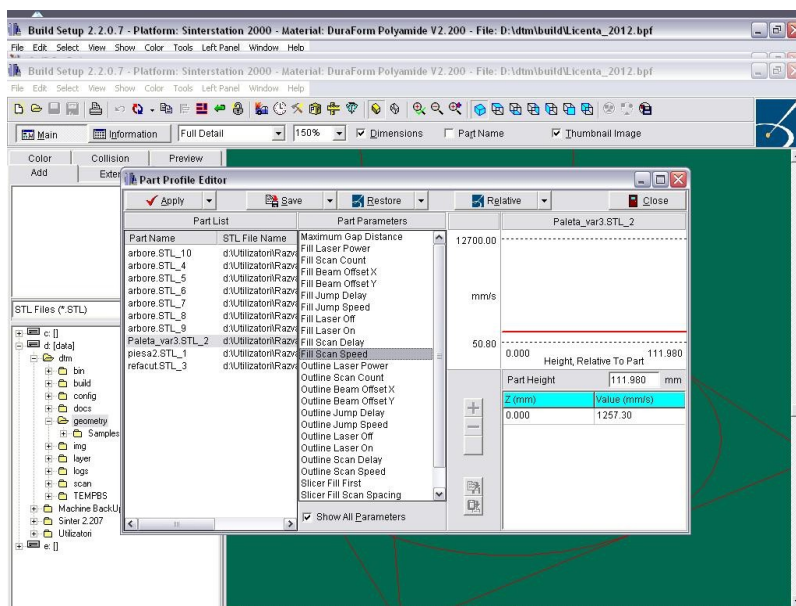


Figure 4.9. Laser scanning speed

Total		Warm-up Stage	Build Stages	Cool-down Stage
Wait for Temperature Time	0:00:00	0:00:00	0:00:00	0:00:00
Add Powder Layer Time	8:22:06	1:52:09	6:19:13	0:10:44
Scan Time	9:52:38	NA	9:52:38	NA
Summary	18:14:44	1:52:09	16:11:51	0:10:44

Part No.	Part Name	Part Height	Total Scan Time	Fill Scan Time	Outline Scan Time	Total Volume (cm³)	Build Volume (%)
1	piesa2.STL_1	101.800	3:22:00	3:22:00	0:00:00	182.203	31.883
2	Paleta_var3.STL_2	111.980	2:29:58	2:29:58	0:00:00	154.588	27.051
3	refacut.STL_3	101.800	3:01:06	3:01:06	0:00:00	176.219	30.836
4	arbore.STL_4	48.864	0:08:25	0:08:25	0:00:00	8.325	1.457
5	arbore.STL_5	48.864	0:08:21	0:08:21	0:00:00	8.325	1.457
6	arbore.STL_6	48.864	0:08:21	0:08:21	0:00:00	8.325	1.457
7	arbore.STL_7	48.864	0:08:35	0:08:35	0:00:00	8.326	1.457
8	arbore.STL_8	48.864	0:08:49	0:08:49	0:00:00	8.510	1.489
9	arbore.STL_9	48.864	0:08:38	0:08:38	0:00:00	8.325	1.457
10	arbore.STL_10	48.864	0:08:20	0:08:20	0:00:00	8.325	1.457

Figure 4.10 An example of an analysis bulletin related to model size and manufacturing time

This project has been funded with support from the European Commission. This publication [communication] reflects the views only of the authors, and the Commission cannot be held responsible for any use which may be made of the information contained therein.

Once the pre-processing part of the models is finished, it can be move on to the actual manufacturing part, the models being loaded in BUILD SETUP, after which using the second software package of the Sinterstation machine, where the command and control parameters are set, such as operating temperature (the initial temperature of C for the heating zone will be set, as shown in Figure 4.7). The permissible oxygen level inside the machine's working chamber is also adjusted (5% is allowed inside the machine's oxygen chamber). The atmosphere in which plastic powders are treated is a controlled, being a nitrogen-based atmosphere. This is absolutely necessary to avoid the risk of ignition of plastic parts during the SLS manufacturing process. Once these conditions are met, layers of 0.10 mm are deposited, up to the total of 15 mm necessary to achieve the base of the package, as presented above.

After the deposition of these layers, the sintering process starts automatically, the actual manufacture of the package being carried out layer by layer until the maximum height of the package on the Z axis is reached.

Once the manufacturing package is completed, it enters the area of the last required cooling cycle, as shown in Figure 4.7, the temperature set for this cycle being C. In this phase no more layers of powder are deposited.

The models are finally buried in powder in the work area, being cleaned during a post-processing stage, with the help of special cleaning brushes, to avoid the risk of breaking certain fine details of the models, an exhaust system being permanently used at the same time for vacuuming the excess dust. The final parts that were made on the SLS machine, after their post-processing step are shown in the image in Figure 4.11.

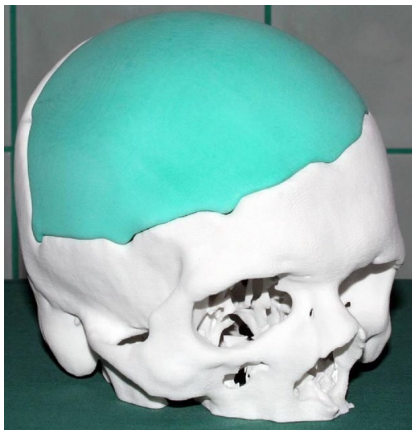


Figure 4.11. Medical model made of polyamide material on SLS machine using Sinterstation 2000 equipment (UTC-N)

This project has been funded with support from the European Commission. This publication [communication] reflects the views only of the authors, and the Commission cannot be held responsible for any use which may be made of the information contained therein.

5 Realizing of silicone rubber moulds by Vacuum Casting method

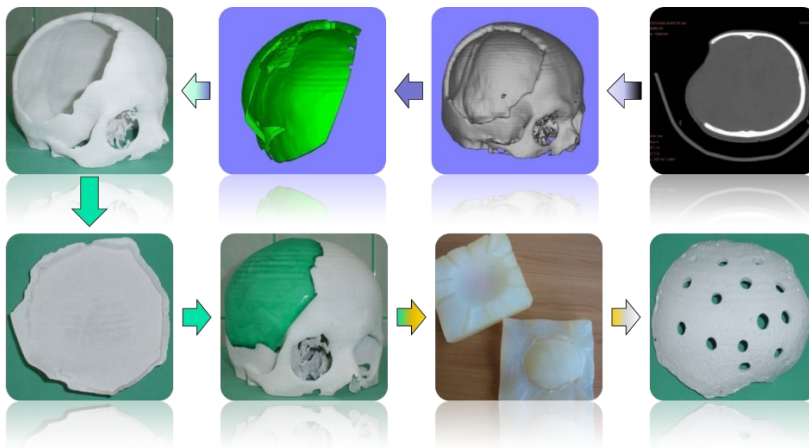


Fig. 5.1. Required steps for obtaining a customized implant using indirect

Manufacturing a silicone rubber mould (Figure 5.1) for a customized implant requires the following steps:

- 1) Checking the master model which was obtained using an Additive Manufacturing Technology. In this example, the model was obtained through Selective Laser Sintering Process, using Polyamide, PA6 material.
- 2) Cleaning the master model and applying chemical substances to prevent sticking of the silicone on model's surface. For this purpose, a green coloured Release Agent was used. The dried process of the model took 2 hours, at room temperature.
- 3) Manufacturing of a shaped box, using MDF as a building material (wood with glossy surface), in which the master model can fit and to it can be casted the silicone rubber (CS) in a liquid state. For economic reasons this box must be made approximately 20-25 mm larger than the size of the master model, Figure 5.2.

This project has been funded with support from the European Commission. This publication [communication] reflects the views only of the authors, and the Commission cannot be held responsible for any use which may be made of the information contained therein.

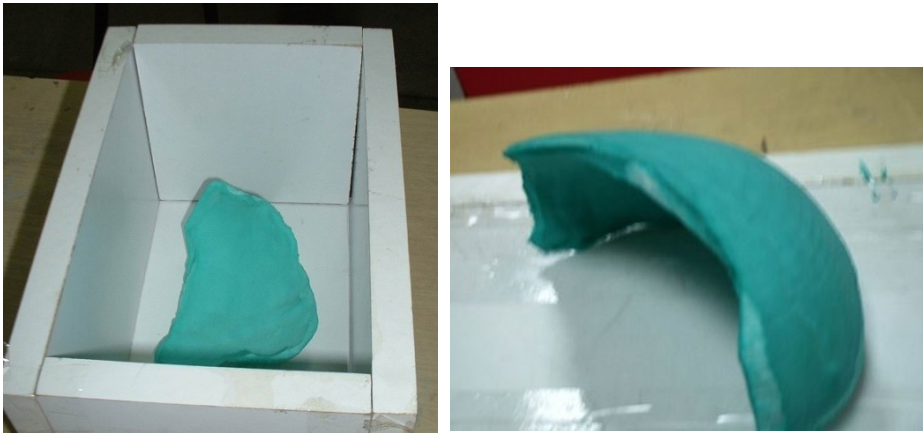


Fig. 5.2. The box shaped from wood and the physical model of the destroyed area

- 4) Suspension of the model into the box. The model must be suspended into the box and to not touch the bottom of the box. There are many ways to suspend the model. Due to the small size of this master model, it was chosen to anchor the model with the help of nylon threads, in walls of wooden box after its previous drilling. Drilling was done with a helical drill with a cylindrical shaft, Drill 2 STAS 573-80/Rp 3. Due to the small size of the holes, the future implant that will be casted into the silicone mould will not be affected.
- 5) Preparation of the silicone rubber mixture. Silicone rubber which has been casted over the model was obtained by mixing silicone "ESSIL 291 RESIN" (Figure 5.3a) and catalyst "ESSIL 291 CATALYSEUR" (Figure 5.3b). The catalyst had role for hardener.

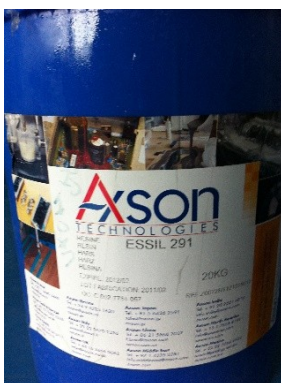
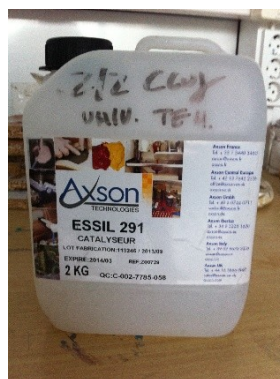


Figure 5.3. a) ESSIL 291 RESIN



b) ESSIL 291 CATALYSEUR

This project has been funded with support from the European Commission. This publication [communication] reflects the views only of the authors, and the Commission cannot be held responsible for any use which may be made of the information contained therein.

By determining the volume of the box (9 cm x 8 cm x 8 cm = 576 cm³) was obtained by approximating, the quantities of silicone, respective catalyst, which must be used (600 g silicon and 60 g catalyst). The ratio of silicone and catalyst was 10:1. The two components were mixed in a container whose volume is at least 5times larger (Figure 5.4. a, b, c).

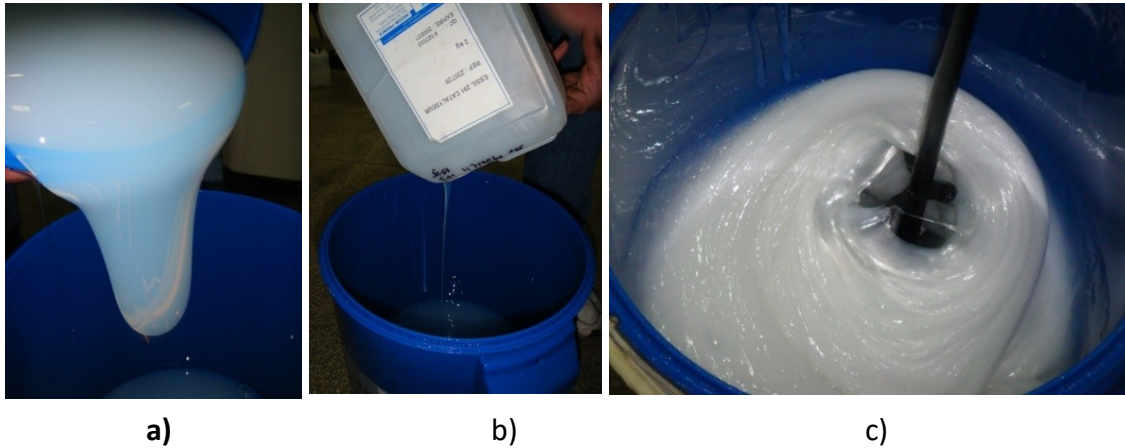


Figure 5.4.a,b,c Mixing of the components

- 6) Introducing the mixture into a vacuum chamber (MCP-001 Machine PLC) for degassing, where it stayed until most of the air bubbles are gone.
- 7) Casting the mixture in the box over the model. The model must be covered, so the mixture was casted onto with approximately 5 cm over the model (Figure 5.5 a,b).

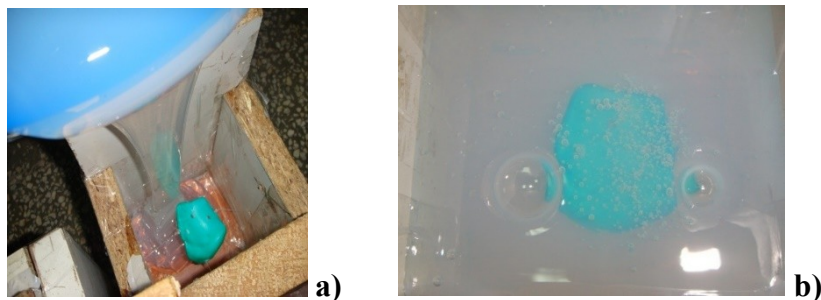


Figure 5. 5. a,b Casting the silicone over the model

- 8) As shown in Figure 5.6, during the casting have been formed many air bubbles. If these are located close to the model, may lead to deviations from its original shape of the master model and will influence the shape of the future implant too. Therefore,

This project has been funded with support from the European Commission. This publication [communication] reflects the views only of the authors, and the Commission cannot be held responsible for any use which may be made of the information contained therein.

the forming box with silicone rubber is inserted again into the vacuum chamber to remove air bubbles accumulated at casting proces, around the master model.



Figure 5.6. Removing the air bubbles from the mould

9) Further, the box containing silicone rubber mould, was introduced into a polymerization oven, where the solidification process of the silicone rubber block was occurred. The mould remained in the oven 2 hours, at 50° C temperature. Another possibility for polymerization is to let it at room temperature for 24h.

10) After full polymerization, the silicone rubber block was removed from the box. With the help of a cutter, following the separation plane between the two half moulds (which was made considering the complex shape of the part) the block was cut. This has been facilitated by the use of a transparent silicone rubber. By opening the silicone rubber mould, the master model was extracted (Figure 5.7 a,b,c,d).

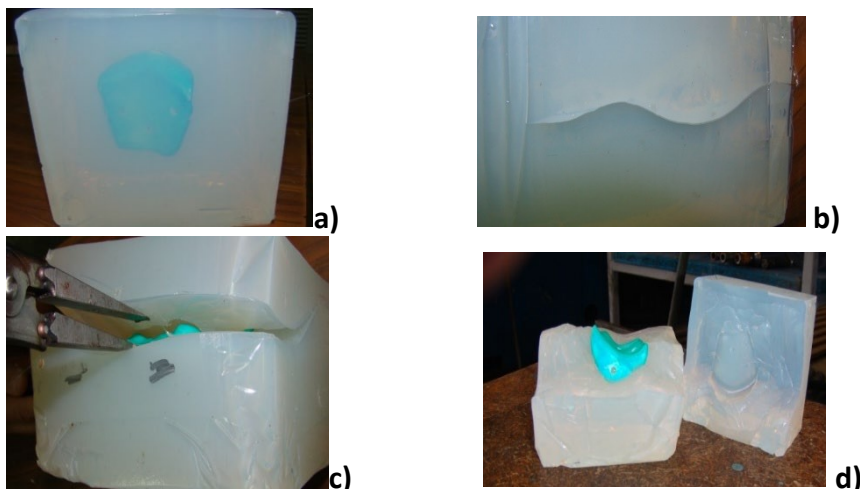


Figure 5.7. Silicone rubber mould

This project has been funded with support from the European Commission. This publication [communication] reflects the views only of the authors, and the Commission cannot be held responsible for any use which may be made of the information contained therein.

6 Realizing of the real implant made of PMMA material using silicone rubber moulds

The pattern of the implant was used to build a silicone rubber mould after the CT scan and 3D model were completed. PMMA-based radiopaque bone cement was placed into the silicone rubber mould and pushed into place. The final custom-made implant's margins were modestly and manually processed after unmoulding to remove any excess. To prevent the development of an epidural hematoma, holes were drilled into the plate's surface. Ethylene oxide was used to sterilize the plates.

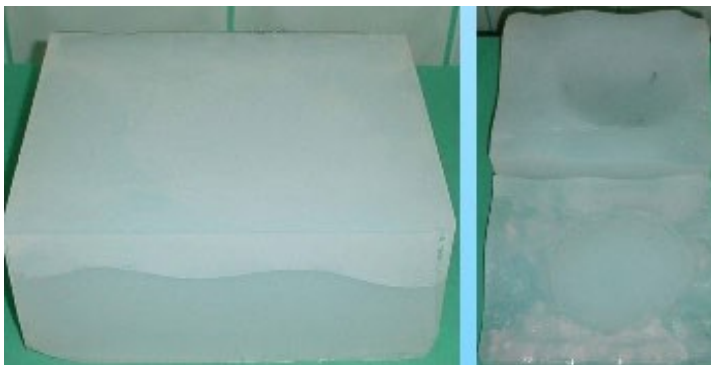


Figure 6.1. Silicone rubber mould in which the PMMA-based radiopaque bone cement was cast. The thickness of the mould's walls and the excess material appearing at one of the drain channels

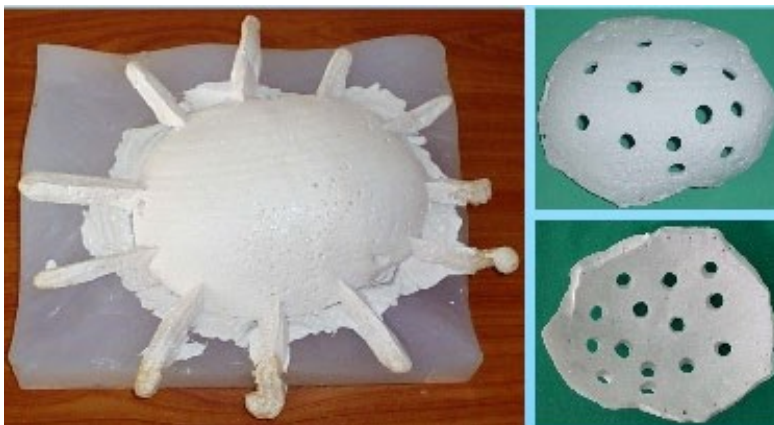


Figure 6.2. Custom made cranioplasty plate (before implantation).

This project has been funded with support from the European Commission. This publication [communication] reflects the views only of the authors, and the Commission cannot be held responsible for any use which may be made of the information contained therein.

The bone deficiency was disclosed, and custom-made implants were placed under the patient's general anaesthesia. To add stability, the plates were sutured to the defect's bony edges with 1-0 silk sutures. Additional CT scans of the patient were acquired postoperatively to assess the symmetry restored by the surgery. The calvaria, the roof of the neurocranium, and the cranial base make up the neurocranium, which is the covering of the brain. The frontal, parietal, and occipital bones make up the calvaria. The volume of the neurocranium (calvaria) was measured in this study. The rebuilt cranial volume was calculated from postoperative CT images using Xelis (INFINITT Healthcare, Seoul, Korea).

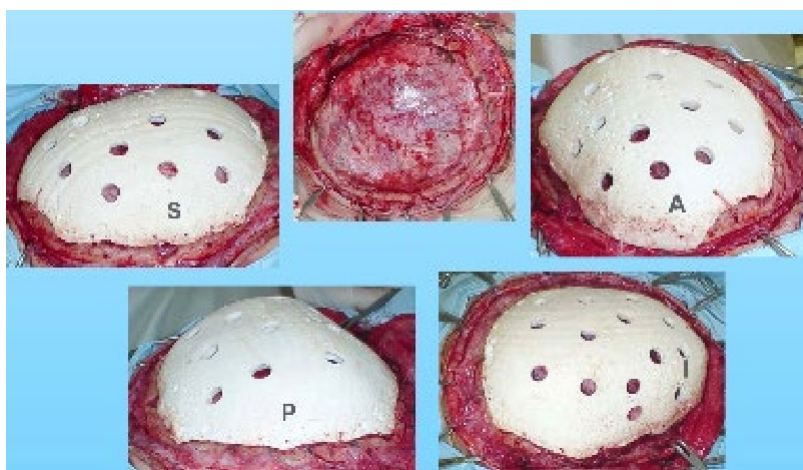


Figure 6.3. Intraoperative view (the plate is exactly positioned into the defect)

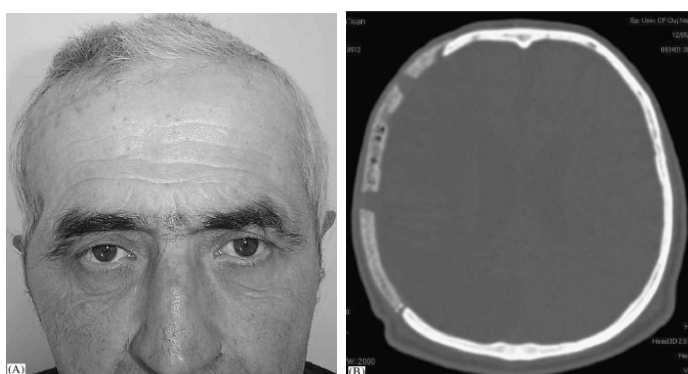


Figure 6.4. Postoperative aspect revealing the restored symmetry and (B) postoperative CT, note the perfect marginal adaptation of the reconstruction plate

This project has been funded with support from the European Commission. This publication [communication] reflects the views only of the authors, and the Commission cannot be held responsible for any use which may be made of the information contained therein.

7 Conclusions

To correct major skull deformities, either intra-operative vault reconstruction or a "custom manufactured cranial implant" might be chosen before surgery. Time, greater risk to the patient, insufficient protection from trauma and infection, and generally suboptimal cosmesis are among downsides of intra-operative repair. Custom-made cranioplasty implants, on the other hand, have the advantages of a shorter operative time, less invasive surgery, better cosmetic results, faster recovery, and lower expenses due to the shorter operative time.

Custom-made implants should be explored for cranioplasty because to the several advantages of custom-made implants, including reduced surgical times, no donor site morbidity, and enhanced cosmetic results.

RP techniques have been used to create custom-made implants in numerous cases. A silicone rubber mould was utilized in this procedure. Because of its fluidity, the silicone rubber enables for the retention of the plate's surface morphology and marginal features during the impression process. The implant's stability has enhanced thanks to the precision of the marginal replicas. The graft can be created accurately if the PMMA graft is allowed to polymerize in the bone defect. During the polymerization of PMMA, however, the temperature rises, causing damage to the critical structure nearby.

Finally, custom-made cranial implants created by 3D modelling, rapid prototyping, and additive manufacturing were particularly useful for fixing big deformities. There was a significant improvement in morphology and function. Infection, plate rejection, or major long-term consequences were not found. This approach could be used to repair bones at additional locations.

This project has been funded with support from the European Commission. This publication [communication] reflects the views only of the authors, and the Commission cannot be held responsible for any use which may be made of the information contained therein.

8 References

- [CAP16] Capulli A.K., Mac Queen L.A., Sheehy, S. P., Parker, K.K., Fibrous scaffolds for building hearts and heart parts, *Advanced Drug Delivery Reviews*, Vol. 96 (2016), pp. 83-102. <https://doi.org/10.1016/j.addr.2015.11.020>
- [PAC15] Păcurar, R. Păcurar, A. chapter “Applications of the Selective Laser Melting Technology in the Industrial and Medical Fields” , 26 pages, published in the book entitled „New Trends in 3D Printing”, edited by: dr. Igor V Shishkovsky, Open-access book, IN-Tech Publishing House, Rijeka, Croatia, 2016, ISBN 978-953-51-4668-1
- [ROT06] Rotaru H., Băciuț M., Stan H., Bran S., Chezan H., Iosif A., Tomescu M., Kim S.G., Rotaru A., Băciuț G., Silicone rubber mould cast polyethylmethacrylate-hydroxyapatite plate used for repairing a large skull defect, *Journal of Cranio-Maxillofacial Surgery*, Vol. 34 (2006), pp. 242-246. doi:10.1016/j.jcms.2006.01.005
- [ROT12] Rotaru H., Stan H., Florian I.S., Schumacher R., Park Y.T., Kim S.G., Chezan H., Balc N., Baciut M., Cranioplasty With Custom-Made Implants: Analyzing the Cases of 10 Patients, *Journal of oral and maxillofacial surgery: official journal of the American Association of Oral and Maxillofacial Surgeons*, Vol. 70 (2012), pp. 169–176. doi:10.1016/j.joms.2011.09.036
- [www 01] Multi Jet Fusion printing process - <https://www.materialise.com/it/manufacturing/tecnologie-di-stampa-3d/multi-jet-fusion>; accessing date: 20.05.2021.
- [www 02] CT (Computed Tomography) Scan - <https://my.clevelandclinic.org/health/diagnostics/4808-ct-computed-tomography-scan>; accessing date: 20.05.2021
- [www 03] How does a CT or CAT scan work? - <https://www.medicalnewstoday.com/articles/153201?c=73707002470>; accessing date: 20.05.2021
- [www 04] Computed Tomography (CT) - <https://hkhjoshua.wordpress.com/2014/10/17/new-post/>; accessing date: 20.05.2021

This project has been funded with support from the European Commission. This publication [communication] reflects the views only of the authors, and the Commission cannot be held responsible for any use which may be made of the information contained therein.

BRIGHT

Erasmus+ strategic partnership for Higher Education

**BOOSTING THE SCIENTIFIC EXCELLENCE AND
INNOVATION CAPACITY OF 3D PRINTING METHODS
IN PANDEMIC PERIOD**

TOOLKIT 2

**DESIGN AND SLM MANUFACTURING
OF CUSTOM FACIAL IMPLANT USED
TO RECONSTRUCT THE
SUPRAORBITAL MARGIN AND
ZYGOMATIC BONE**

Project Title	Boosting the scientific excellence and innovation capacity of 3D printing methods in pandemic period 2020-1-RO01-KA226-HE-095517
Output	IO2 – BRIGHT e-toolkit manual for digital learning in producing medical parts by 3D printing methods in the context of the pandemic
Toolkit	Toolkit 2 Design and SLM manufacturing of custom facial implant used to reconstruct the supraorbital margin and Zygomatic bone
Date of Delivery	November 2021
Authors	Cosmin COSMA, Petru BERCE, Nicolae Balc
Version	Final variant

Contents

1. Introduction	38
2. Theoretical background.....	39
2.1 Realizer 250 equipment and working principle.....	39
2.2 SLM Realizer 250 machine	40
2.3 Powders for SLM process.....	41
2.4 Conventional plates used in maxillofacial surgery.....	42
2.5 Frequent risk of fracture	43
3. Work methodology.....	44
3.1 CT reconstruction	44
3.2 Implant design	47
3.3 Pre-processing	50
3.4. Configure the SLM process parameters	53
3.5 SLM simulation	56
3.6 Estimation of production time and cost.....	57
3.7 SLM-manufacturing of implant.....	58

This project has been funded with support from the European Commission. This publication [communication] reflects the views only of the authors, and the Commission cannot be held responsible for any use which may be made of the information contained therein.

1. Introduction

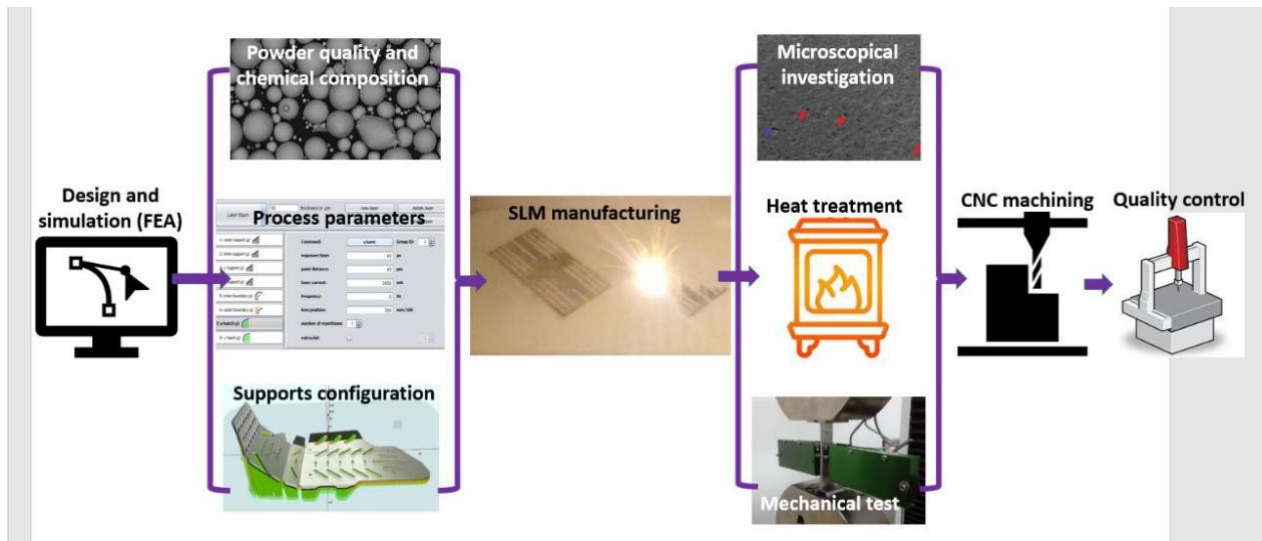
Over the last two decades, the concept of product customization has received increased attention from both academia and industry. Recent developments in digital fabrication technologies have made product personalization not only technically doable but also economically profitable [Pradel]. Selective laser melting (SLM) is capable to fabricate directly custom products. In healthcare, product customization is already an established practice using SLM technology. In this domain, cost considerations are less prominent and personalized components provide incomparable advantages. The basic component of SLM systems is the Nd:YAG laser, which emits continuous light in the infrared spectrum with a wavelength of 1064 nm. SLM process is capable to produce metallic parts with 99.9% relative density. Most of the SLM research were developed using the following powders as stainless steel, pure titanium, titanium alloy (Ti6Al4V), Co-Cr, and nickel (Inconel 625, Inconel 718) [Yap], [Lietaert], [Leordean], [Fateri]. The ongoing transition to digital manufacturing prompts new possibilities of SLM process. The main benefits of SLM parts include [Aniwa]:

- **It is possible to fabricate complex components** that would have to be broken down into several pieces with conventional methods (examples casting or CNC milling).
- Compared to CNC milling or turning, **SLM manufacturing produces less waste** as it only consumes the material needed for a certain part. Moreover, it is possible to re-use the unmelted powder.

In the last years, custom SLM implants were developed to treat total knee arthroplasty [Murr], chondrosarcoma localized in calcaneum [Imanishi], and maxillofacial reconstructions [Rotaru], [Parthasarathy], [Armencea]. The results of these pilot surgical interventions are acceptable, the SLM implants being integrated into the body without any signs of rejection and improving patients' health.

2. Theoretical background

SLM WORKFLOW



2.1 Realizer 250 equipment and working principle

Founded by Dr. Matthias Fockele, one of the two physicists that developed and patented the SLM (Figure 2.1), Realizer company was one of the leading producers of SLM machines. In 1999, the company delivered the world's first SLM machine for metals at the research centre in Karlsruhe [Realizer]. DMG Mori announced the acquisition of the majority Realizer stake (50.1%) in 2017 [Sher].

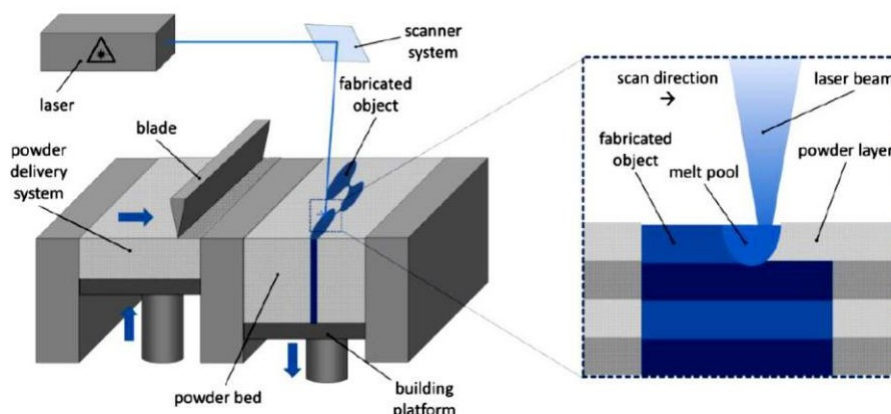


Fig. 2.1. Working principle of SLM. Source: www.realizer.com

This project has been funded with support from the European Commission. This publication [communication] reflects the views only of the authors, and the Commission cannot be held responsible for any use which may be made of the information contained therein.

2.2 SLM Realizer 250 machine

TUCN additive manufacturing lab buy in 2008 a SLM Realizer 250 machine (Germany). This SLM machine costs 0.5 mil. € and under slice-by-slice principle is capable to produce customized implants. The machine is equipped with a 200 W solid fiber laser (type Nd:YAG) and emits continuous light in the infrared spectrum with a wavelength of 1064 nm. The main technical characteristics are presented in Figure 2.2. Other technical data are as following: ± 0.10 mm dimensional accuracy, 50 μm common layer thickness, less than 0.5% internal porosity, always required supports, inert gas argon or nitrogen depends on powertype, heated platform up to 250°C, typical surface roughness Ra between 8 μm to 10 μm , and 100-1500 mm/s scanning speed.

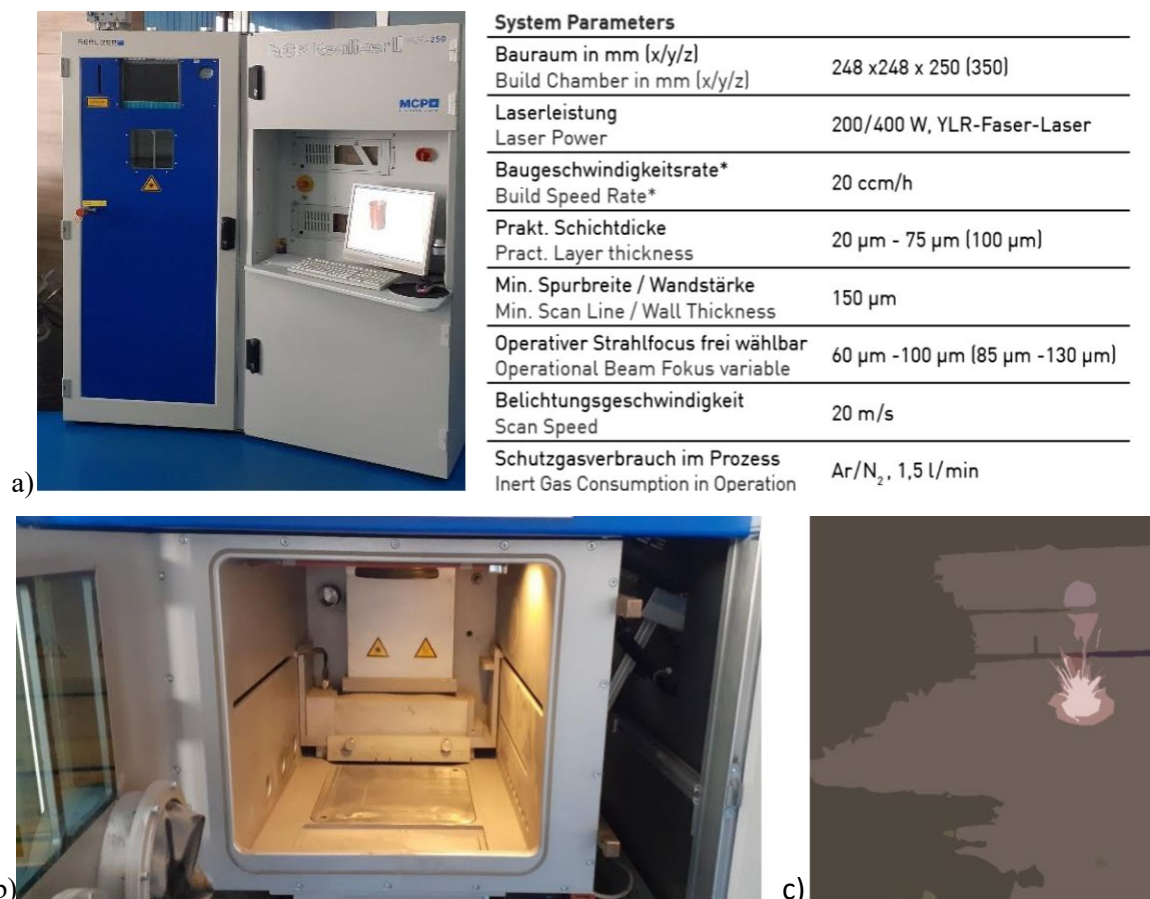


Fig. 2.2. SLM Realizer 250 machine: a) Technical data, b) Manufacturing chamber, c) Graphical animation of laser scanning

This project has been funded with support from the European Commission. This publication [communication] reflects the views only of the authors, and the Commission cannot be held responsible for any use which may be made of the information contained therein.

2.3 Powders for SLM process

Generally, this machine works with the following gas atomized powders as tool steel and stainless steel, pure titanium (Ti), titanium alloy (Ti6Al4V), Co-Cr, aluminum, and nickel (Inconel 625, 718). Information about particles shape and size are essential in controlling the SLM process. The shape of grains is spherical and have a diameter between 10 μm to 90 μm (Figure 2.3). The particle size distribution is described in percentiles, common is offer d90 value. This d-value indicate that 90% of particles are finer than this diameter according to laser diffraction result. It was observed that d90 value for normal SLM powder ranging from 20 μm to 60 μm . Moreover, the particle flowability can be measured using a hall flowmeter funnel with an orifice of 2.5 mm and is possible to calculate the flow rate (s/50g). The hall flow rate is expressed as the time required for a 50 g powder sample to be discharged by gravitational force through the flowmeter funnel (ASTM B213). Typical flow rate is between 15s to 40s per 50g of powder.

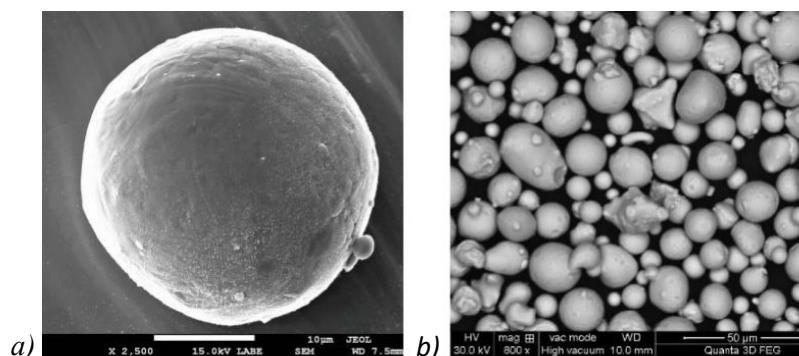


Fig. 2.3. SLM powders: a) Co-Cr alloy, b) pure Titanium

Some of the most representative powder makers are as follows: Bego, Carpenter Additive, CNPC Powder, Fehrmann Alloys, GE Additive, Höganäs, Metalpine, Mimete, Oerlikon Additive, Osaka Titanium Techn., Safina, Sandvik Osprey, and Scheftner Dental Alloys. The prices listed below are just indications for biocompatible powders.

Titanium Alloy TiAl6V4:	420 – 540 €/kg
Pure Titanium Grade 1 or 2:	360 – 480 €/kg
Stainless Steel 316L (1.4404):	70 – 110 €/kg
Cobalt Chromium Alloy (CoCrWMo):	240 – 370 €/kg

This project has been funded with support from the European Commission. This publication [communication] reflects the views only of the authors, and the Commission cannot be held responsible for any use which may be made of the information contained therein.

2.4 Conventional plates used in maxillofacial surgery

The technological evolution has greatly contributed to the modernization of the medical field, through the improvement of the quality of products as well as of the medical act [Cosma'2017]. This trend is triggered by an aging society, with a higher life expectancy. The implants or plates commercialized currently do not cover the multitude of medical cases that deal with individual osseous problems that appeared because of traumas, malformations, or osseous tumors. Figure 2.4 presents standard plates conventional manufactured used in maxillofacial surgery to treat simple fractures, being made of pure titanium Grade II.

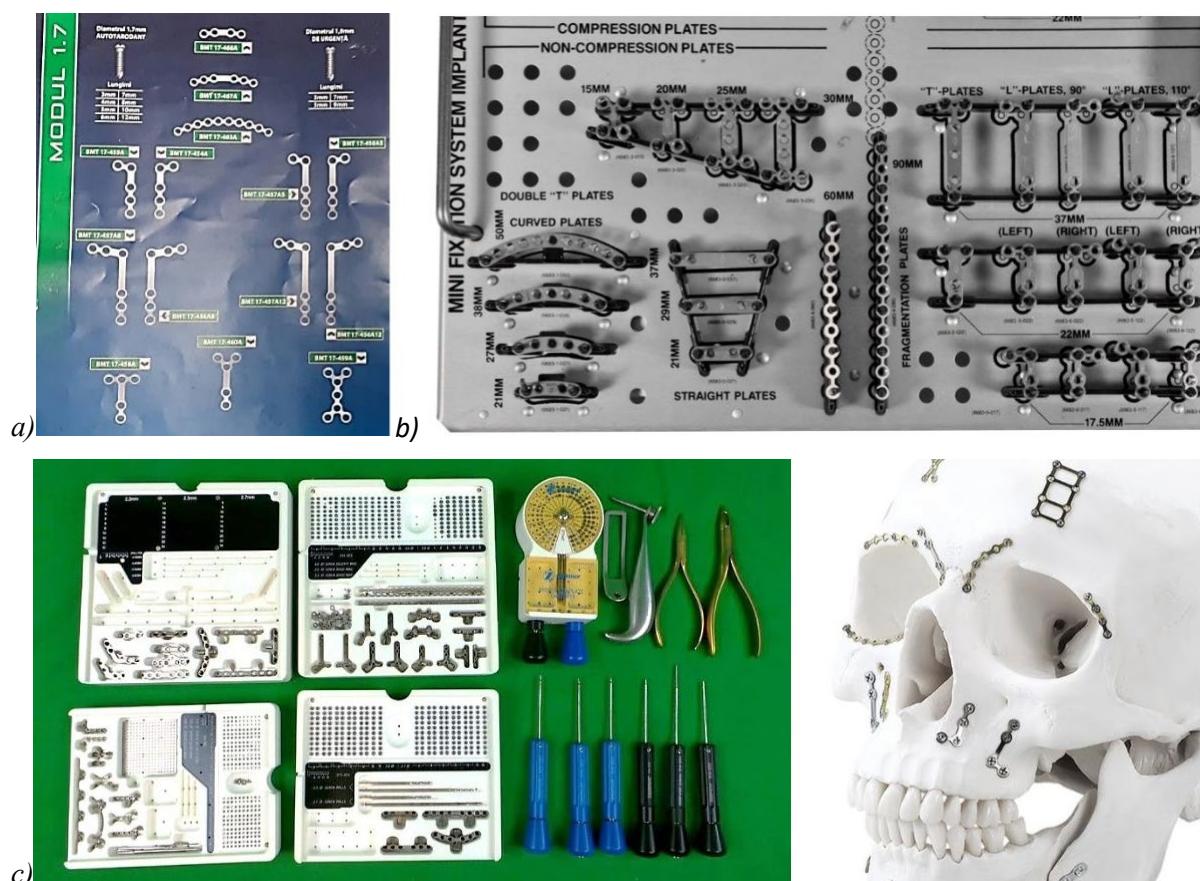


Fig. 2.4. Standard plates conventional manufactured used in maxillofacial surgery to treat fractures, being made of pure titanium, produced by: a) BioMicron Transilvania; b) Striker; c) Zimmer

This project has been funded with support from the European Commission. This publication [communication] reflects the views only of the authors, and the Commission cannot be held responsible for any use which may be made of the information contained therein.

2.5 Frequent risk of fracture

A recent report published by National Clinical Research Center for Oral Diseases (Shanghai, China) shows that the various fracture patterns depend on the mechanism and degree of the externally applied forces, with the usually reported causes including automobile traffic accidents (37%), work accidents (21%), bike accidents (19%), falls (13%), striking an object (7%) [Casole]. This 10-year retrospective study reveal that the most common fractured bones of facial were the zygomatic arch, nasal bone, orbital floor, zygomaticomaxillary area, and mandible bone [Casole]. The most affected patients have between 19 to 29 years old (28%) and between 30 to 39 years old (22%). In general, all the patients suffer also postinjury complications such as malocclusion, limited mouth opening, infraorbital nerve palsy, and blindness. The summary of this extended report is detailed in Figure 2.5.

Considering this report and others [Rotaru], [Parthasarathy], the present laboratory work is focused on a complex facial bone which is frequent fractured as zygomatic bone.

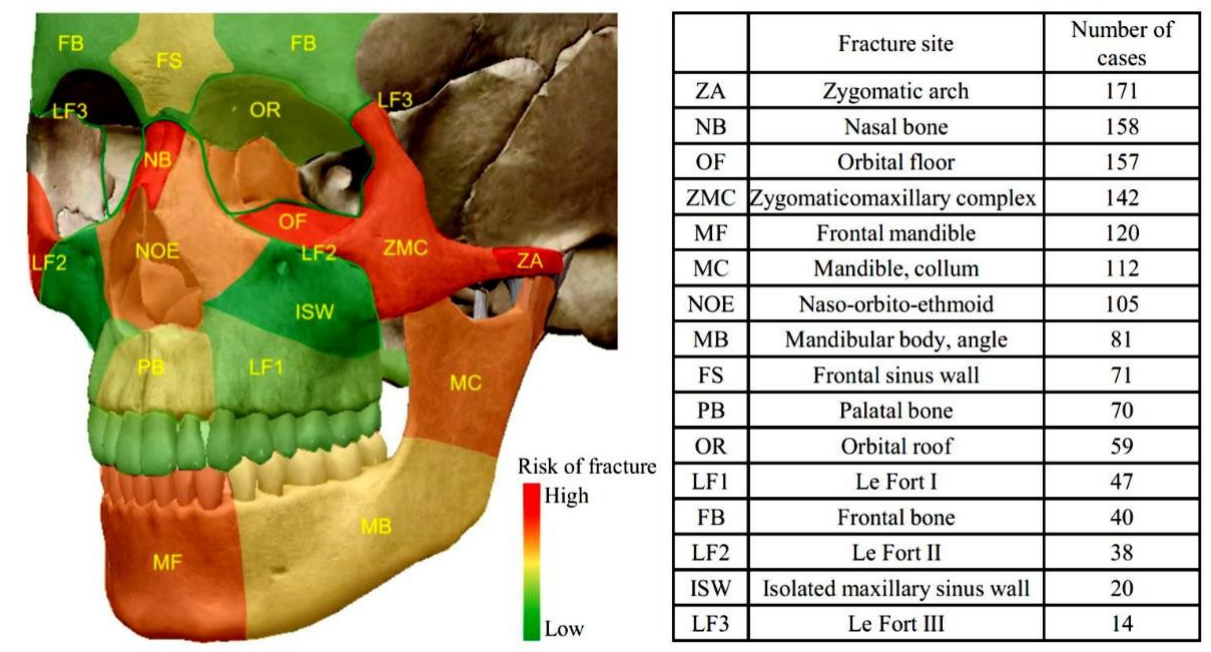


Fig.2.5 Facial skeleton showing the frequent risk of fracture [Casole]

This project has been funded with support from the European Commission. This publication [communication] reflects the views only of the authors, and the Commission cannot be held responsible for any use which may be made of the information contained therein.

3. Work methodology

3.1 CT reconstruction

To support the surgeons in complex reconstruction cases, various studies were developed, and the method of design-manufacturing was established. Using computer tomography (CT) images is it possible to design and fabricate directly customized anatomical implants using SLM process and biocompatible alloys. The customized implants are precisely adjusted to the implant area, eliminating the restrictions of shape, reducing the length of the surgical intervention through preparatory simulations, and they can have physical-mechanical features like those manufactured through conventional technologies [Rotaru], [Parthasarathy]. All these aspects lead to the diminishment of the chances of infection or rejection by the body, as well as to the more rapid recovery of the patient.

InVesalius is public health software that performs analysis and segmentation of virtual anatomical models, enabling the creation of physical models with the aid of additive manufacturing [InVesalius]. From 2D images obtained through CT, the program allows to create 3D anatomical representations of bones (Figure 3.1). It was named in honor of the Belgian dr. Andreas Vesalius (1514-1564), widely considered the father of modern anatomy. This software was developed by Center for Information Technology Center Renato Archer. The use of visualization technologies and 3D analysis of CT images, when combined with additive manufacturing, can assist the surgeon in diagnosing, surgical planning, and simulation of complex bone defects.



Figure 3.1. InVesalius software

This project has been funded with support from the European Commission. This publication [communication] reflects the views only of the authors, and the Commission cannot be held responsible for any use which may be made of the information contained therein.

The present laboratory work is focused on a complex facial bone which is frequent fractured as zygomatic bone. Figure 3.2 details the anatomy of skull (anterior view), marking with red squares the targeted facial bones as frontal zygomatic bone, orbital surface of zygomatic bone, and supraorbital margin.

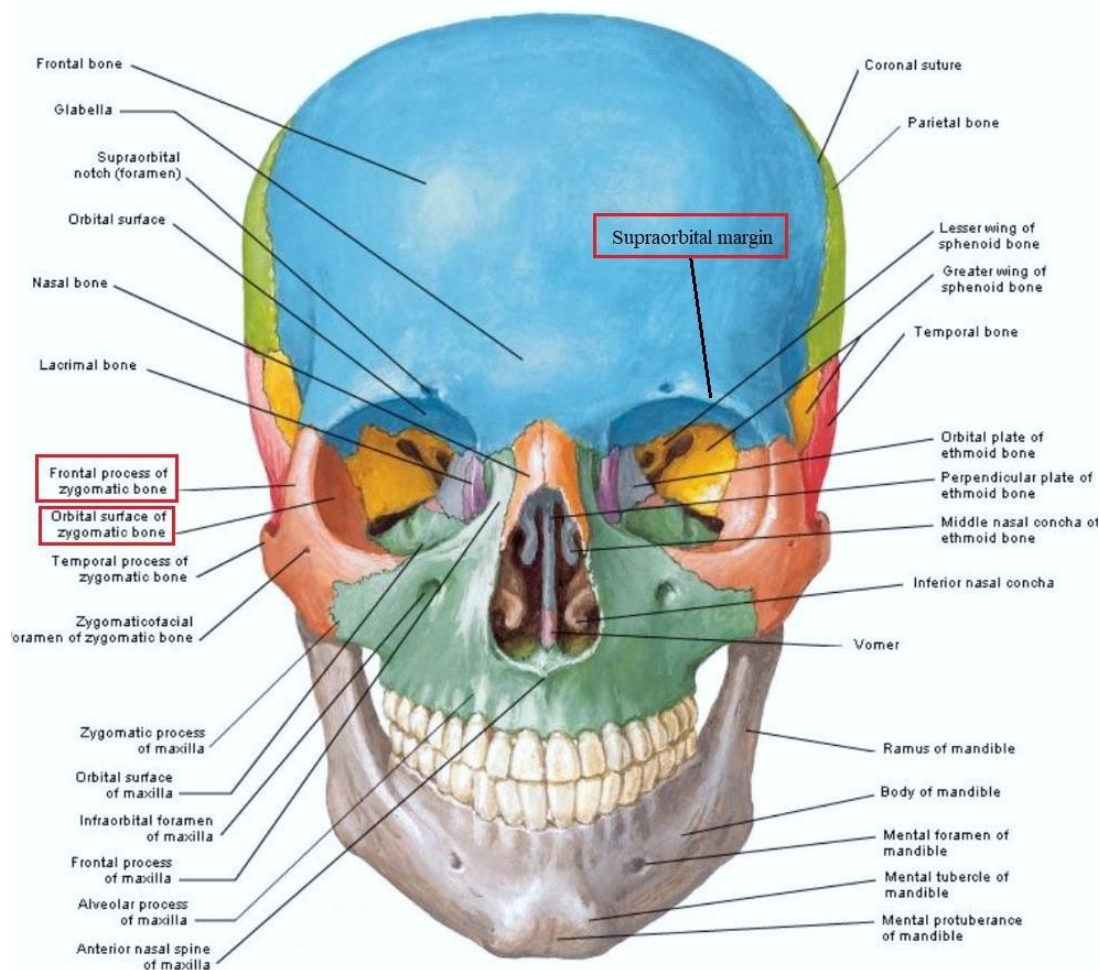


Fig. 3.2. Anatomy of facial bones [Chung]

In this work, we used CT images of a 69-year-old female who volunteered for us to reconstruct 3D models. The CT images were taken with a Promax scanner (Planmeca, Finland). The following scan parameters were used: 88 kV, 7 mA, 0.2 mm layer thickness, 400 slices, and 12 s exposure time. Using the CT images, the surgeons could establish the diagnosis and

This project has been funded with support from the European Commission. This publication [communication] reflects the views only of the authors, and the Commission cannot be held responsible for any use which may be made of the information contained therein.

suggest a treatment method [Armencea]. The DICOM images were imported in InVesalius software for medical data processing and adjustments (Figure 3.3 and Figure 3.4).

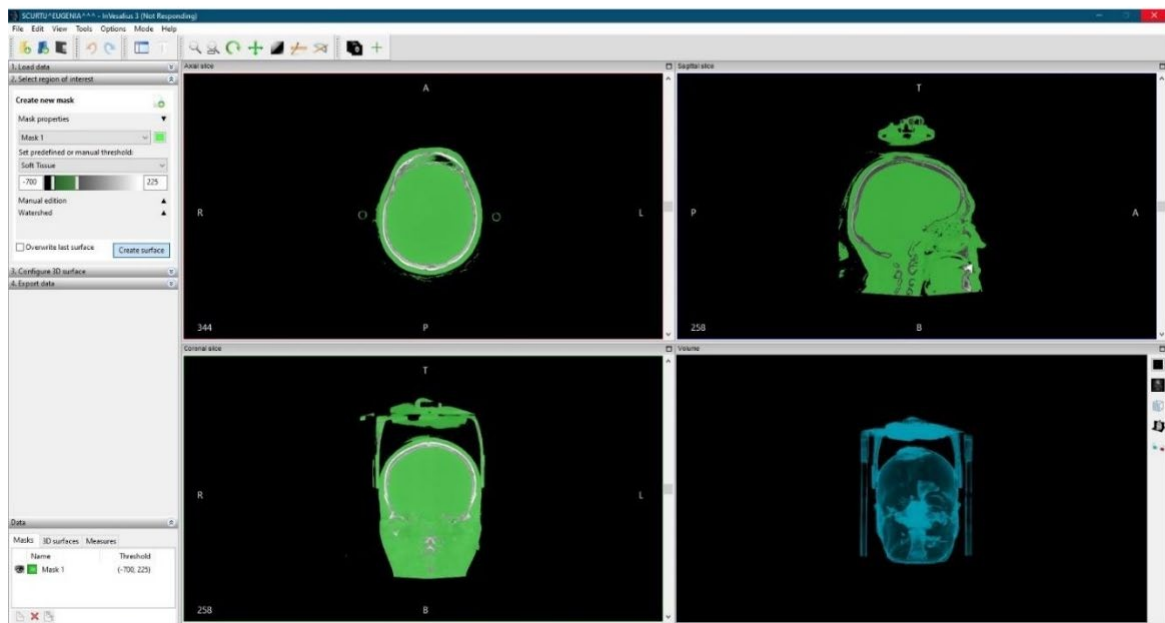
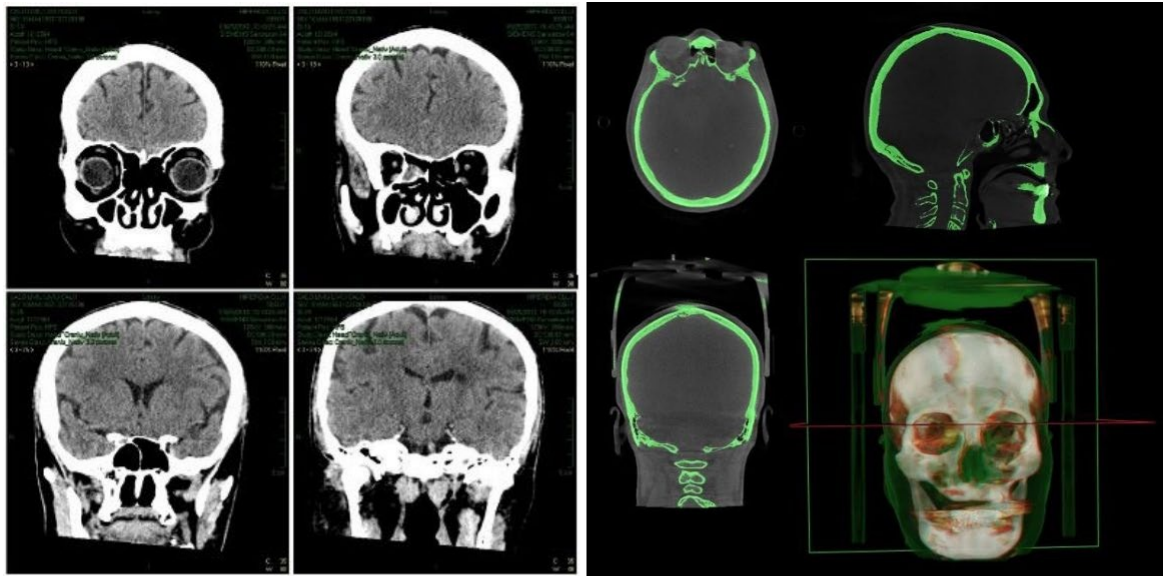


Fig. 3.3. CT reconstruction of patient facial bones

This project has been funded with support from the European Commission. This publication [communication] reflects the views only of the authors, and the Commission cannot be held responsible for any use which may be made of the information contained therein.

Figure 3.4 is showing the virtual reconstruction of facial bones and soft tissues (skin), where the defect area is marked with red color. Steps undertaken were threshold segmentation, surface generation and .STL exportation of virtual bone.

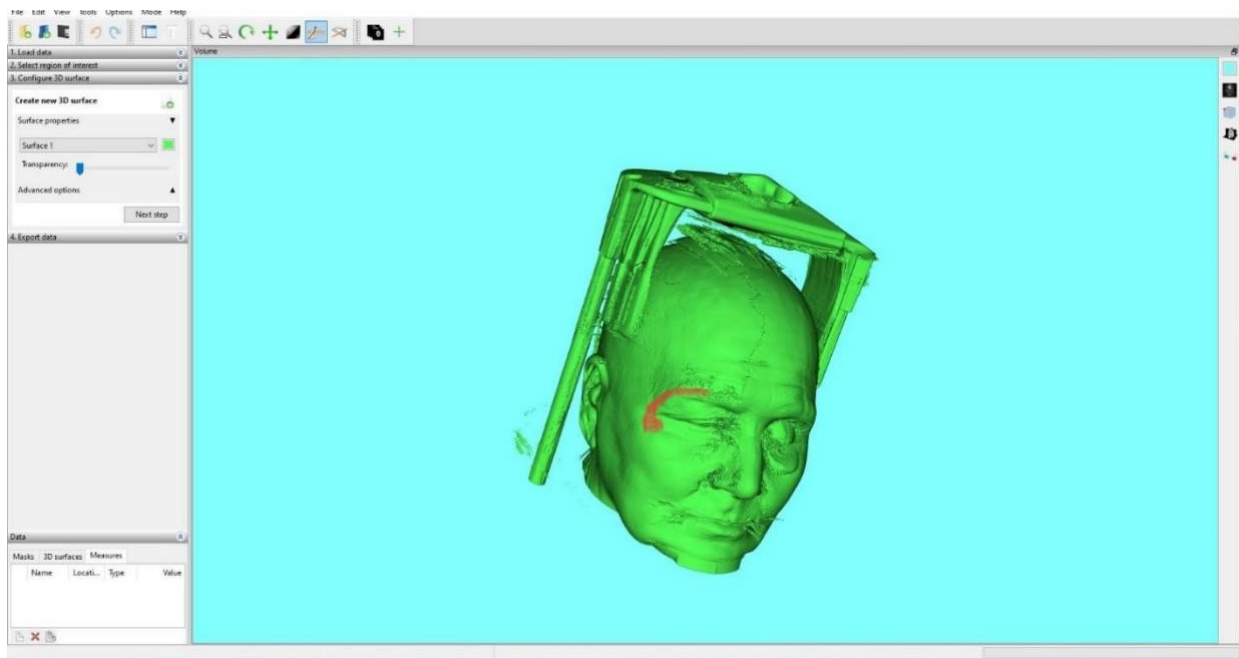


Fig. 3.4. Virtual reconstruction of facial bones and soft tissues (skin); The defect area is marked with red color, location supraorbital margin and frontal zygomatic bone

3.2 Implant design

During the digitization and processing of CT images, we obtained the 3D mask of the targeted facial bones which were exported in STL format. Figure 3.5 shows the virtual model of supraorbital margin and frontal zygomatic bone. This virtual reconstruction of custom implant can be used to treat a large bone defect located in supraorbital margin, frontalzygomatic bone, and its orbital surface. If the targeted area is destroyed, the initial model of implant should be created using mirror function (see Ref. [Armencea'2019]). This initial version of implant will be used as master model. To fix and repair all the errors from the virtual model (.STL file), Autodesk Meshmixer software was used. This free software is a prototype design tool based on high-resolution dynamic triangle meshes.

This project has been funded with support from the European Commission. This publication [communication] reflects the views only of the authors, and the Commission cannot be held responsible for any use which may be made of the information contained therein.

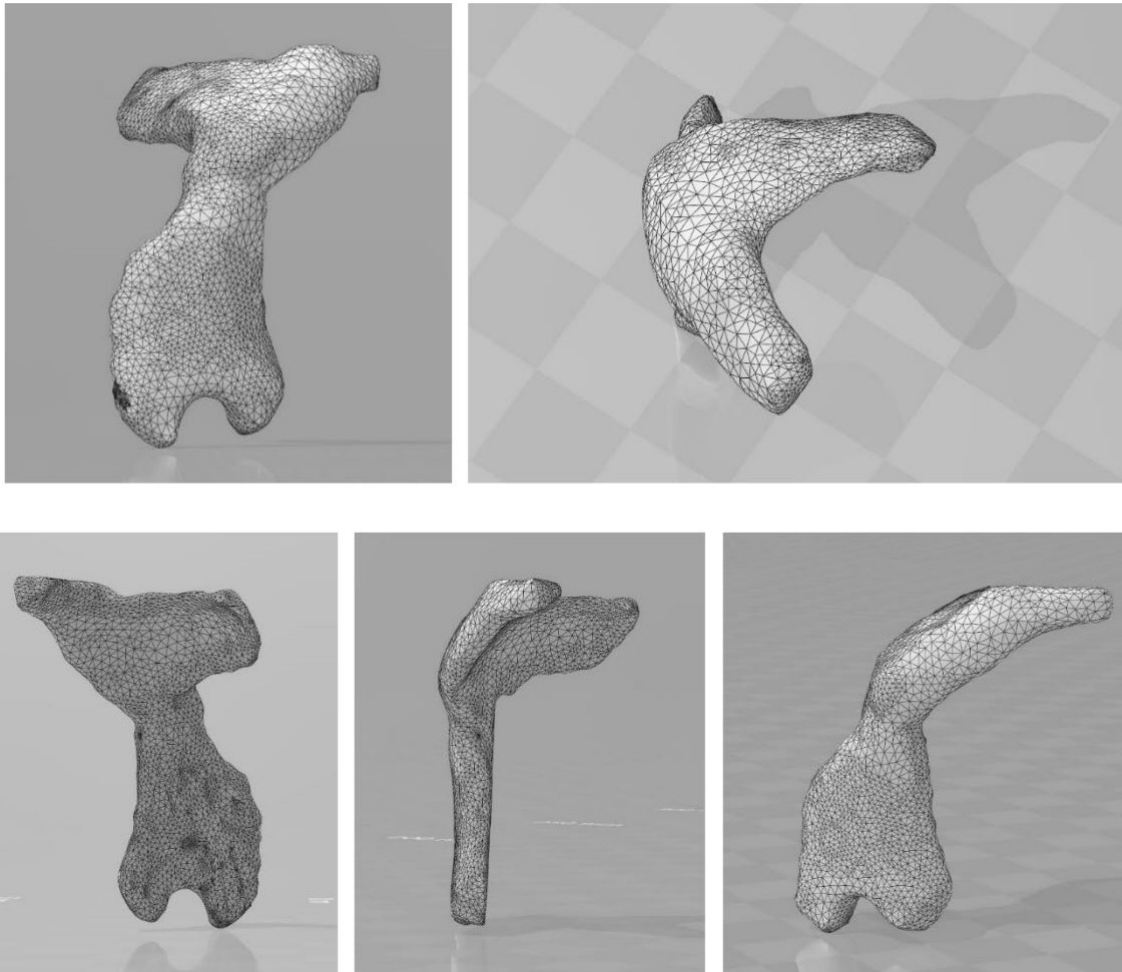


Fig. 3.5 Initial version of facial implant (master model)

After the implant model was clean off surface errors and defects, the model was imported in SolidWork software. Here, the implant was prepared considering two directions as following weight reduction and fixation zones. For weight reduction of implant, 32 holes with 1.1 mm diameter were used to perforate the orbital surface of zygomatic area (see Figure 3.6). For fixing the implant, 2 holes with 2.6 mm diameter were created. Taken into consideration the mechanical properties of Ti processed by SLM, advanced topological optimization and reduction of weight can be applied on this implant using finite element analysis simulations. In this way, the design of custom implant can be optimized under SolidWorks Simulations or ANSYS analysis.

This project has been funded with support from the European Commission. This publication [communication] reflects the views only of the authors, and the Commission cannot be held responsible for any use which may be made of the information contained therein.



Fig. 3.6. Creating 2 fixing holes with 2.6 mm diameter and perforate the orbital surface of zygomatic bone with 32 holes with 1.1 mm diameter

To improve the fixation of implant, we added a superior fixing area. Figure 3.7 presents the final design of implant. The final design of Ti implant has 2.13 cm³ and 9.64 g (Figure 3.8). If is necessary, repair all the geometrical defects from STL file such as: connecting unmatched edges, closing holes, aligning triangular normal, resolving overlapping areas. After we accomplished these steps, the edges of implant surface were smoothed in Meshmixer software.

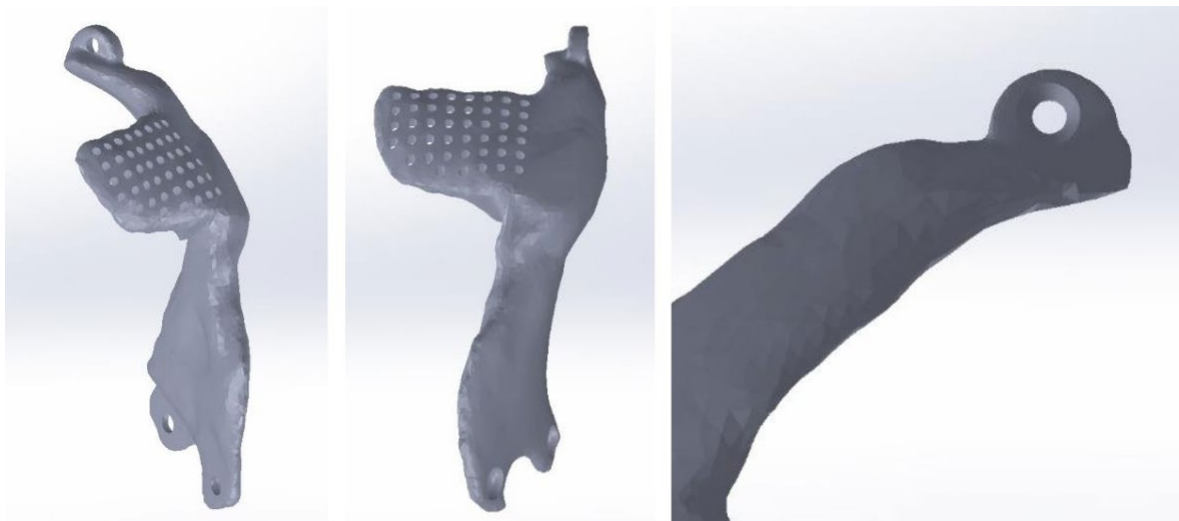


Fig. 3.7. Final design of implant after a fixing area was added superior; In total are 3 holes for fixing the implant with screw bones

This project has been funded with support from the European Commission. This publication [communication] reflects the views only of the authors, and the Commission cannot be held responsible for any use which may be made of the information contained therein.

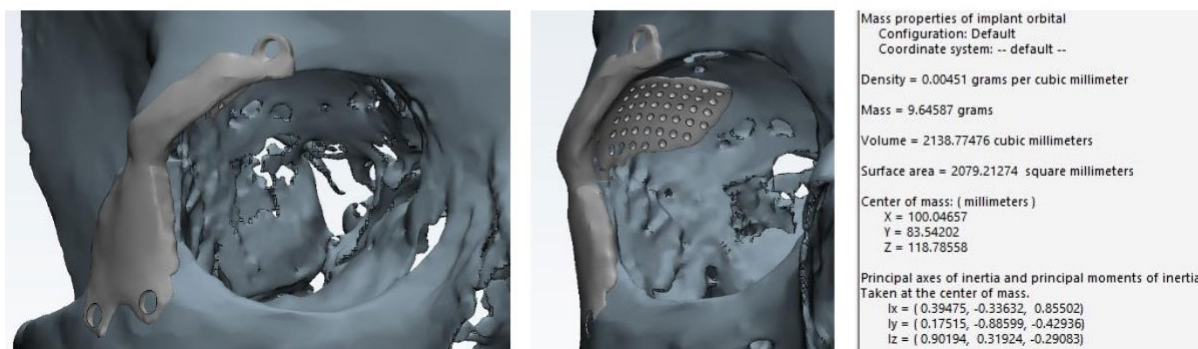


Fig. 3.8. Final design of Ti implant, weight 9.64 g, volume 2.13 cm³

The designed implant should fit perfectly to the orbit's topographic characteristics. This process enables the precise reconstruction of the defects, even when there are significant parietal fractures on both sides of the head [Avinent]. Particular focus was placed on orbit complicated geometry.

3.3 Pre-processing

To fabricate the implant, we will use pure Ti powder which corresponds to standard Ti Grade 1, having a purity of 99.5%. Identify and note the powder cost and the main physical-mechanical properties in Table 1. The Ti powder should have spherical granules with proper diameter for SLM printing and high biocompatibility.

Table 1. Physical-mechanical properties of Ti implants SLM-manufactured

Commercial name	Yield Tensile strength (MPa)	Ultimate Tensile strength (MPa)	Elongation or Strain (%)	Young Modulus (GPa)	Density [g/cm ³]	Hardness [HRC or HB]	Powder diameter [µm]	Supplier

Angled surfaces more than 45° are possible to be built without supports structures according to multiples experimental studies [Cosma'2019] and German Standard VDI 3405 [VDI]. A self-supporting angle describes the feature's angle relative to the build

This project has been funded with support from the European Commission. This publication [communication] reflects the views only of the authors, and the Commission cannot be held responsible for any use which may be made of the information contained therein.

platform (XY plane). A sketch of this principal is illustrated in Figure 15 where is presented a cross-section of a profile which has different δ angles between the surfaces and the SLM plate. This sketch demonstrates the importance of building orientation on SLM plate and how we can improve the design of parts.

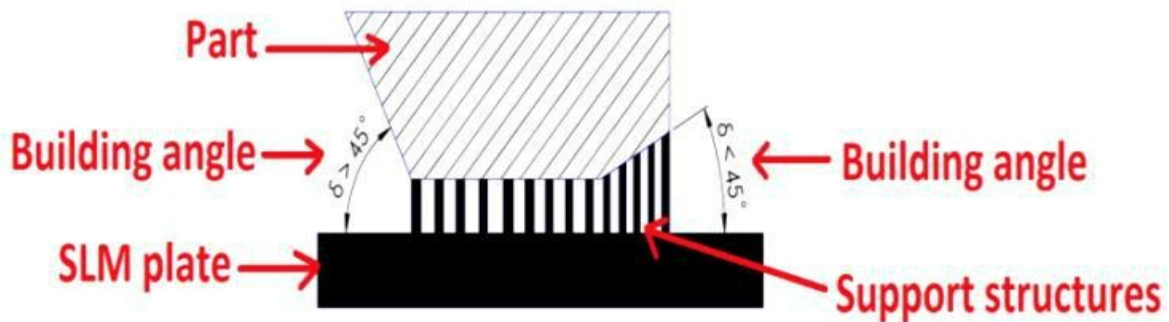


Fig. 3.9. Support structures needed to anchor surfaces. Surfaces with angles higher than 45° are possible to fabricate without supports [Cosma'2019]

Now, you should establish the best building orientation of implant to have a reduced production time. Use RDesigner software from Realizer machine and an example is listed in Figure 3.10. For easily removing the supports, the distance between the implant and the build platform should be 3 mm. The part orientation is a critical aspect, and it should be adapted/optimized for each model according to user needs (example: reduced build time, low surface roughness, or high mechanical resistance on a specified direction).

Also configure the proper support structures to anchor the model. Support structures are required to sustain the next layer built upon, to anchor the part on the build plate and to prevent the warping effect. RDesigner offer the possibility to model a new type of them called "lattice supports". The lattice pattern can be configured in different ways, modifying the unit cell between 0.5 mm to 2.5 mm. This type of lattice support is illustrated in Figure 3.10.

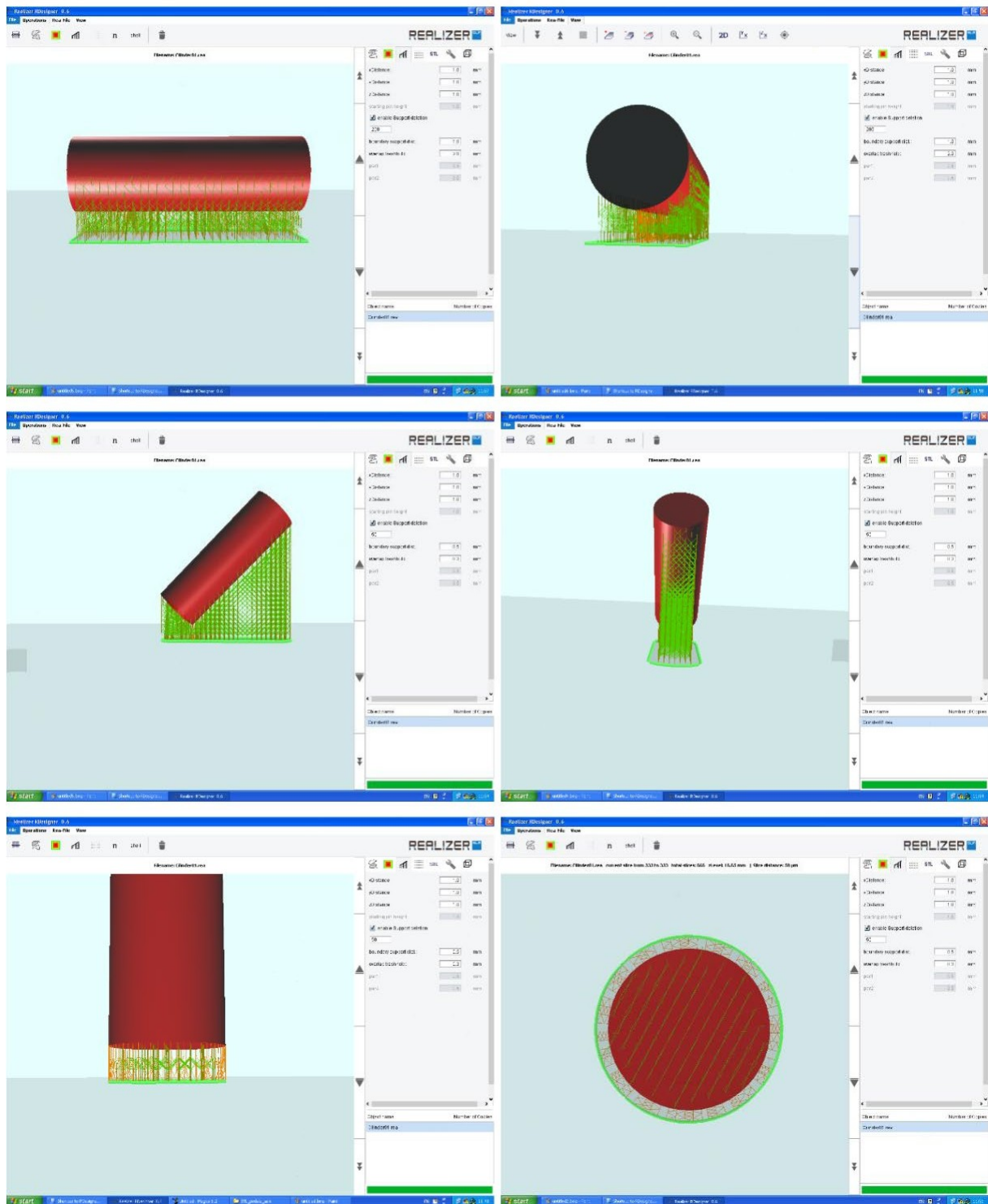


Fig. 3.10. Different building orientations of implant and its support structures, RDesigner software: Horizontal, angled at 45°, and vertical

This project has been funded with support from the European Commission. This publication [communication] reflects the views only of the authors, and the Commission cannot be held responsible for any use which may be made of the information contained therein.

Figure 3.11 shows the optimal building orientation of implant on SLM platform, and its support structures generated. The lattice unit of support structure was setup at $x=y=z=1.0$ mm. These steps were elaborated in RDesigner software.

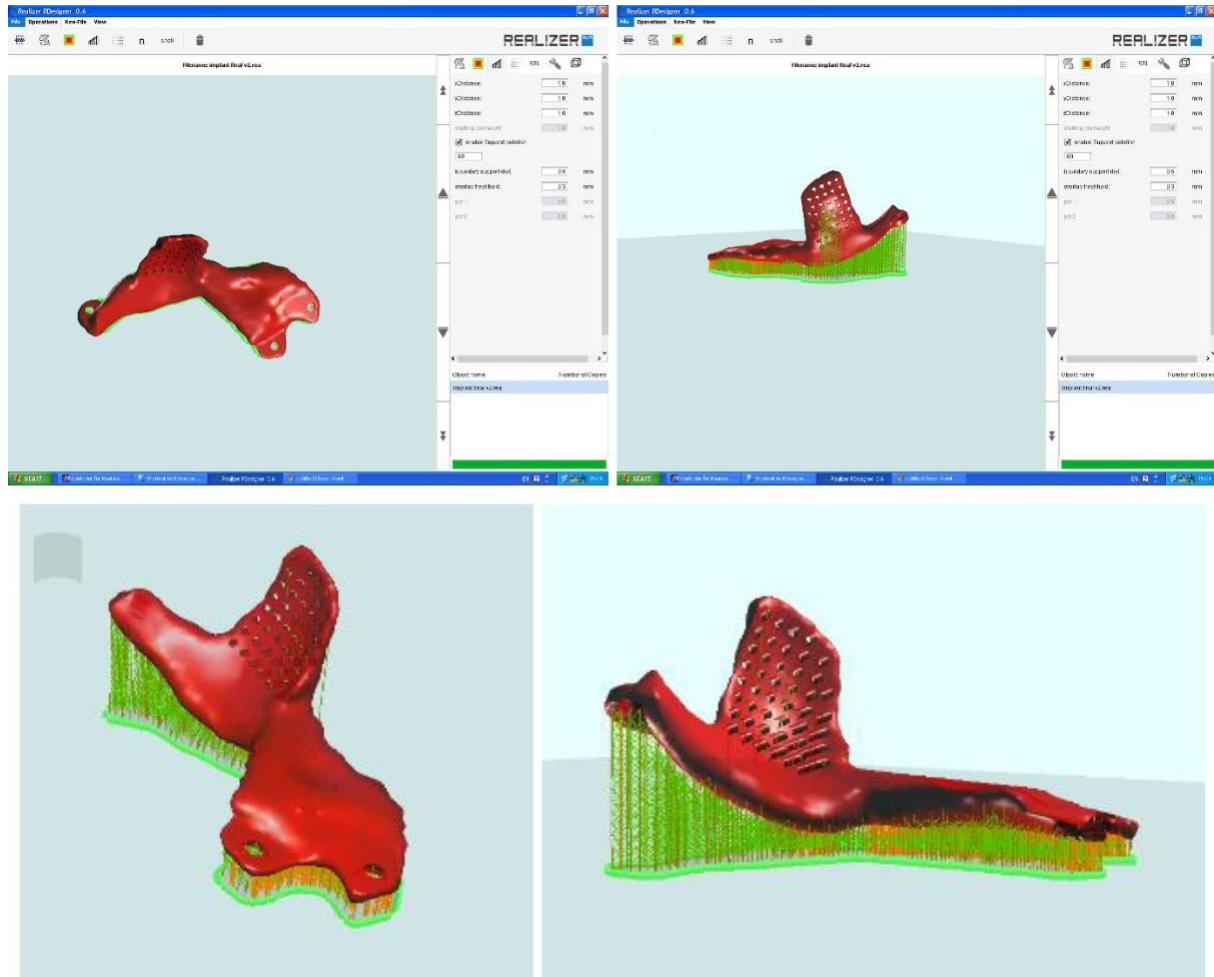


Fig. 3.11. Optimal building orientation of implant on SLM platform and its support structures generated; Lattice unit of support structure $x=y=z=1.0$ mm

3.4. Configure the SLM process parameters

Setup the thickness of a layer powder (typically $50 \mu\text{m}$) and slice the model. By default, RDesigner saves build jobs in its own REA material file. In addition to the slice data and generated build paths for laser tracks, this REA file contains all the SLM process parameters (laser power, scanning speed, hatch distance, etc.). To configure the SLM process parameters,

This project has been funded with support from the European Commission. This publication [communication] reflects the views only of the authors, and the Commission cannot be held responsible for any use which may be made of the information contained therein.

REditor software is used. This software tool is useful to optimize the SLM parameters, to define the scanning strategy, to organize the laser scanning steps (e.g., first scan the Outer- boundary, after scan the hatch area, and in the end the inner-boundary). An example is shown in Figure 3.12 where different functions are included as following: Outer-boundary, Inner- boundary, Hatch in X and Y direction. Beside these functions, the parameters for lattice support structures can be configured in the following function: X and Y Support (see Figure 3.12). Each function should be configured, and the main parameters can vary between:

- Laser power (10-200 W), expressed in mA where 5000 mA = 200 W;
- Scanning speed (100-2000 mm/s), expressed by Exposure Time and Point Distance;
Example: Scanning speed 357 mm/s with Exposure Time 140 μ s and Point Distance 50 μ m (see Figure 3.12).

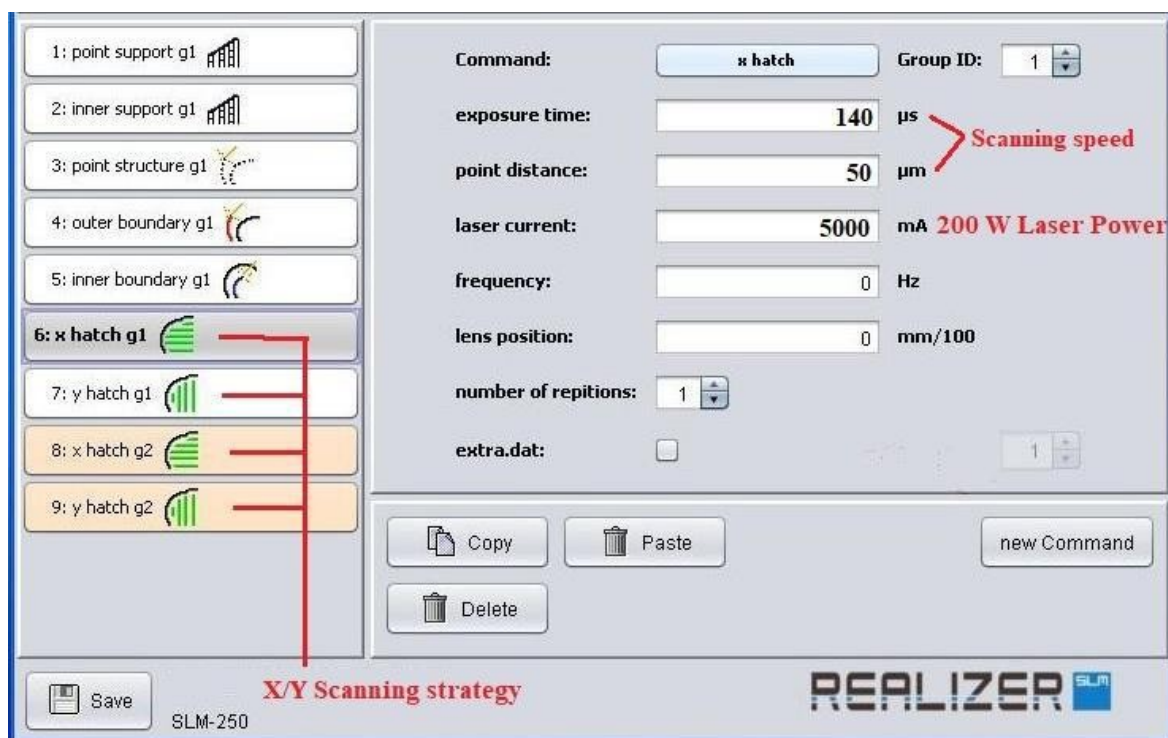


Fig. 3.12. Configure the SLM process parameters in REditor software

Moreover, the laser scanning strategy is another important aspect. Usually, we used an alternating X/Y strategy which allows a scanning in X direction of “n” layer and in Y direction of “n + 1” layer (rotating each hatch scan 90°) [Cosma’2020]. An example is shown in Figure 3.13. The advantage of this hatch pattern is that it can contribute to a high build rate compared with stripe hatch or chessboard pattern. On the other side, this scanning strategy can cause a rise of residual stress phenomena compared to the chessboard hatch pattern, and a special attention must be given to process parameters.

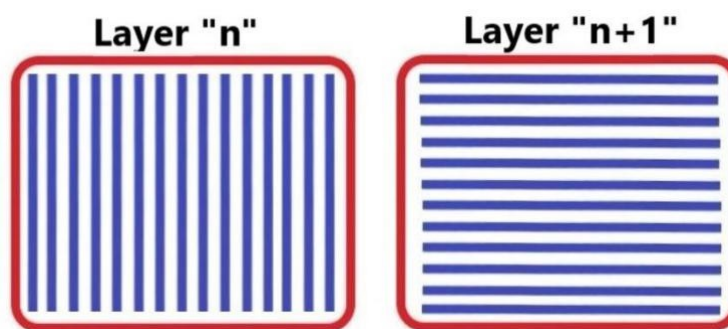


Fig. 3.13. X/Y alternating laser scanning strategies; Laser functions used to scan the part: Outer-boundary – Red, Hatch area – Blue [Cosma’2020]

To summarize this step, the main SLM parameters for Ti implant will be:

- Slice thickness 50 μm , resulting 466 slices;
- Scanning strategy X/Y;
- Hatch area 120 laser power and 357 scanning speed;
- Outer-boundary area 120 laser power and 500 mm/s scanning speed;
- Inner-boundary area 120 laser power and 500 mm/s scanning speed;
- Support structures 120 laser power and 750 mm/s scanning speed.

These SLM parameters were tested previously and conduct to a stable processability without technological defects.

3.5 SLM simulation

Since the cost of SLM fabrication is high, simulations are often used to predict the behavior of the part during processing. Using created REA file of the SLM job, manufacturing simulation can be elaborated. Figure 3.14 shows a simulation of SLM manufacturing in RDesigner at different slices.

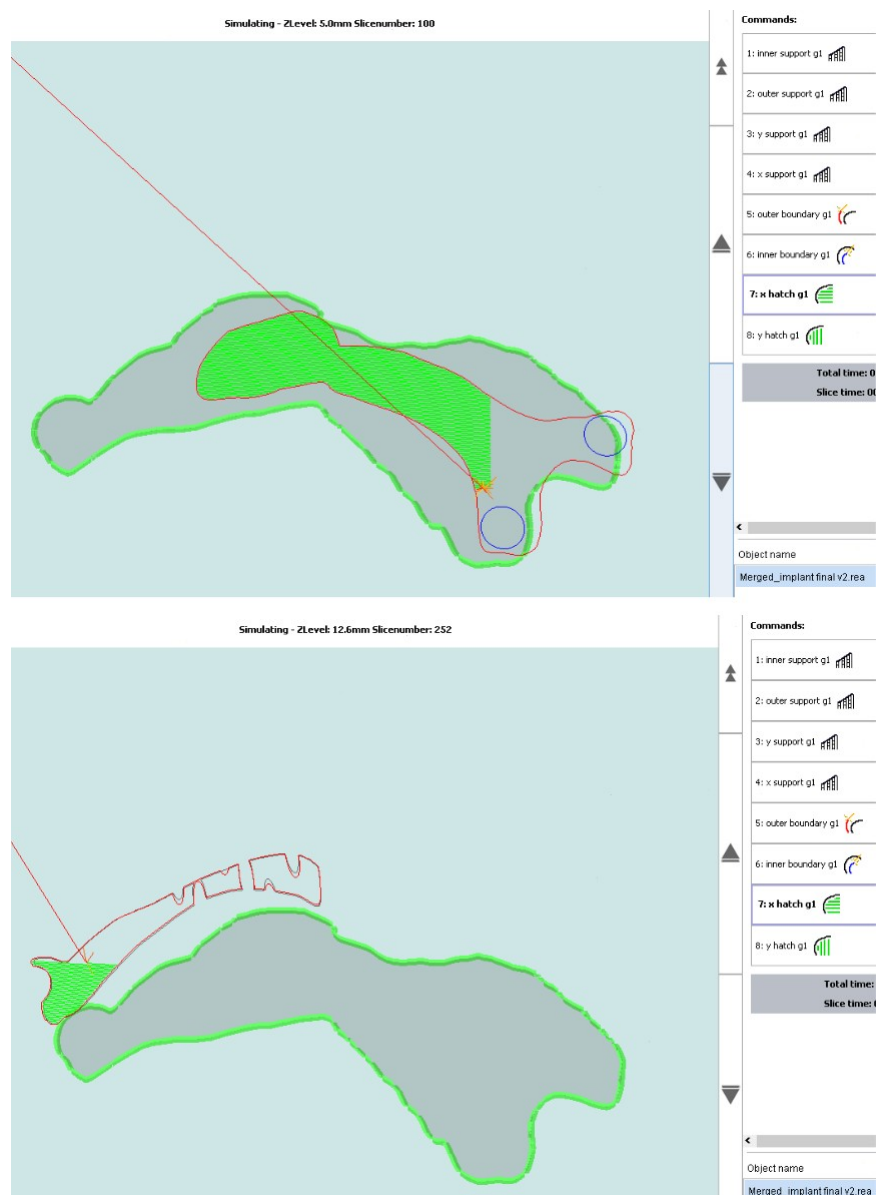


Fig. 3.14. SLM simulations at 100 and 252 slices

This project has been funded with support from the European Commission. This publication [communication] reflects the views only of the authors, and the Commission cannot be held responsible for any use which may be made of the information contained therein.

Figure 3.15 shows a zoom capture of SLM simulation at slice 100 and 101 respectively. Here it can be seen the effect of X/Y laser scanning strategy. At layer 100, the laser scans the section in X direction, and the next layer is scanned in Y direction.

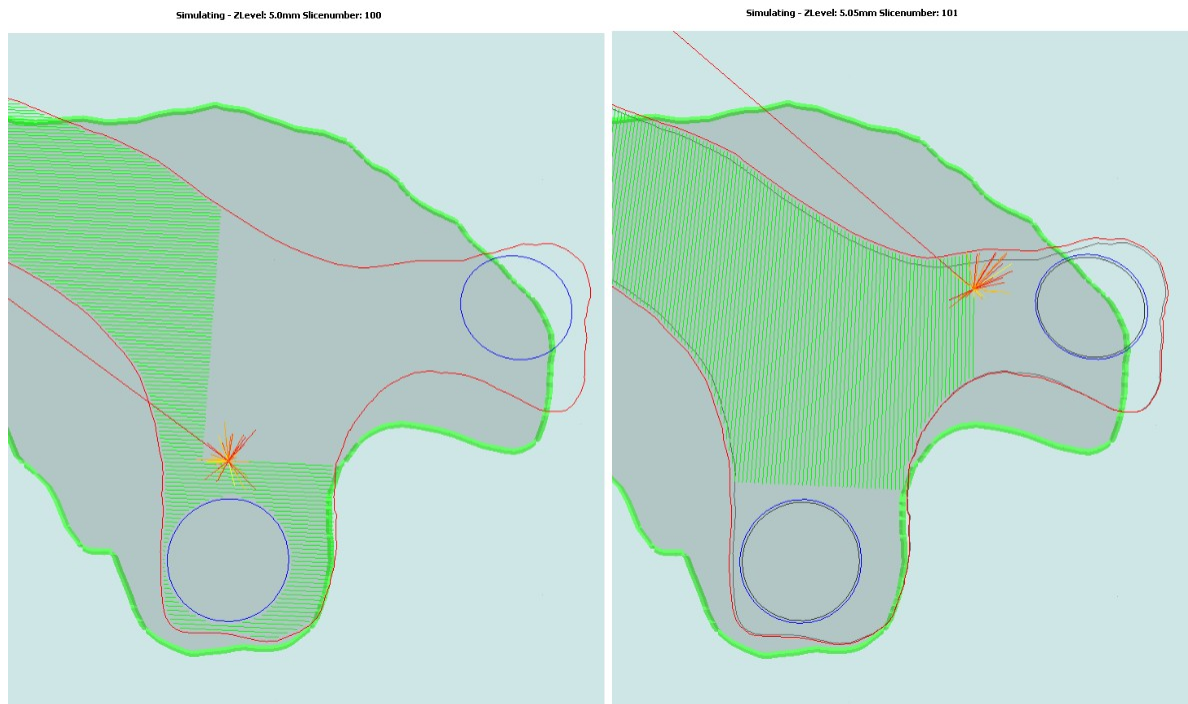


Fig. 3.15. SLM simulations at 100 and 101 slices

3.6 Estimation of production time and cost

Figure 3.16 shows an estimation of manufacturing costs using RCalculator tool. Importing the REA file with all the SLM parameters and implant slices, this app calculates the production cost (448 €) and time to fabricate it (6.36 h). Regarding the production costs, they vary between 50 € to 80 € per hour being influenced by multiple factors as material, part complexity, etc. Post-processing procedures will add supplementary fees for stress relief treatment, support removal, finish/polishing, CNC machining, and surface treatments.

This project has been funded with support from the European Commission. This publication [communication] reflects the views only of the authors, and the Commission cannot be held responsible for any use which may be made of the information contained therein.

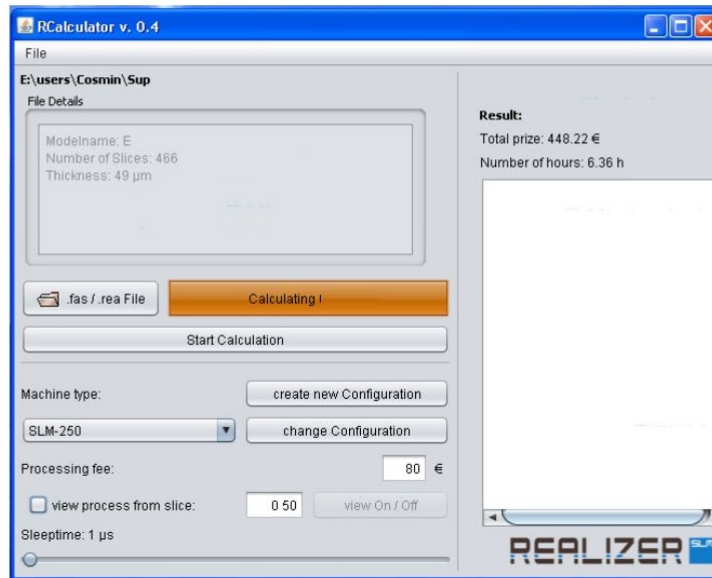


Fig. 3.16. Production cost and time to manufacture the designed Ti implant, RCalculator software

3.7 SLM-manufacturing of implant

Figure 3.17a shows how the Realizer machine is prepared, more exactly the base plate is calibrated to reference level. The platform should be brought in the right Z-height. This height can be controlled with a spatula. The steps are:

1. Raise platform by 0.10 mm and drive the recoater to the front and to the back.
2. Repeat till you can see the complete platform through the powder bed.
3. Press “Set Zero” for the elevator in Motors page to determine the actual position of the platform as zero position (Figure 3.18 b).

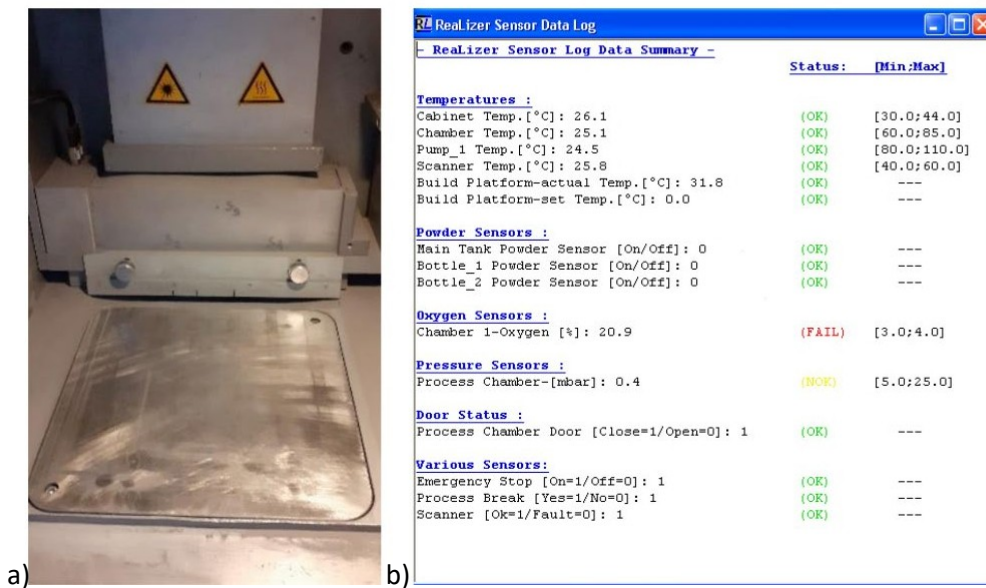


Fig. 3.17. a) Preparing the SLM base plate at reference level; b) Control all the machine sensor

To start the Realizer 250 machine, the following routine steps should be done in Realizer software [MCP]:

1. Control all the data from sensors (see Figure 3.17b) and clean the cover of the F-Theta lens with glasses wipes.
2. Close the build chamber and start flooding routine by pressing “Flood ON” in Motors page (Figure 3.18 b).
3. Turn the heating on if desired.
4. When the machine has reached an oxygen value lower than 1% (Figure 3.18 a) turn off the flooding routine by pressing “Flood OFF” in Motors page (Figure 3.18 b).
5. Turn on the gas pump by pressing “Gas pump on” (Figure 3.18 b) till you have reached an oxygen value of 0.2% (Figure 3.18 a).
6. If 0.2% or lower is reached turn of flooding routine (“flood off”) and press “Gas On”.
7. Now you must level the platform by driving the recoater to the front of the base plate, drop a little bit of powder by putting a value of 10.000 in the command box of loader 2 in Motors page. Afterwards drive the recoater back to the end of the build chamber.
8. Import the REA file you want to fabricate.

This project has been funded with support from the European Commission. This publication [communication] reflects the views only of the authors, and the Commission cannot be held responsible for any use which may be made of the information contained therein.

9. Start the laser in Laser page (Figure 3.18 c).
10. Start the job by pressing the yellow “GO” in the Realizer software.
11. Then put in the slice you want to start from. First layer to be built is usually “0” and Press “OK”. *Now the machine starts the fabrication.* During the fabrication, the oxygen concentration should be lower than 2% in an argon protection gas.

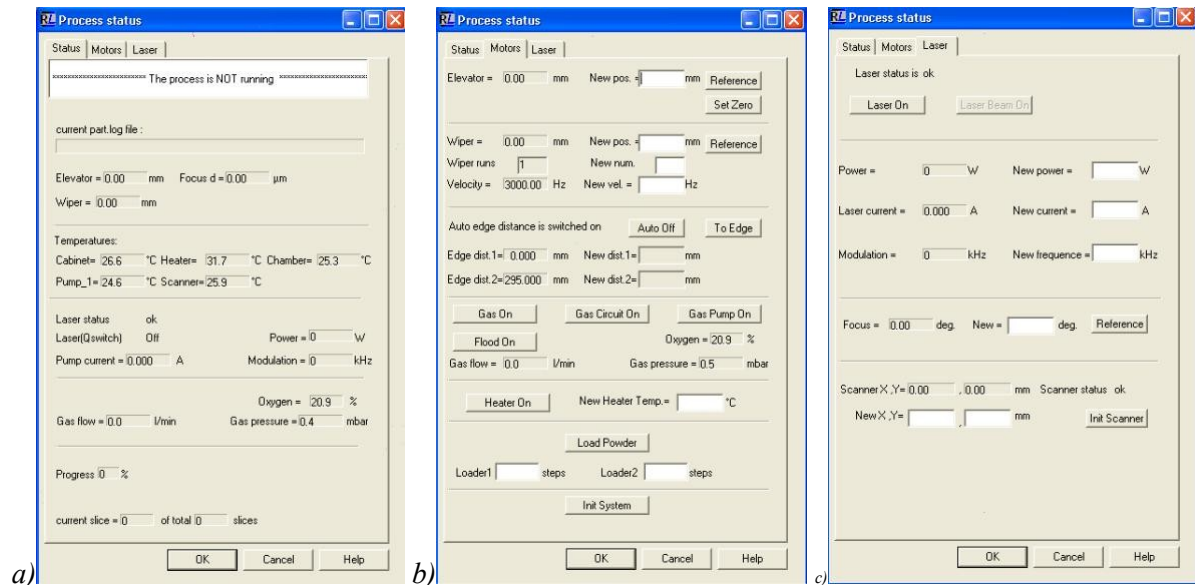


Fig. 3.18. Realizer software: a) Process status (wiper position, scanner/pump/cabinet/platform temperature, oxygen level, etc.); Technological parameters setting up: b) Motors page (temperature of base plate, on/off gas pump, elevator position); c) Laser page

Figure 3.19 shows some images during the SLM manufacturing at 258 slice. The SLM parameters and conditions conduct to proper fabrication without any unfavorable issues or defects. The production time was 6.51 h, being slightly longer than the theoretically estimated time in RCalculator tool (6.36 h - Section 3.6 Estimation of production time and cost).

This project has been funded with support from the European Commission. This publication [communication] reflects the views only of the authors, and the Commission cannot be held responsible for any use which may be made of the information contained therein.

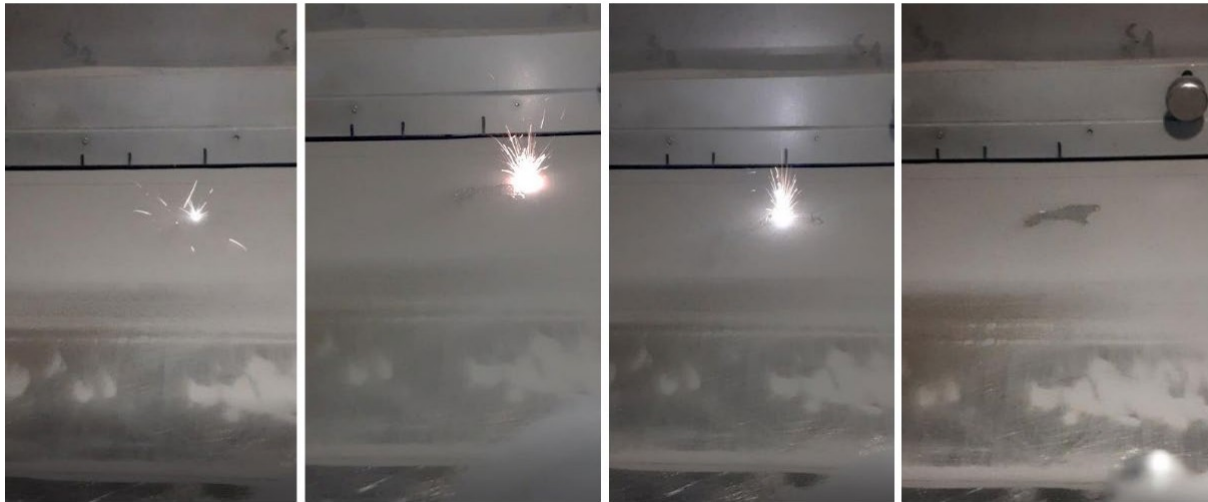


Fig. 3.19. SLM manufacturing of Ti implant

Figures 3.20-3.22 detail some diagrams generated during the SLM fabrication of Ti implant. In general, the time needed to scan a powder layer varied between 25 s to 30 s being influenced by the area that needs to be irradiated by Nd:YAG laser. The laser power was maintained constant at 120 W for each scanning function. The build platform and working chamber recorded a temperature up to 44°C and 30°C respectively. The gas pressure was limited to 11.0-11.2 mbar. After the SLM machine scan the first 60 layers, the oxygen content decrease from 1.5% to 0.4% in an argon atmosphere.

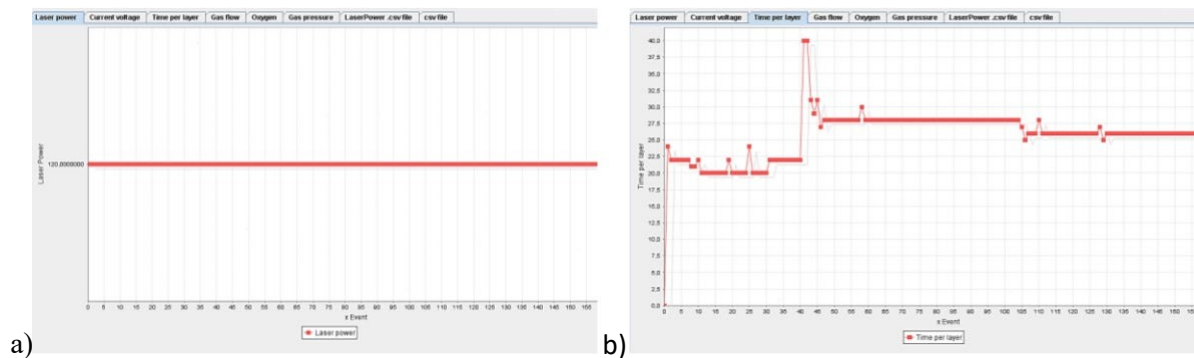


Fig. 3.20. Diagrams generated during the SLM fabrication by machine sensors:

a) Laser power, b) Time per each layer expressed in seconds

This project has been funded with support from the European Commission. This publication [communication] reflects the views only of the authors, and the Commission cannot be held responsible for any use which may be made of the information contained therein.

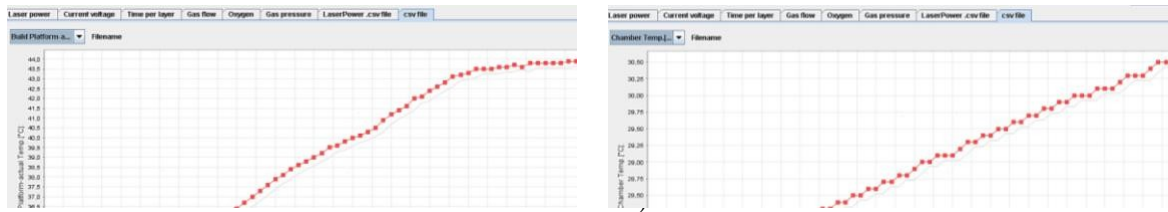


Fig. 3.21. Diagrams generated during the SLM fabrication by machine sensors: a) Build platform, b) Working chamber

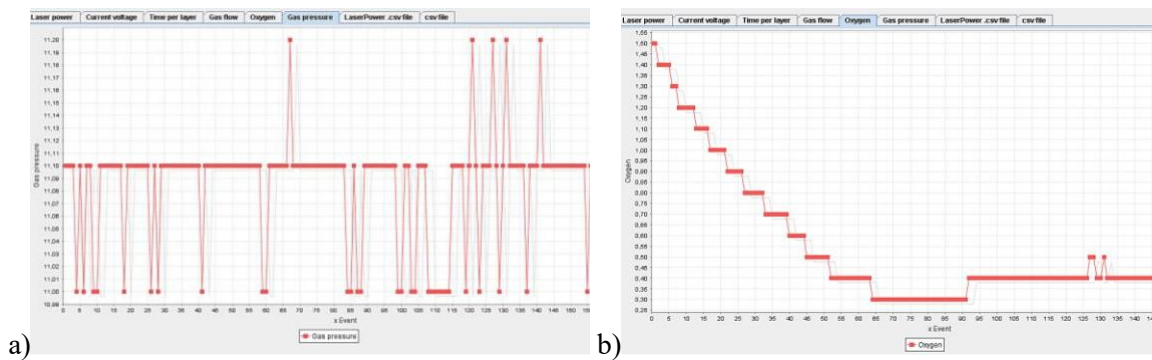


Fig. 3.22. Diagrams generated during the SLM fabrication from working chamber zone: a) Gas pressure, b) Oxygen content

Figure 3.23 shows the step undertaken to clean the implant after SLM-manufacturing. Using a brush, the un-melted powder is removed and recycled for future works. To recycle the un-used powder, a vibratory sieve shaker is operated.



Fig. 3.23. Cleaning the implant of powder

This project has been funded with support from the European Commission. This publication [communication] reflects the views only of the authors, and the Commission cannot be held responsible for any use which may be made of the information contained therein.

To clean the anatomical surface of implant, a pneumatic biax tool can be used (biax compressed air angle grinder). The polishing of Ti implant is done with milling tools and carborundum abrasive discs mounted on a micro-motor at 10,000-15,000 rpm (Figure 3.24). The below image shows the implant with as-built surfaces and polished.



Fig. 3.24. Biax micro-motor used to polish the implant

This project has been funded with support from the European Commission. This publication [communication] reflects the views only of the authors, and the Commission cannot be held responsible for any use which may be made of the information contained therein.

BRIGHT

Erasmus+ strategic partnership for Higher Education

BOOSTING THE SCIENTIFIC EXCELLENCE AND INNOVATION CAPACITY
OF 3D PRINTING METHODS IN PANDEMIC PERIOD

TOOLKIT 3FIXATOR MADE BY STEREOLITHOGRAPH (Digital light processing method)

Project Title	Boosting the scientific excellence and innovation capacity of 3D printing methods in pandemic period 2020-1-RO01-KA226-HE-095517
Output	IO2 – BRIGHT e-toolkit manual for digital learning in producing medical parts by 3D printing methods in the context of the pandemic
Toolkit	Toolkit 3 Fixator made by Stereolithography (Digital light processing method)
Date of Delivery	November 2021
Authors	Aleksandar Miltenović, Milan Banić, Nikola Vitković, Miloš Simonović
Version	Final variant

This project has been funded with support from the European Commission. This publication [communication] reflects the views only of the author, and the Commission cannot be held responsible for any use which may be made of the information contained therein.



Content

1	Introduction	66
2	Stereolithography process	66
3	Generating geometry and preparation for printing	67
4.	Materialise Magics	71
5.	3D printing	93
6.	Postprocessing	96
7.	Conclusions	98

This project has been funded with support from the European Commission. This publication [communication] reflects the views only of the author, and the Commission cannot be held responsible for any use which may be made of the information contained therein.



1 Introduction

In orthopedic surgery, it is vital to use proper fixation techniques to treat various medical conditions. Here is a requirement to provide the best possible medical treatment to a patient with a bone fracture. Surgeons use internal and external fixation techniques to treat bone fractures.

Nowadays, one of two types of plates and their variants are commonly used for bone fixation is Locking Compression Plates (LCP). These fixation systems are standardly anatomically shaped, and they provide angular stability to the bone.

In this toolkit will be shown printing process with all necessary pre- and postprocessing steps as well as machine settings for successful printing of the part – Locking Compression Plates which fixation plate.

2. Stereolithography Process

Stereolithography, as 3D printing technology, has following steps in the

- Selection of technology and machine
- Generating 3D model in a software for 3D modelling
- Generating STL file
- Defining parameter of machine for printing (at first use)
- Optional correction of object geometry
- Object positioning
- Generating support
- Distribution of model with support at platform for printing
- 3D printing
- Postprocessing

In a similar way, the steps required for modelling of the medical part is going to be presented. Details presented must be just enough for the readers so they can also replicate it at their home institution following the procedure described in the toolkit manual.

Standard for 3D printing is STL file that needs to be generated. Most of used CAD software (Solidworks, Catia, Inventor) has number of restrictions in work with STL files and therefore is

This project has been funded with support from the European Commission. This publication [communication] reflects the views only of the authors, and the Commission cannot be held responsible for any use which may be made of the information contained therein.

necessary using of specialized software for STL file processing. One of those software that can be used for stereolithography is Materialise Magics.

Options that are important for conversion are related for resolution. Most of software are giving button option with high, medium and low resolution as well as options that user can enter his tolerances. As the user want higher resolution and better surfaces, he should choose lower tolerances for possible deviations. This is especially important for the parts with surfaces that are not plane and under angle. As the tolerances are lower the final STL file will be higher. Also, in the cases when printing resolution is low, high STL file resolution is not going to get any result. Therefore is important to know the resolution of the printer. For example, Envisiontec Ultra 3SP has the maximal resolution of 0.025 mm in z direction.

Material consumption is an important issue for parts made by Stereolithography printing process. If the functionality of the part as well as strength is less important, there should be less used material. In that case for stereolithography is important to define the model as hollow and to define technological holes if this is necessary. Preprocessing can be done in 3D modeling software that can be, in some cases, easier comparing with software for manipulation with STL file.

3. Generating geometry and preparation for printing

Part that need to be printed has to be made in some of CAD software for 3D modeling. After the modeling is finished is necessary to convert part into STL file. Today all the software has possibility to convert file into STL (Figure 3. 1 – Autodesk Inventor).

This project has been funded with support from the European Commission. This publication [communication] reflects the views only of the authors, and the Commission cannot be held responsible for any use which may be made of the information contained therein.

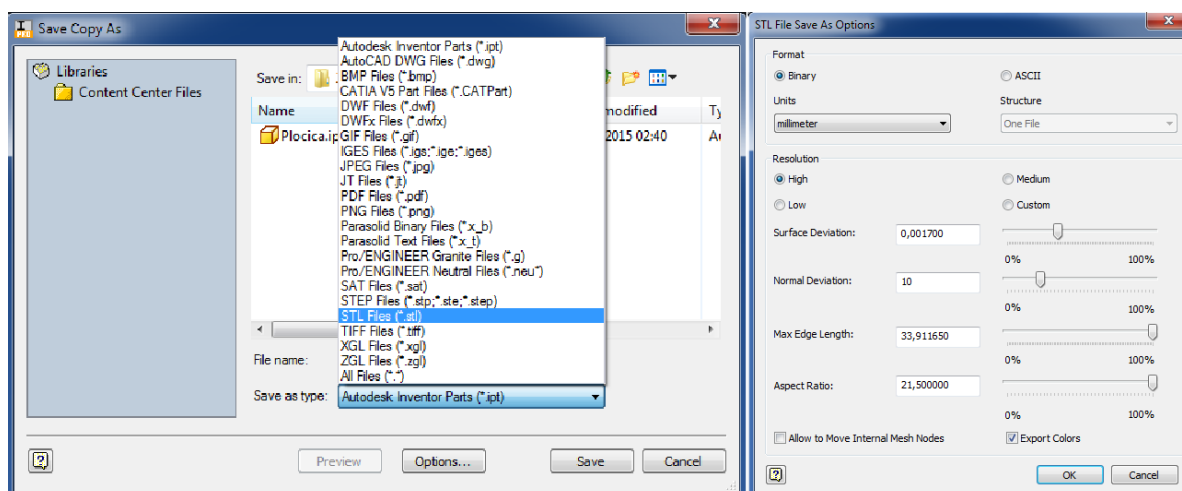


Figure 3.1. Autodesk Inventor windows for converting in STL with possible options

Wall thickness is important for printing process while if the wall dimension is too small there is dangerous that during printing or in postprocessing phase wall can have or got cracks. Some tips for wall thickness is to be at least 1 mm but results will be better if it is 2 mm. Also here should be taken into account the size of the wall and is edge of surface with thickend or not.

Technological holes should be defined for leakage of liquid material. The tip is that the smallest diameter of hole should be 2 mm, but it would be better to have more holes and that diameter is 3 mm. For this is important also to define the logical position of the hole at the part. Position should be at surface that is not important for the part functionality and that will allow liquid material to leak out (Figure 3.2, 3.3, 3.4).

This project has been funded with support from the European Commission. This publication [communication] reflects the views only of the authors, and the Commission cannot be held responsible for any use which may be made of the information contained therein.

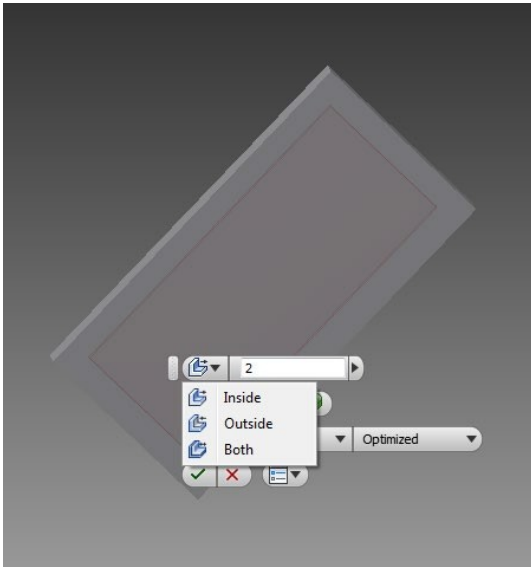


Figure 3.2. Defining hollow and position for technological hole

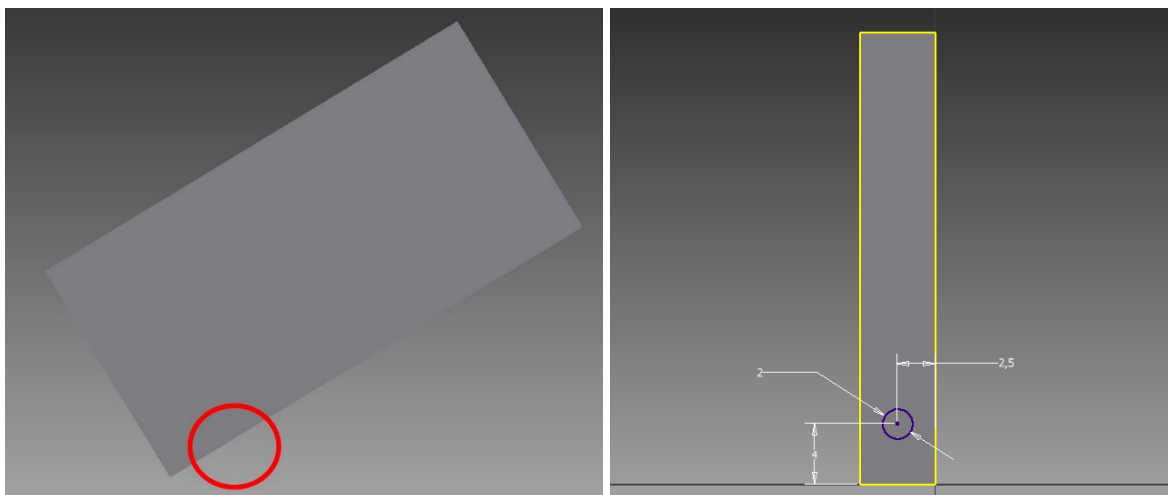


Figure 3.3. Position for technological hole

This project has been funded with support from the European Commission. This publication [communication] reflects the views only of the authors, and the Commission cannot be held responsible for any use which may be made of the information contained therein.

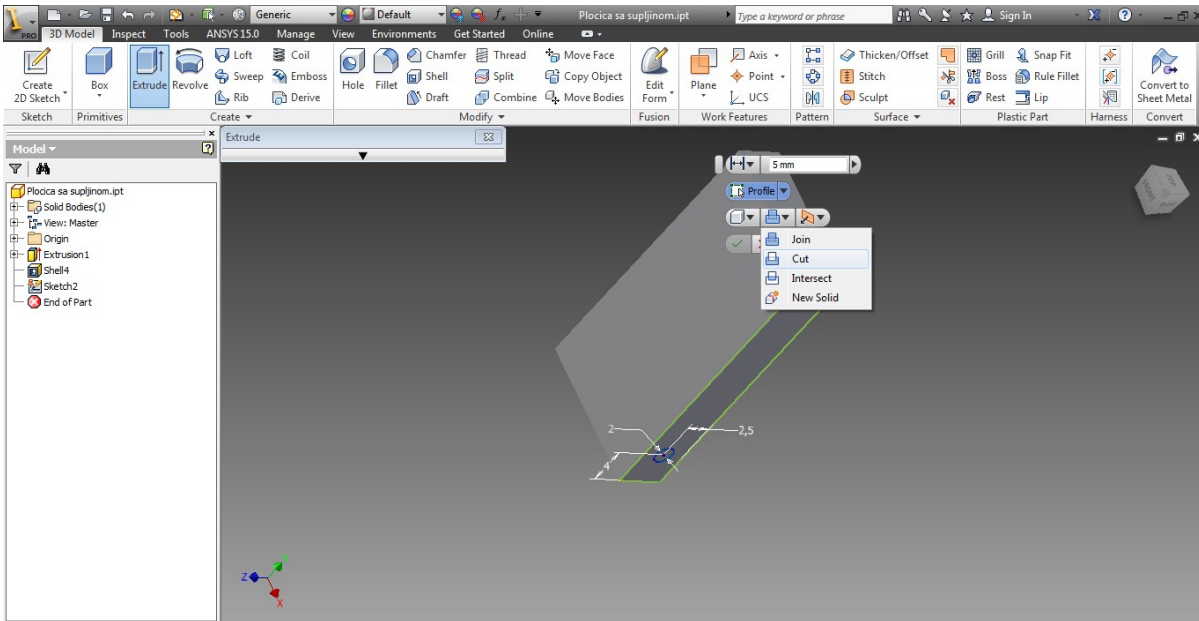


Figure 3.4. Definition of technological hole in CAD software

This project has been funded with support from the European Commission. This publication [communication] reflects the views only of the authors, and the Commission cannot be held responsible for any use which may be made of the information contained therein.

4. Materialise Magics

For the good printing of the part is important to define the machine settings. Materialise Magics offers a lot of parameters that need to be defined in order to have good print. Therefore in Figures 4.5 - 4.43 is going to be presenting defining settings step by step. This is especially important for support settings that enables the good connection to basic platform from one side and to the printed part on other side. This gives smooth postprocessing in which part with support structure need to be separated from platform as well separation of printed part from support.

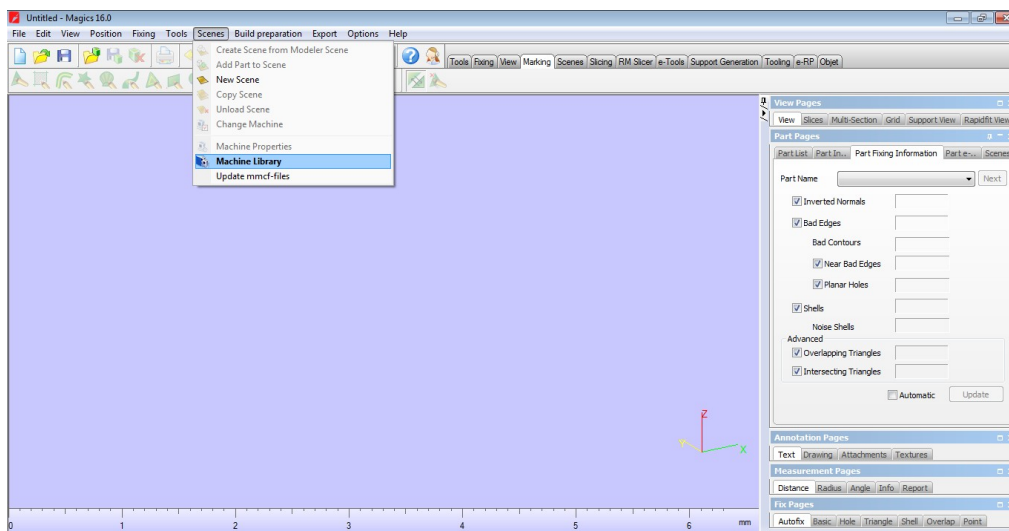


Figure 4.5 Surrounding in Materialise Magics

Figure 4.5 represent Surrounding in Materialise Magics. To access Machine Library is necessary to use card Scenes. After clicking Machine Library is necessary to use Envisiontec Prefactory as it is shown at Figure 4.7.

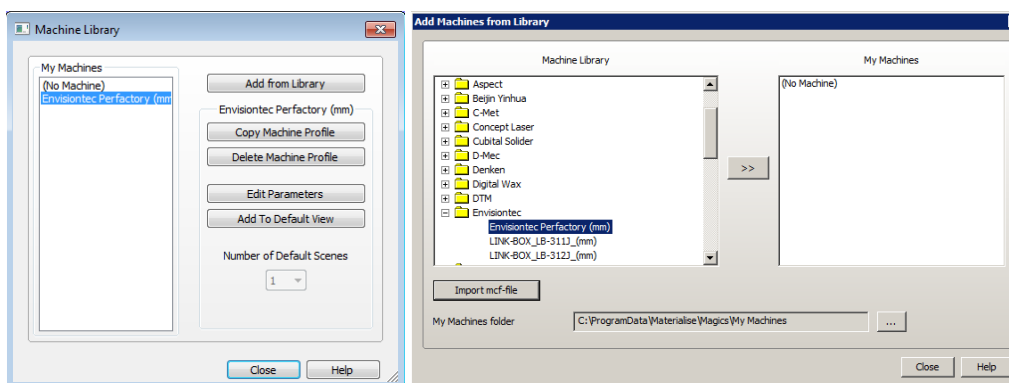


Figure 4.6. Introduction of Envisiontec Prefactory

This project has been funded with support from the European Commission. This publication [communication] reflects the views only of the authors, and the Commission cannot be held responsible for any use which may be made of the information contained therein.

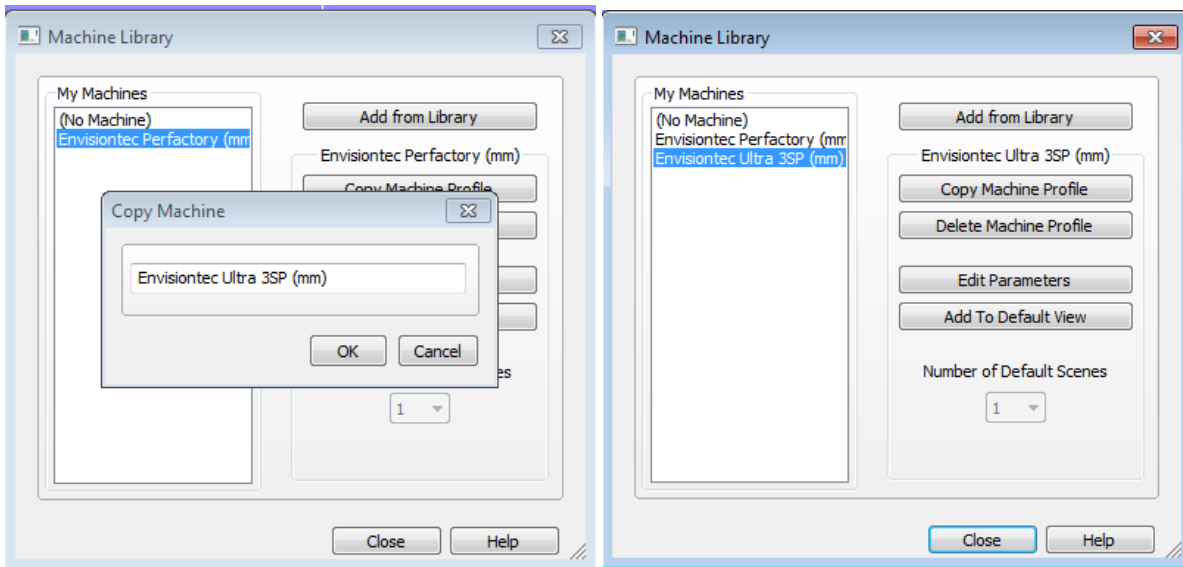


Figure 4.7. Defining 3D printer into Materilise Magics

In Figure 4.7 is shown procedure in which is copied “Evisiontec Perfactory” and changed in the name of 3D printer that is used for printing. In this case is 3D printer “Envisiontec Ultra 3SP” and that is the name used for defining work envioment. In Figure 4.8 is given introducing field for Envisiontec Ultra 3SP envioment.

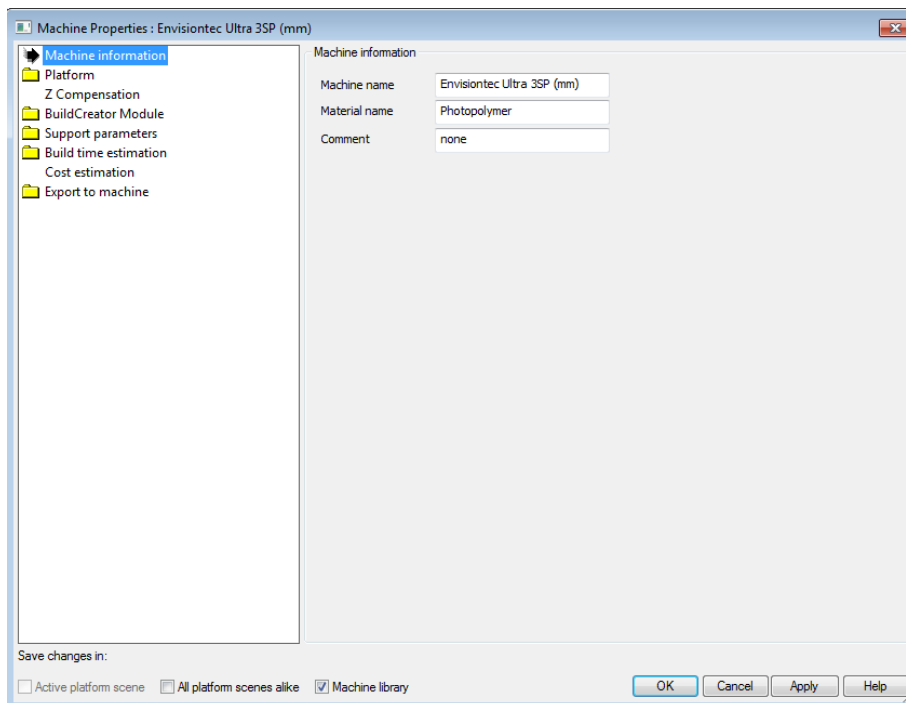


Figure 4.8. Introducing machine settings – machine information

This project has been funded with support from the European Commission. This publication [communication] reflects the views only of the authors, and the Commission cannot be held responsible for any use which may be made of the information contained therein.

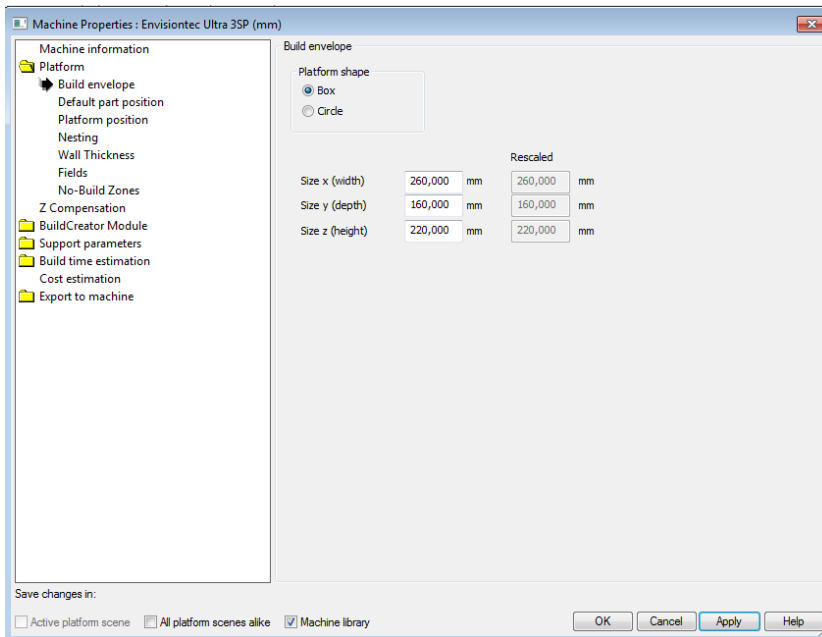


Figure 4.9. Introducing machine settings – platform

In Figure 4.9 are given machine settings for the platform. It has box shape with size 260x160x220mm. In Figure 4.10 is defined default part position for the position of the printing part on platform.

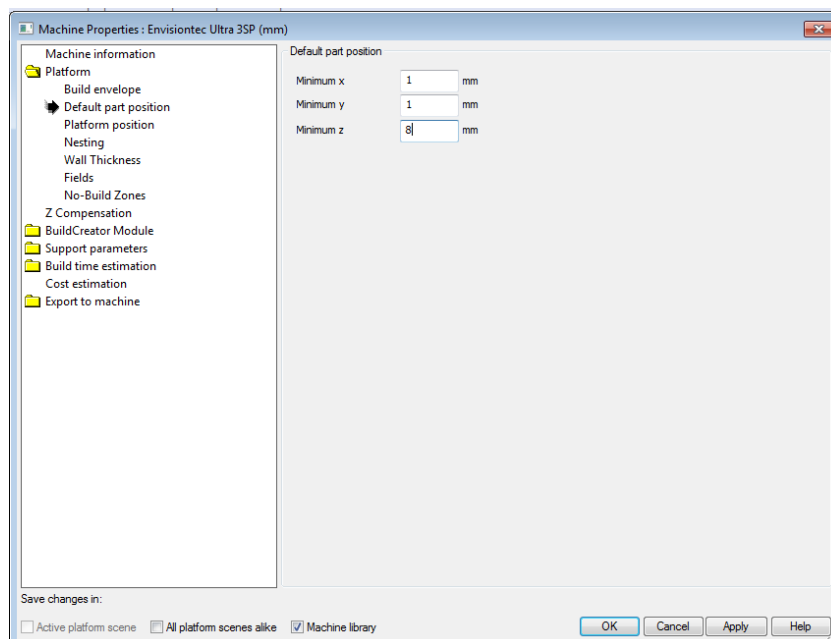


Figure 4.10. Introducing machine settings – default position

This project has been funded with support from the European Commission. This publication [communication] reflects the views only of the authors, and the Commission cannot be held responsible for any use which may be made of the information contained therein.

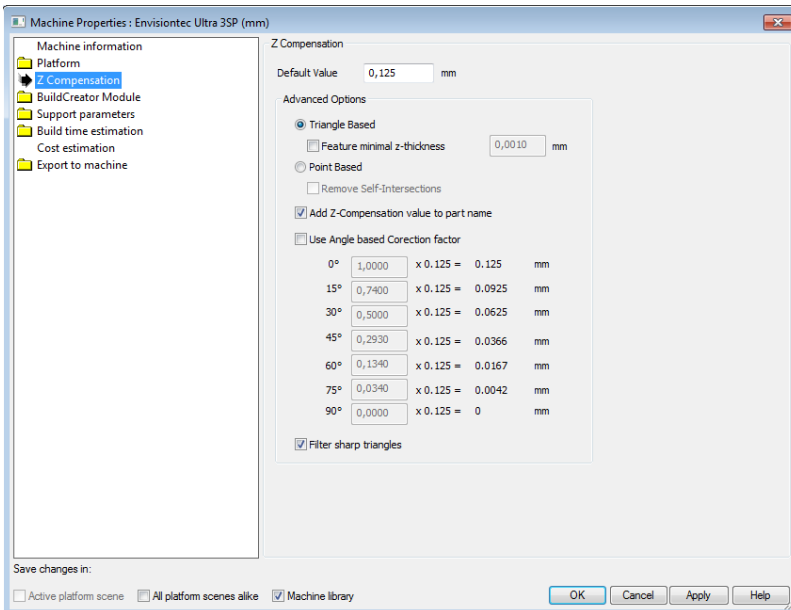


Figure 4.11. Introducing machine settings – platform, z Compensation

In Figure 4.11 is defined z-compensation for the platform – 0.125mm. In Figure 4.12 is defined support format that can be the same as printing part or different. For the successful printing is necessary that the printing part and support has to be entered as two files but with same names.

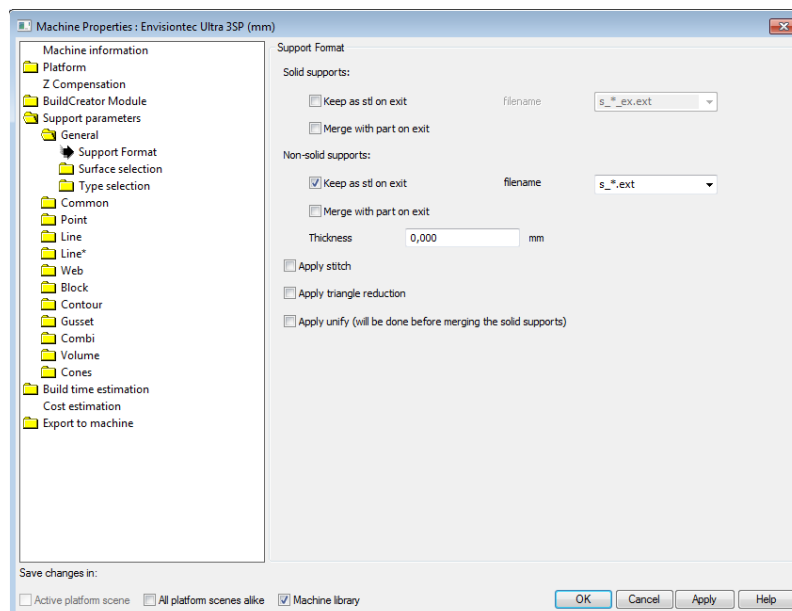


Figure 4.12. Introducing machine settings – support format

This project has been funded with support from the European Commission. This publication [communication] reflects the views only of the authors, and the Commission cannot be held responsible for any use which may be made of the information contained therein.

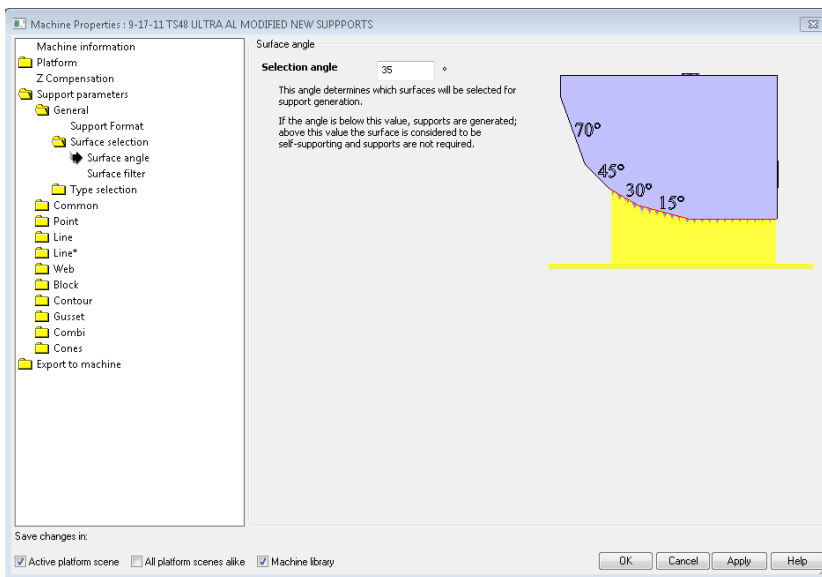


Figure 4.13. Introducing machine settings – surface angle

In Figure 4.13 is defined surface angle in which support will be generated on the part. In this case will be used 35 degrees. In Figure 4.14 is defined surface filter and surface angle.

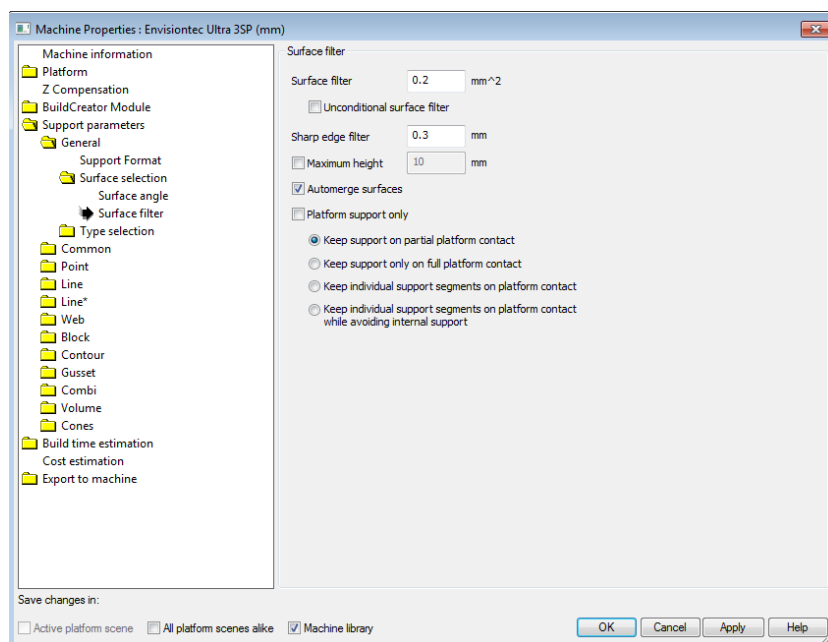


Figure 4.14. Introducing machine settings – surface filter

This project has been funded with support from the European Commission. This publication [communication] reflects the views only of the authors, and the Commission cannot be held responsible for any use which may be made of the information contained therein.

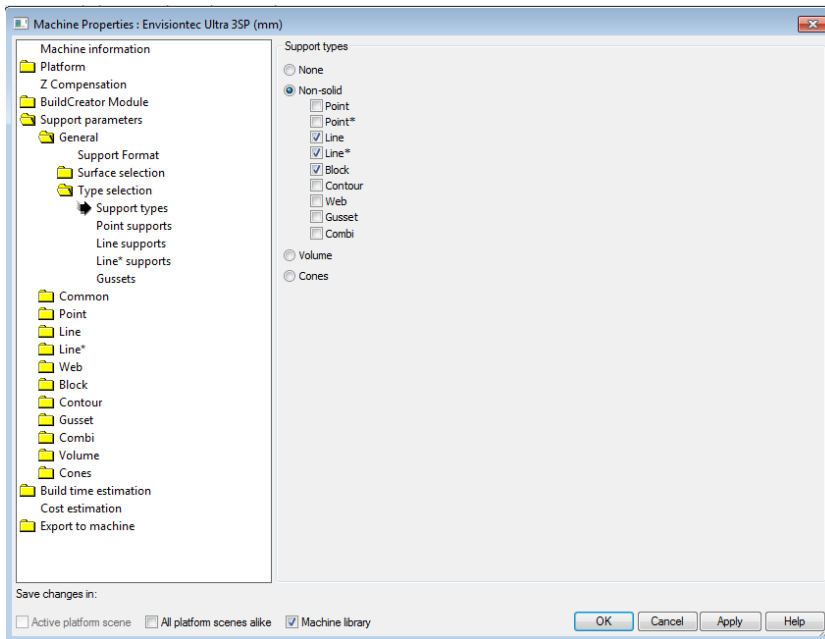


Figure 4.15. Introducing machine settings – support types

In Figure 4.15 is defined surface angle in which support type. In Figure 4.16 is defined basic parameter for support – gusset.

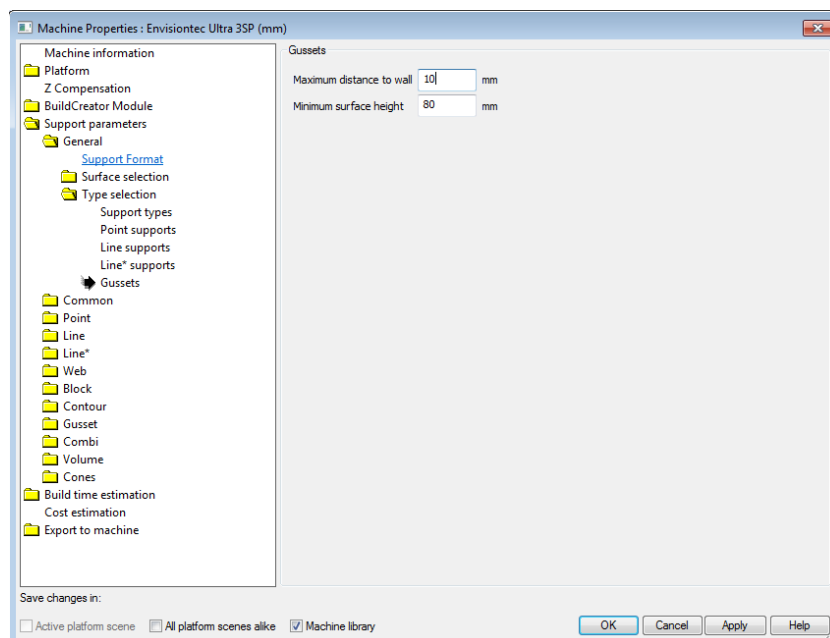


Figure 4.16. Introducing machine settings – gussets

This project has been funded with support from the European Commission. This publication [communication] reflects the views only of the authors, and the Commission cannot be held responsible for any use which may be made of the information contained therein.

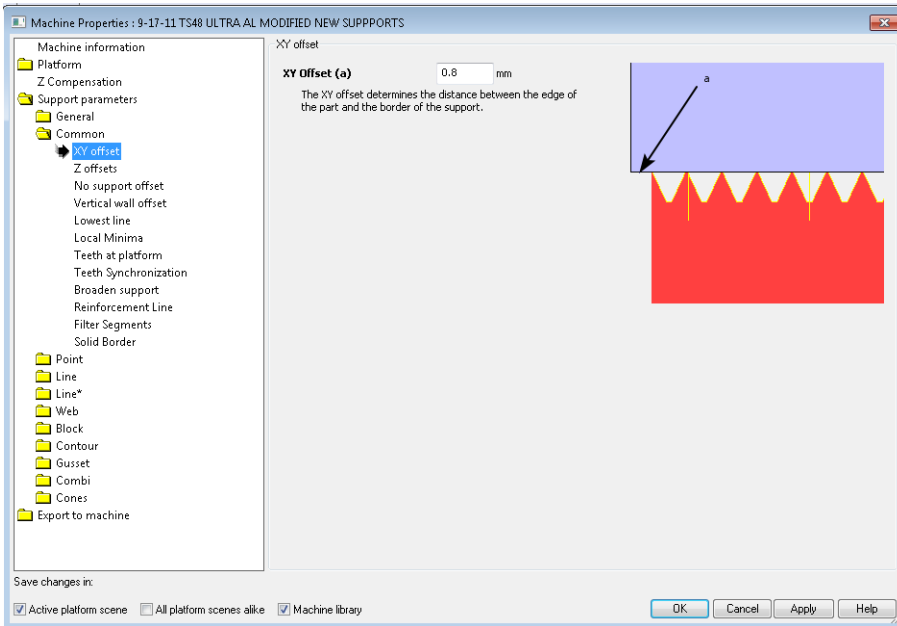


Figure 4.17. Introducing machine settings – XY offset

In Figure 4.17 is defined xy offset for generation of support structure. In Figure 4.18 is defined z offset parameter that has upper and lower value.

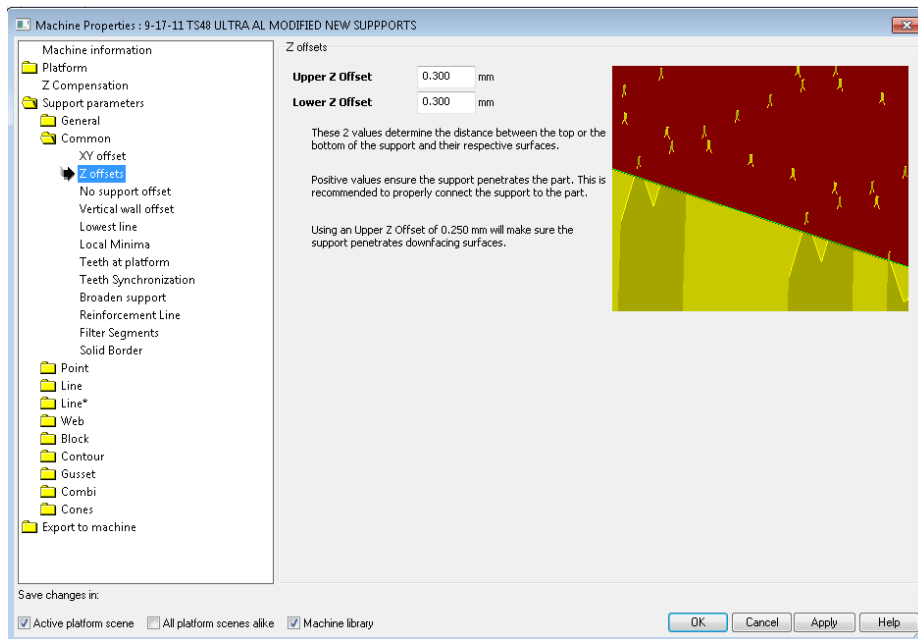


Figure 4.18. Introducing machine settings – Z offset

This project has been funded with support from the European Commission. This publication [communication] reflects the views only of the authors, and the Commission cannot be held responsible for any use which may be made of the information contained therein.

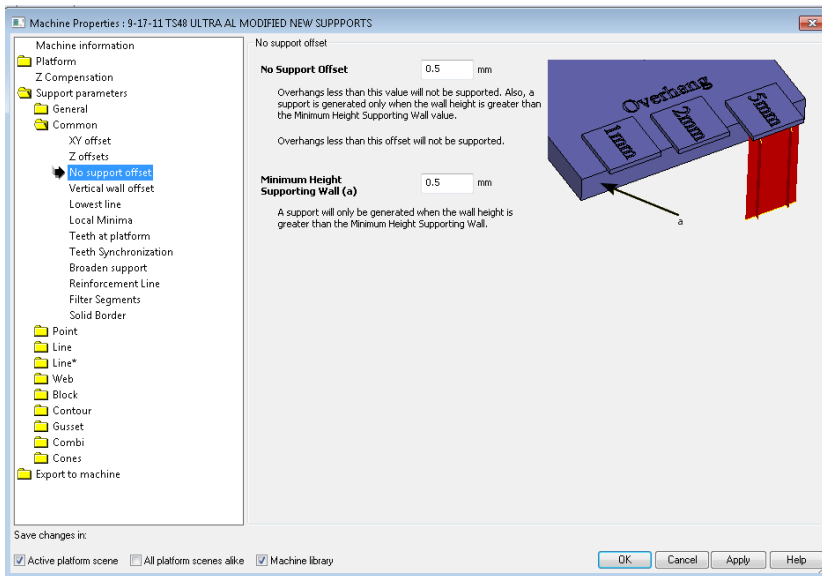


Figure 4.19. Introducing machine settings – No support offset

In Figure 4.19 is defined no support offset with minimum height supporting wall value. In Figure 4.20 is defined vertical wall offset value.

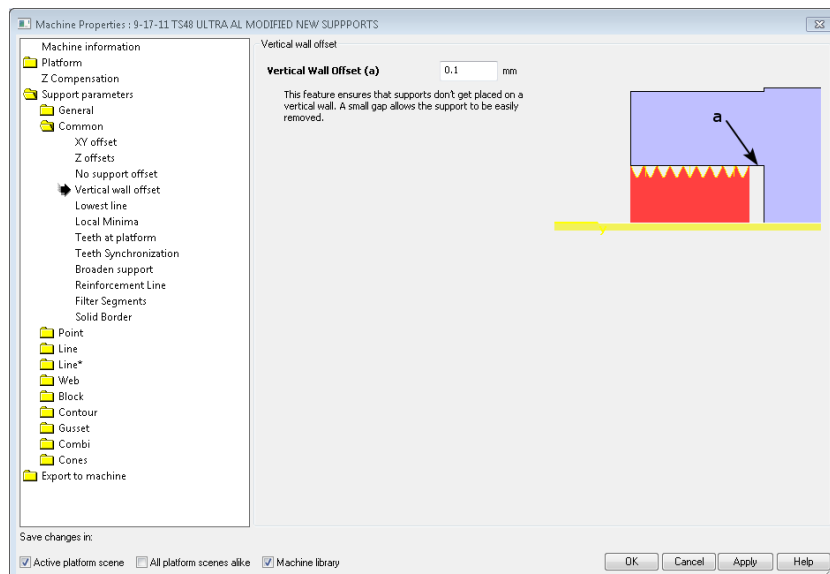


Figure 4.20. Introducing machine settings – Vertical wall offset

This project has been funded with support from the European Commission. This publication [communication] reflects the views only of the authors, and the Commission cannot be held responsible for any use which may be made of the information contained therein.

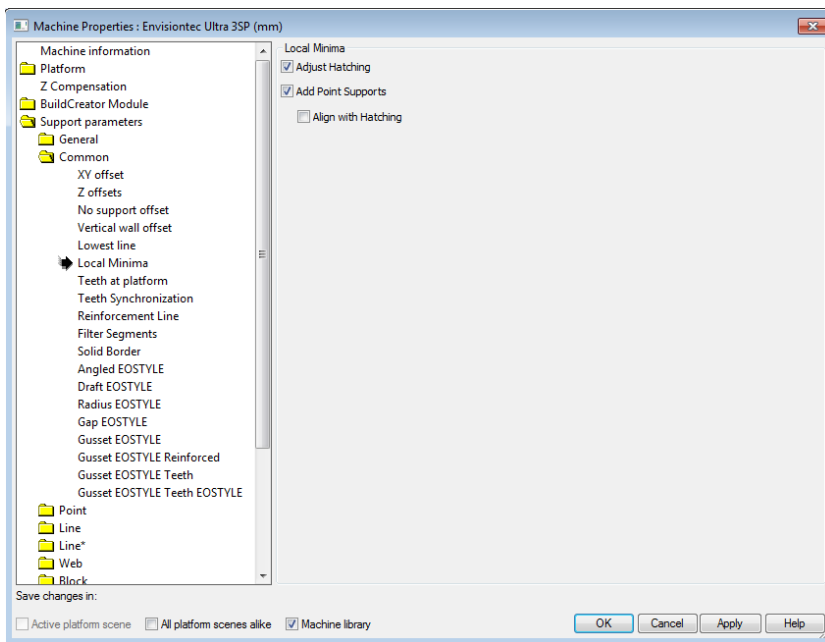


Figure 4.21. Introducing machine settings – local minima

In Figure 4.21 is defined local minima for support. In Figure 4.22 is defined teeth at platform that can go directly of platform or it can be defined with some value.

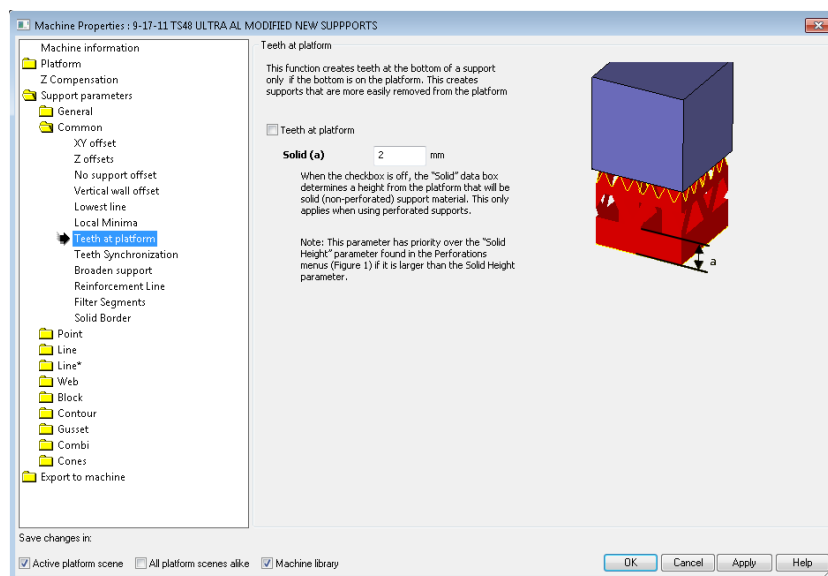


Figure 4.22. Introducing machine settings – Teeth at platform

This project has been funded with support from the European Commission. This publication [communication] reflects the views only of the authors, and the Commission cannot be held responsible for any use which may be made of the information contained therein.

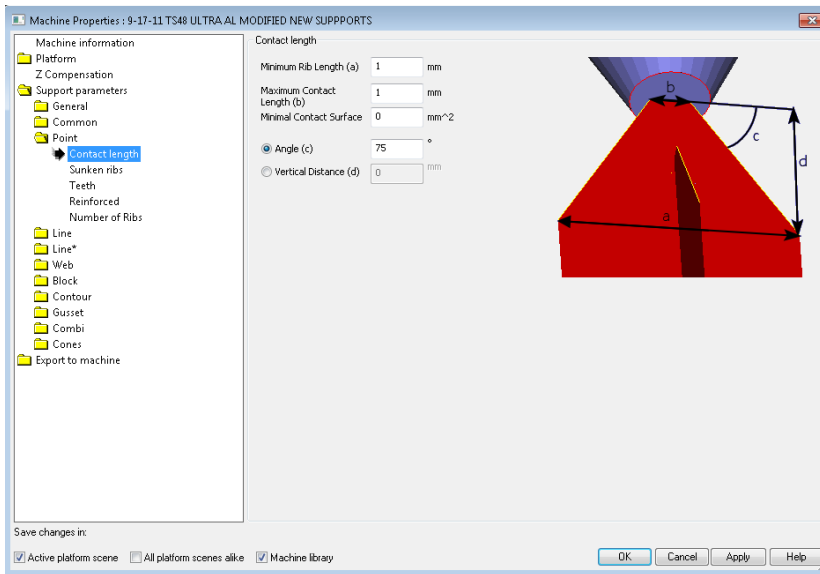


Figure 4.23. Introducing machine settings – Contact length

In Figure 4.23 is defined contact length of support structure. In Figure 4.24 is defined basic parameter for support – gusset.

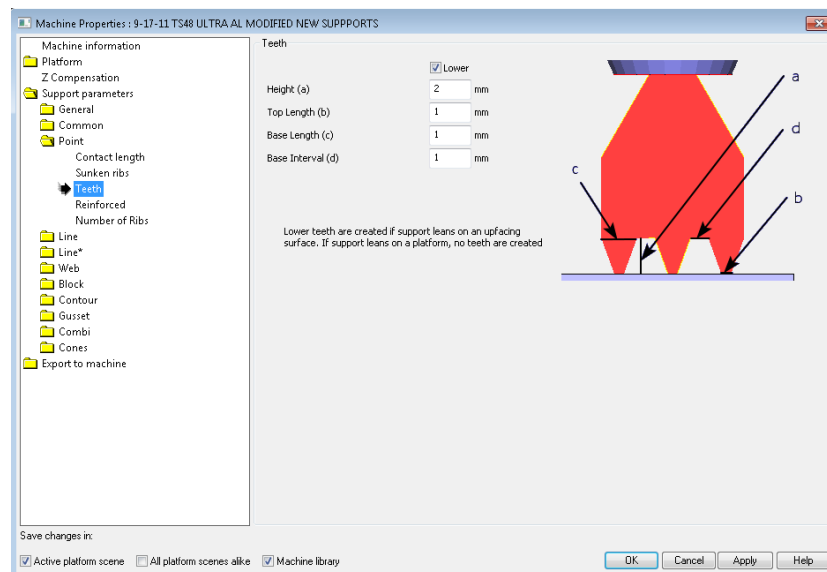


Figure 4.24. Introducing machine settings – Teeth

This project has been funded with support from the European Commission. This publication [communication] reflects the views only of the authors, and the Commission cannot be held responsible for any use which may be made of the information contained therein.

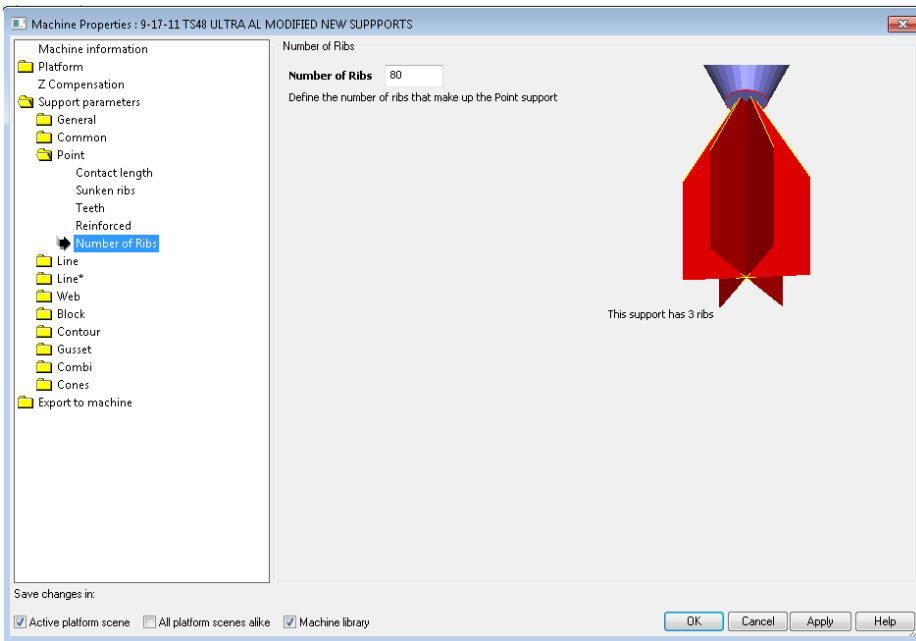


Figure 4.25. Introducing machine settings – number of ribs

In Figure 4.25 is defined number of ribs that are generated on support structure. In Figure 4.26 is defined minimum rib length and maximum contact length.

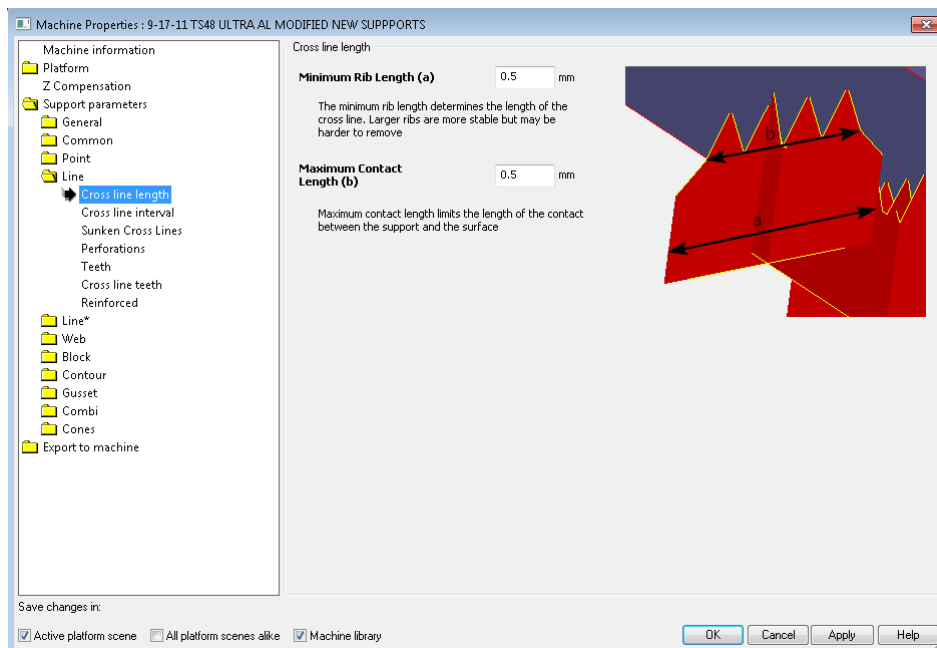


Figure 4.26. Introducing machine settings – cross line length

This project has been funded with support from the European Commission. This publication [communication] reflects the views only of the authors, and the Commission cannot be held responsible for any use which may be made of the information contained therein.

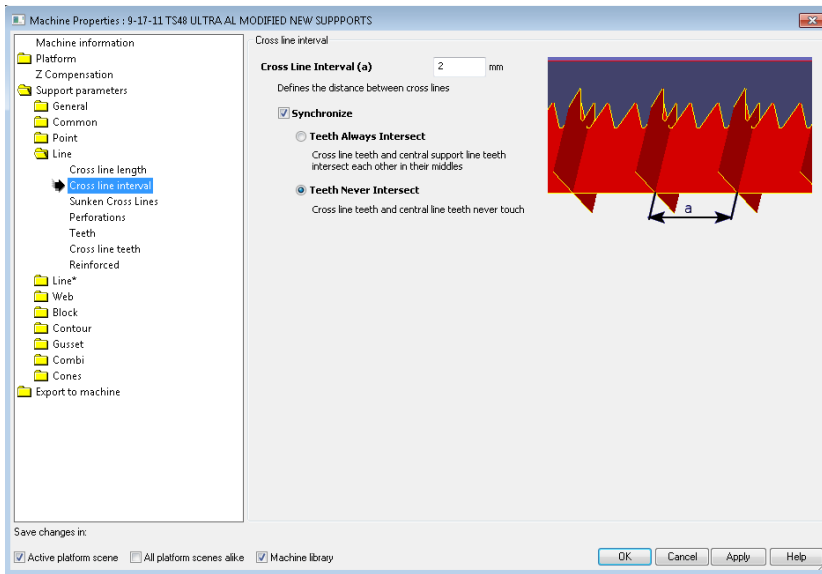


Figure 4.27. Introducing machine settings – Cross line interval

In Figure 4.27 is defined cross line interval. In Figure 4.28 is defined sink cross lines with distance.

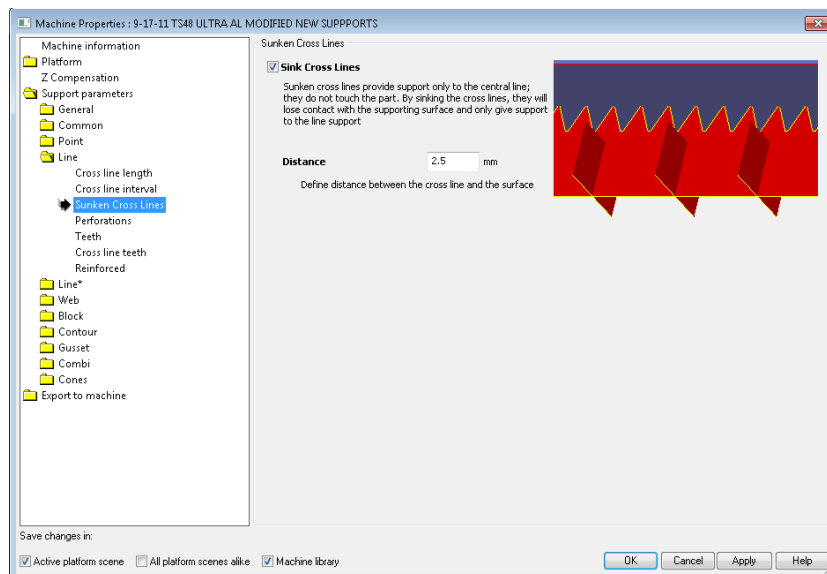


Figure 4.28. Introducing machine settings – sunken cross lines

This project has been funded with support from the European Commission. This publication [communication] reflects the views only of the authors, and the Commission cannot be held responsible for any use which may be made of the information contained therein.

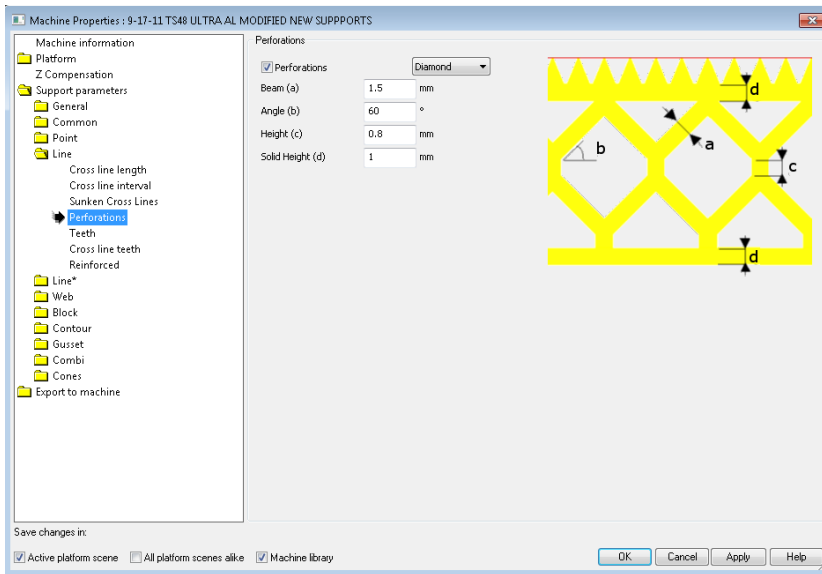


Figure 4.29. Introducing machine settings – perforations

In Figure 4.29 is defined dimensions for perforations. In Figure 4.30 is defined dimensions for teeth.

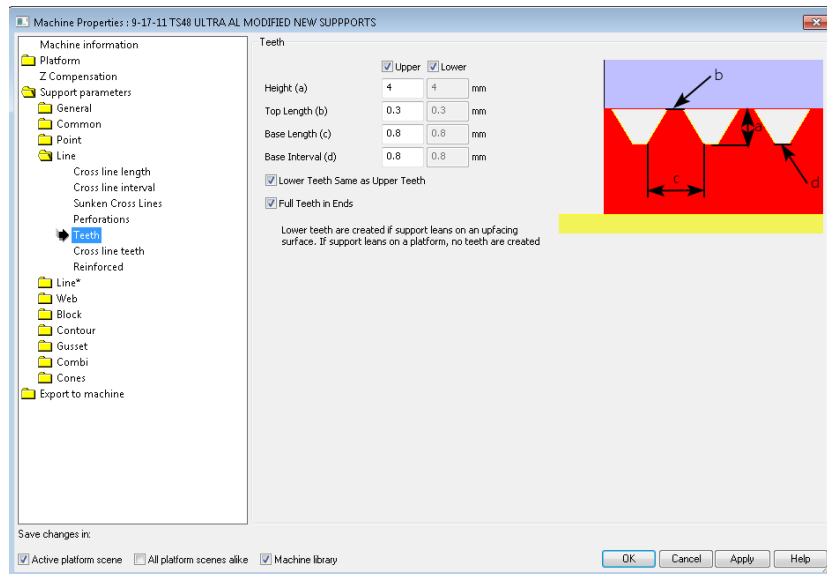


Figure 4.30. Introducing machine settings – line teeth

This project has been funded with support from the European Commission. This publication [communication] reflects the views only of the authors, and the Commission cannot be held responsible for any use which may be made of the information contained therein.

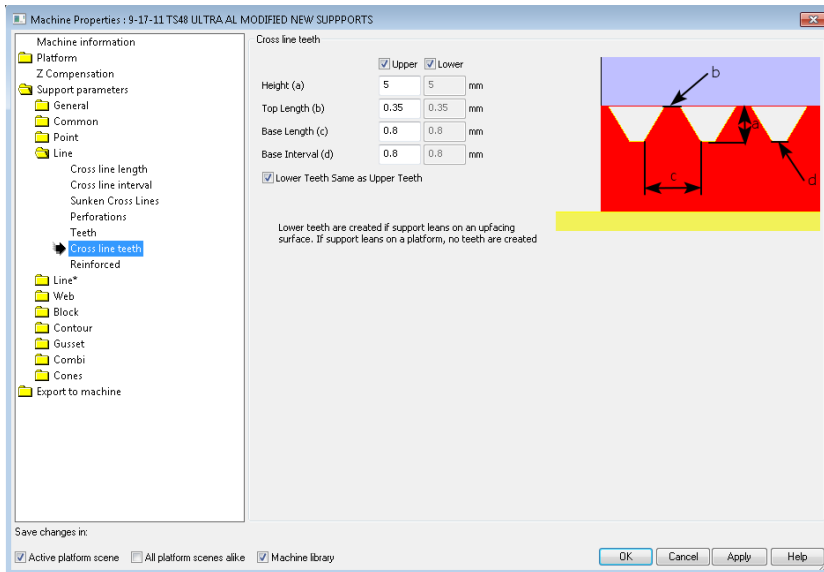


Figure 4.31. Introducing machine settings – cross line teeth

In Figure 4.31 is defined dimensions for cross line teeth. In Figure 4.32 is defined reinforced for line support.

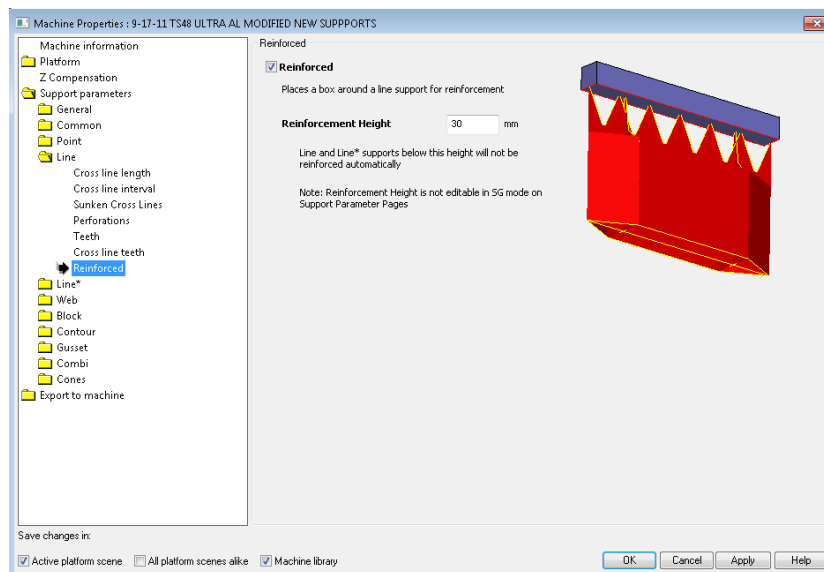


Figure 4.32. Introducing machine settings – reinforced

This project has been funded with support from the European Commission. This publication [communication] reflects the views only of the authors, and the Commission cannot be held responsible for any use which may be made of the information contained therein.

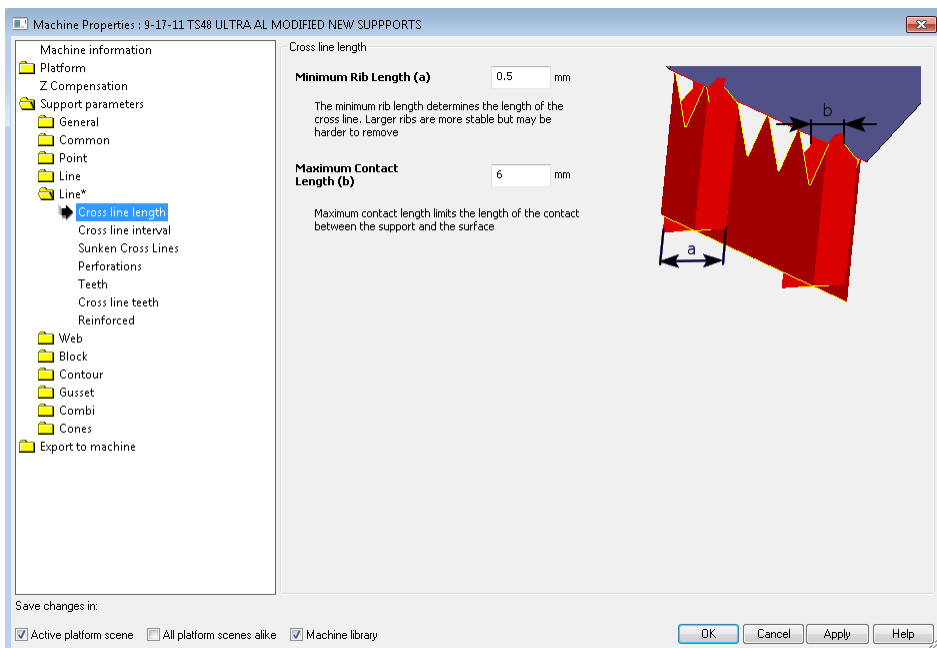


Figure 4.33. Introducing machine settings – cross line length

In Figure 33 is defined cross line length for support. In Figure 4.34 is defined cross line interval for line support structure.

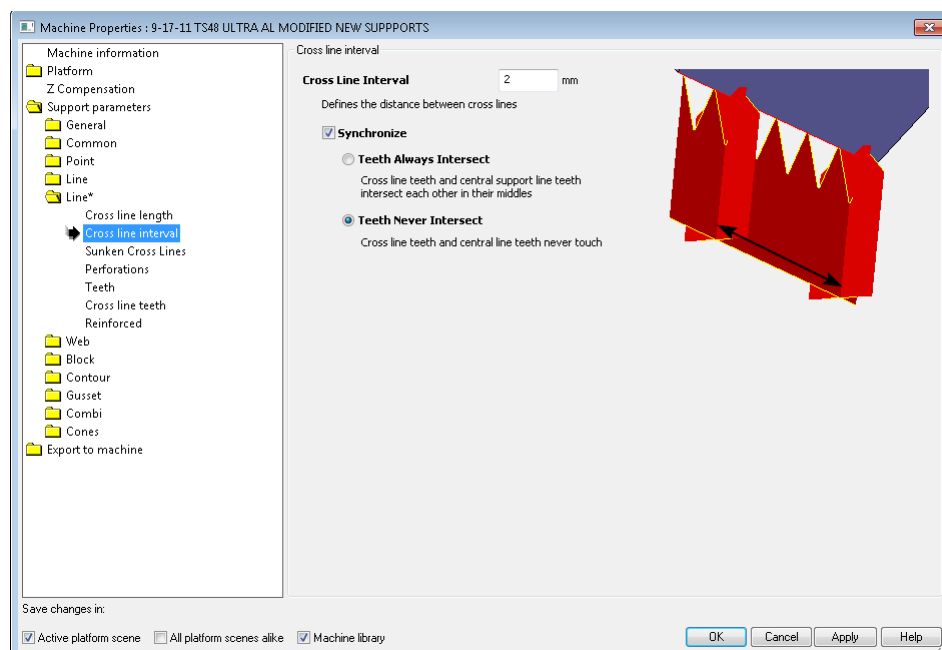


Figure 4.34. Introducing machine settings – cross line interval

This project has been funded with support from the European Commission. This publication [communication] reflects the views only of the authors, and the Commission cannot be held responsible for any use which may be made of the information contained therein.

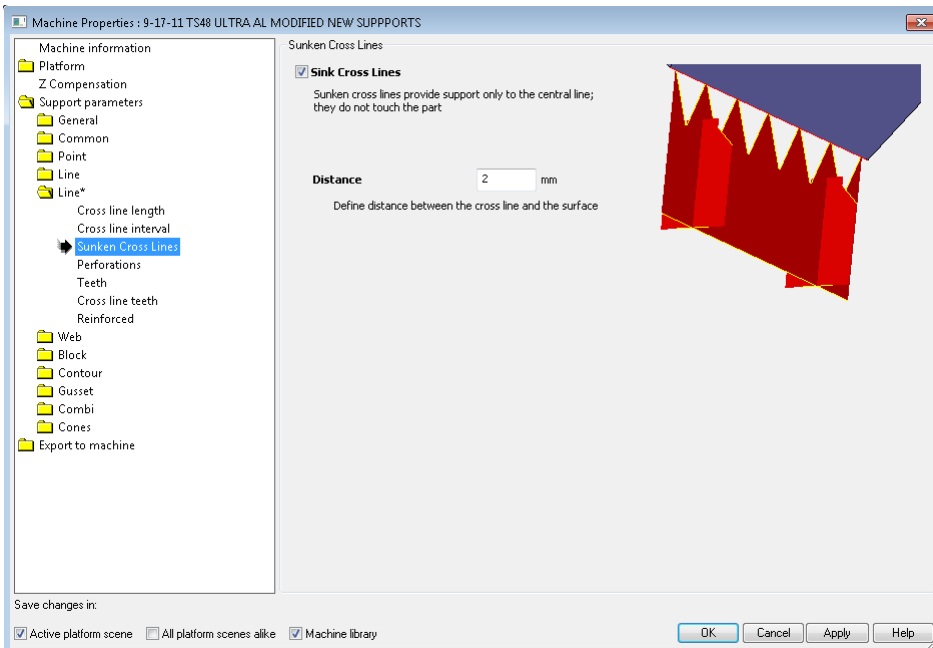


Figure 4.35. Introducing machine settings – sunken cross lines

In Figure 4.35 is defined sunken cross lines. In Figure 4.36 is defined dimensions for perforations.

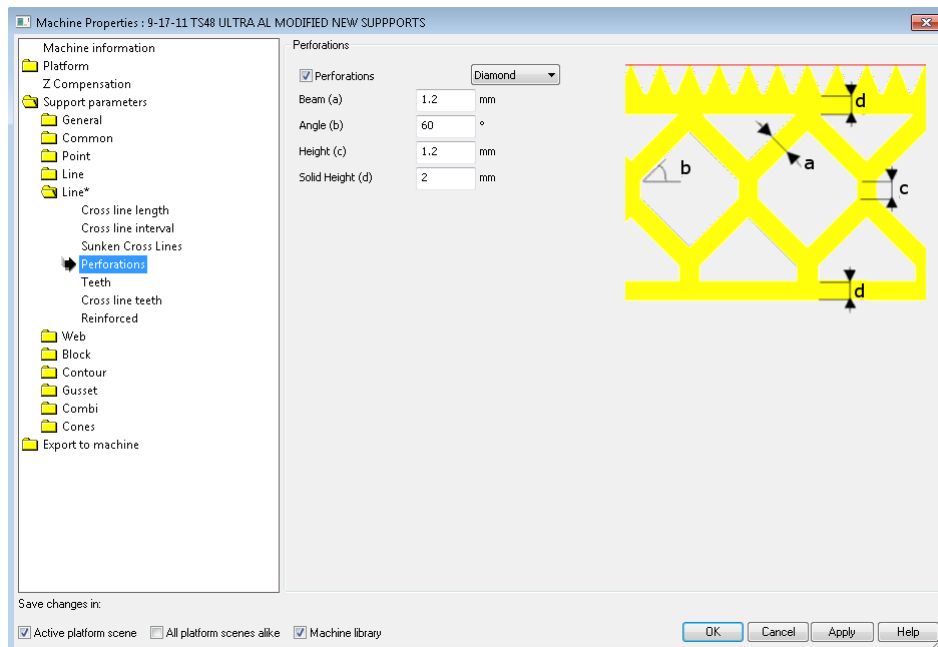


Figure 4.36. Introducing machine settings – perforations

This project has been funded with support from the European Commission. This publication [communication] reflects the views only of the authors, and the Commission cannot be held responsible for any use which may be made of the information contained therein.

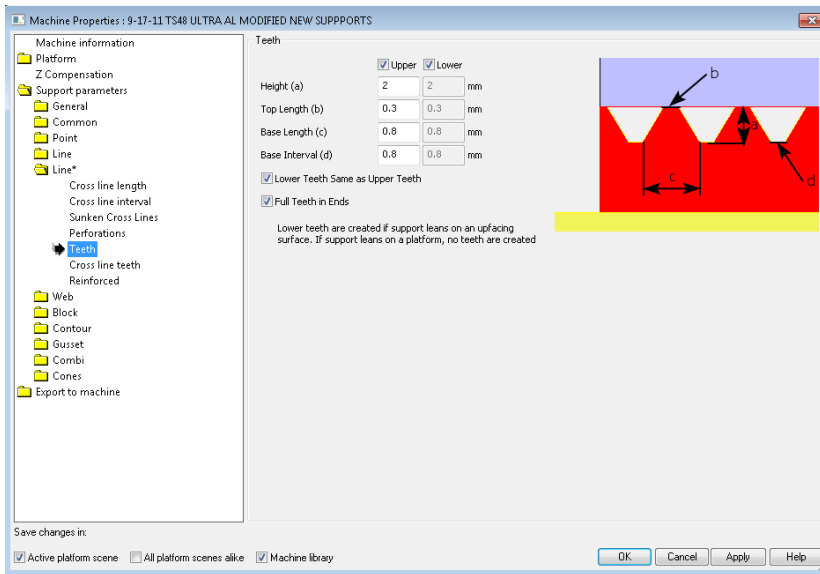


Figure 4.37. Introducing machine settings – teeth

In Figure 4.37 is defined dimensions for teeth. In Figure 4.38 is defined dimensions for cross line teeth.

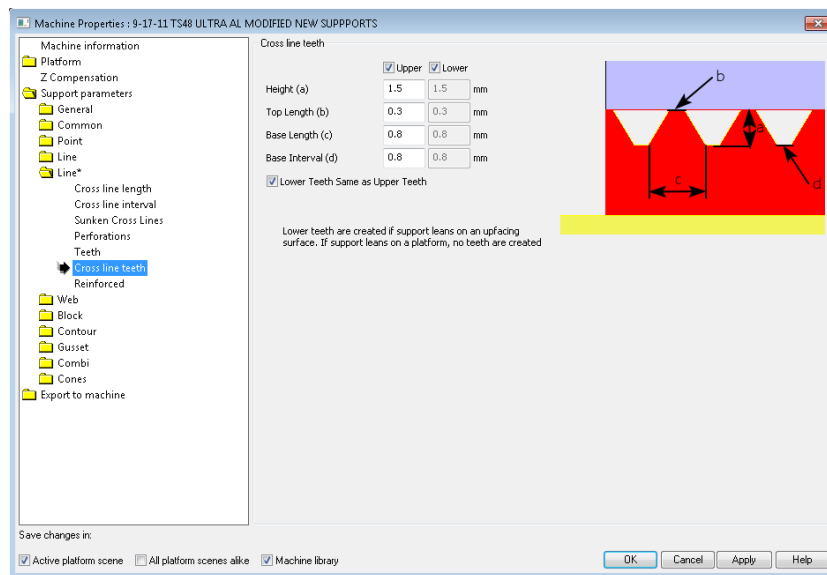


Figure 4.38. Introducing machine settings – cross line teeth

This project has been funded with support from the European Commission. This publication [communication] reflects the views only of the authors, and the Commission cannot be held responsible for any use which may be made of the information contained therein.

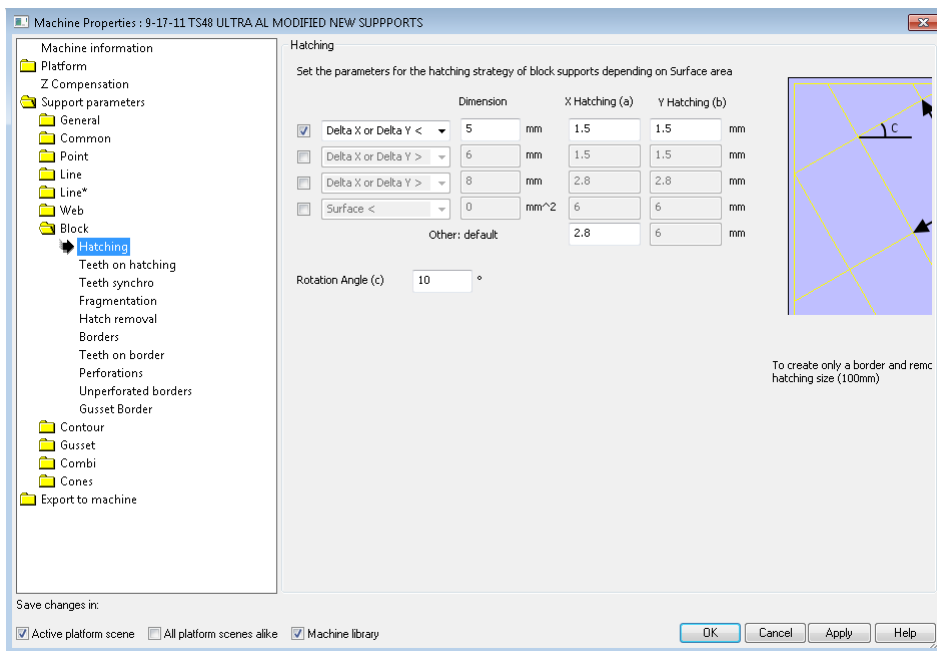


Figure 4.39. Introducing machine settings – hatching

In Figure 4.39 is defined dimensions for hatching as blocks of support structure. In Figure 4.40 is defined dimensions for teeth on hatching.

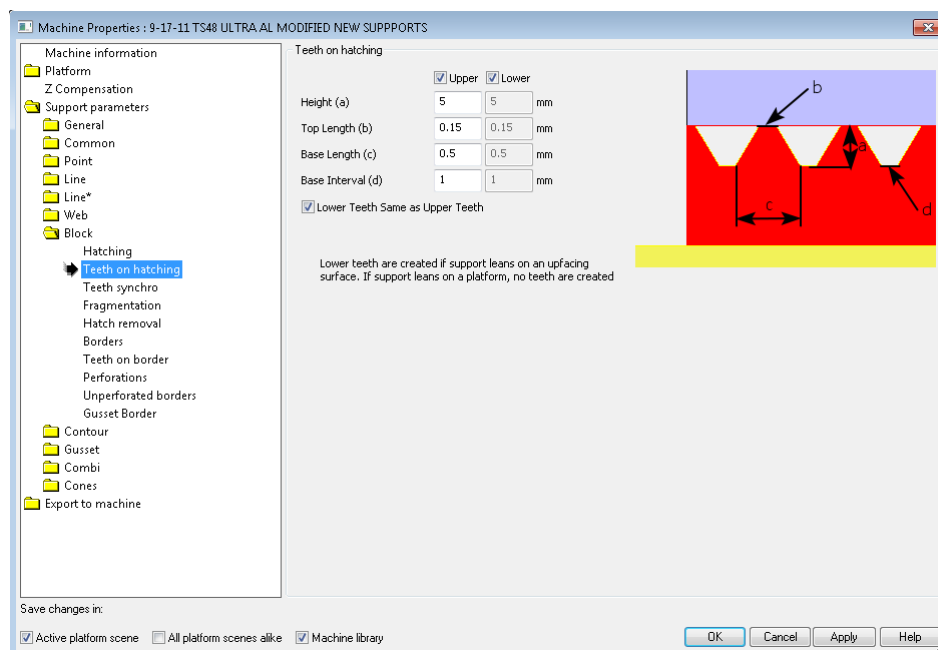


Figure 4.40. Introducing machine settings – teeth on hatching

This project has been funded with support from the European Commission. This publication [communication] reflects the views only of the authors, and the Commission cannot be held responsible for any use which may be made of the information contained therein.

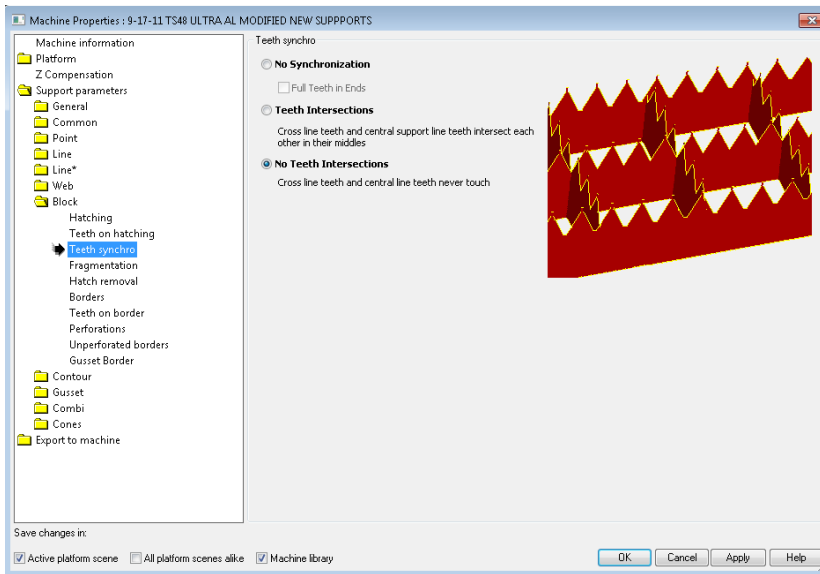


Figure 4.41. Introducing machine settings – teeth synchro

In Figure 4.41 is defined teeth synchro. In Figure 4.42 is defined dimensions for fragmentation.

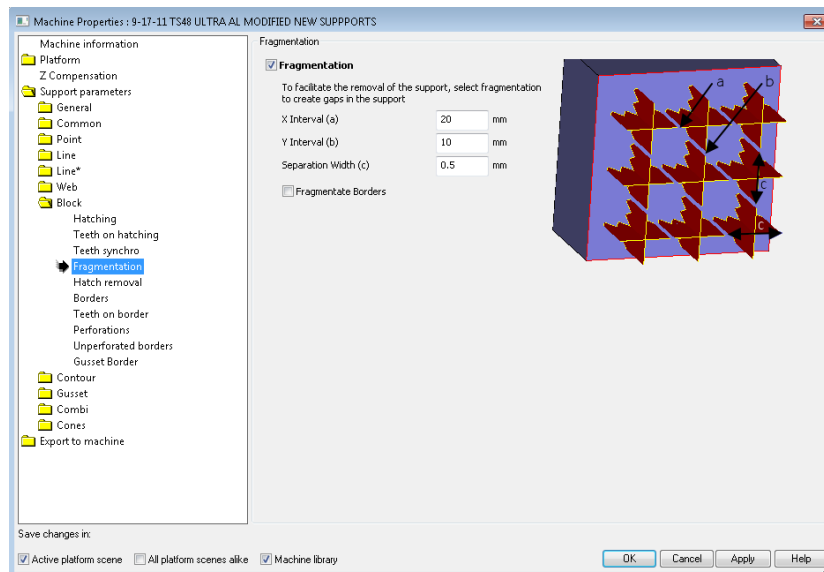


Figure 4.42. Introducing machine settings – fragmentation

This project has been funded with support from the European Commission. This publication [communication] reflects the views only of the authors, and the Commission cannot be held responsible for any use which may be made of the information contained therein.

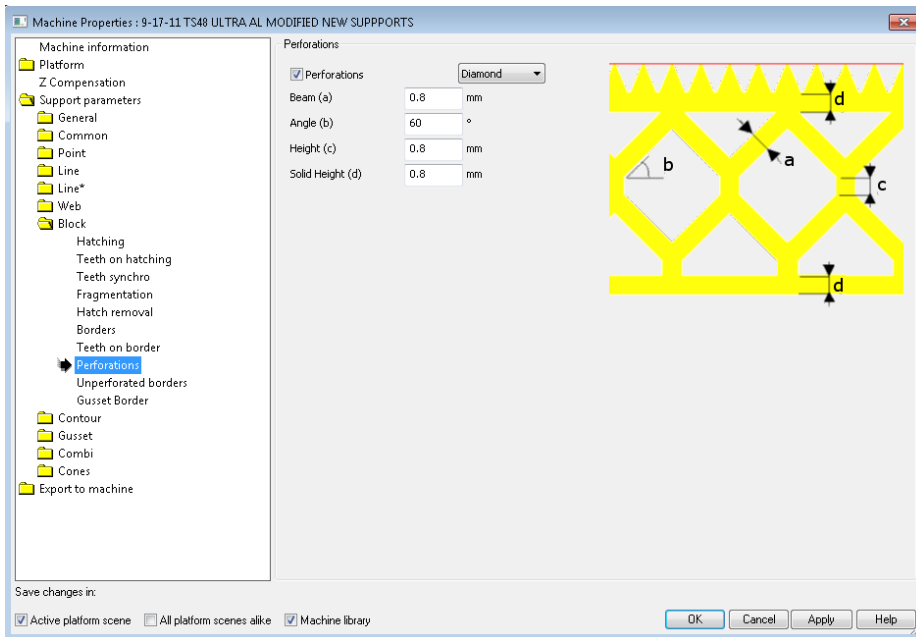


Figure 4.43. Introducing machine settings – block perforations

In Figure 4.43 is defined dimensions for block perforations. In Figure 4.44 is introducing new scene in the software by using card Scenes.

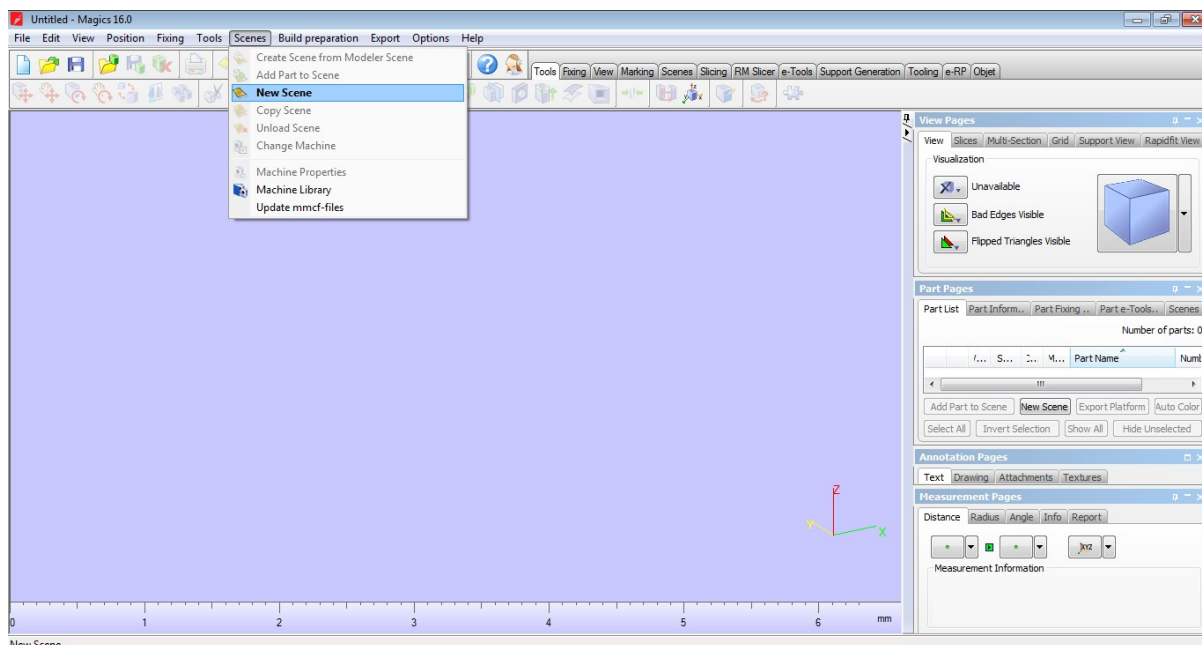


Figure 4.44. New scene

This project has been funded with support from the European Commission. This publication [communication] reflects the views only of the authors, and the Commission cannot be held responsible for any use which may be made of the information contained therein.

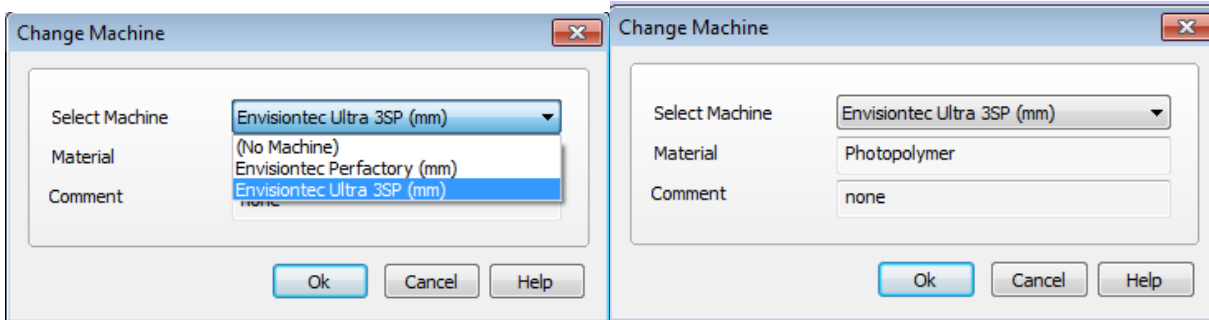


Figure 4.45. Introducing machine settings at new scene

In Figure 4.45 are chosen defined “Envisontec Ultra 3SP” machine. After the definition of machine setting is finished and this needs to be done only once, is possible to continue work with part. Therefore in Figures 4.46 - 4.48 is shown the position and support structure by selection “block” support parameter.

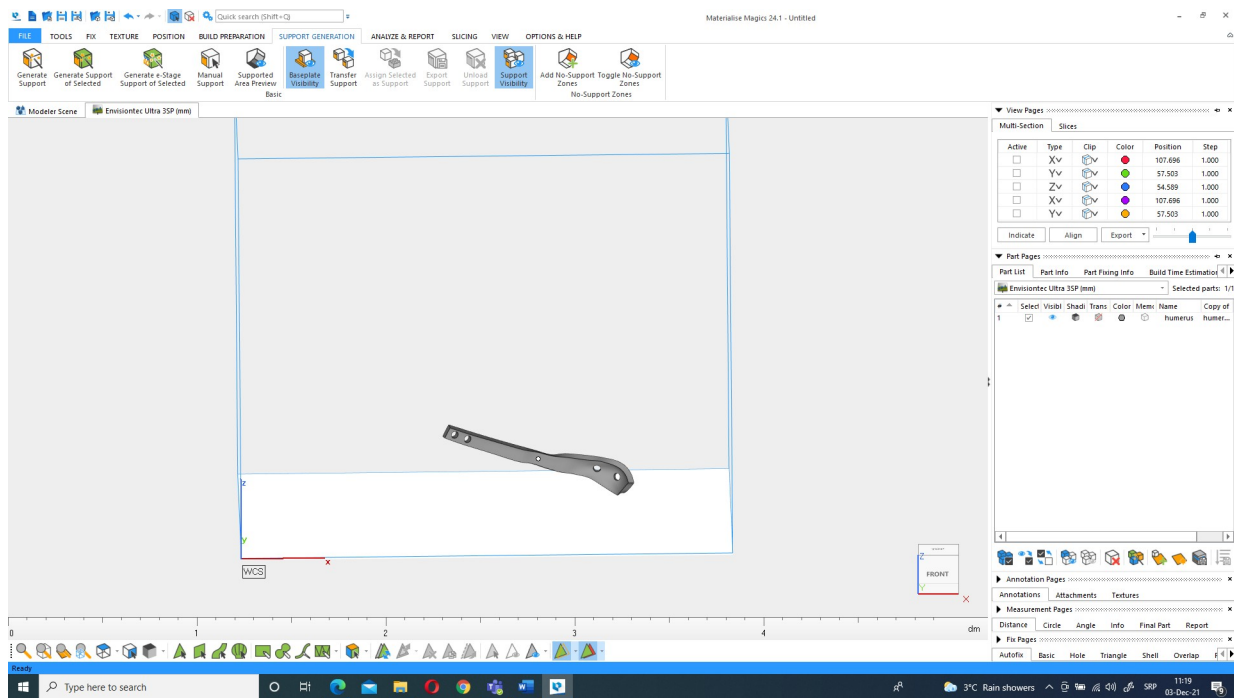


Figure 4.46. Importing part into Material Magics

This project has been funded with support from the European Commission. This publication [communication] reflects the views only of the authors, and the Commission cannot be held responsible for any use which may be made of the information contained therein.

5. Printing of part

The printing process for this part was around 7 hours long. Influence on printing speed is very small comparing to the FDM printing process. Printing process is defined by speed of laser per layer in which there is small difference between big and small image. The most important way to influence the printing speed is the have position of the part has less layers.

Figure 5.49. shows the laser that is on the top over the tank with resin material. Laser is moving left and right and every time makes solidification of one layer. During the printing process, printed part cannot be seen since it is immersed in the tank full of resin. The whole size of printed part is limited with the size of the tank in this architecture of stereolithography printers.



Figure 5.49 Printing of part in the 3D printer

In Figure 5.50 is shows how printed part appears after the printing is finished.

For the postprocessing is important to know that not solidification resin is hazardous and all the operation need to be done so that human skin do not have contact with resin. At Figure 5.51. is shown separation of part with support structure from the platform and in this process is important to use skin protecting gloves. After the part is separated from the platform is very important to clean part as well as platform since for the next printing is important not to contaminate resin in the tank where platform is going to be immersed.

This project has been funded with support from the European Commission. This publication [communication] reflects the views only of the authors, and the Commission cannot be held responsible for any use which may be made of the information contained therein.

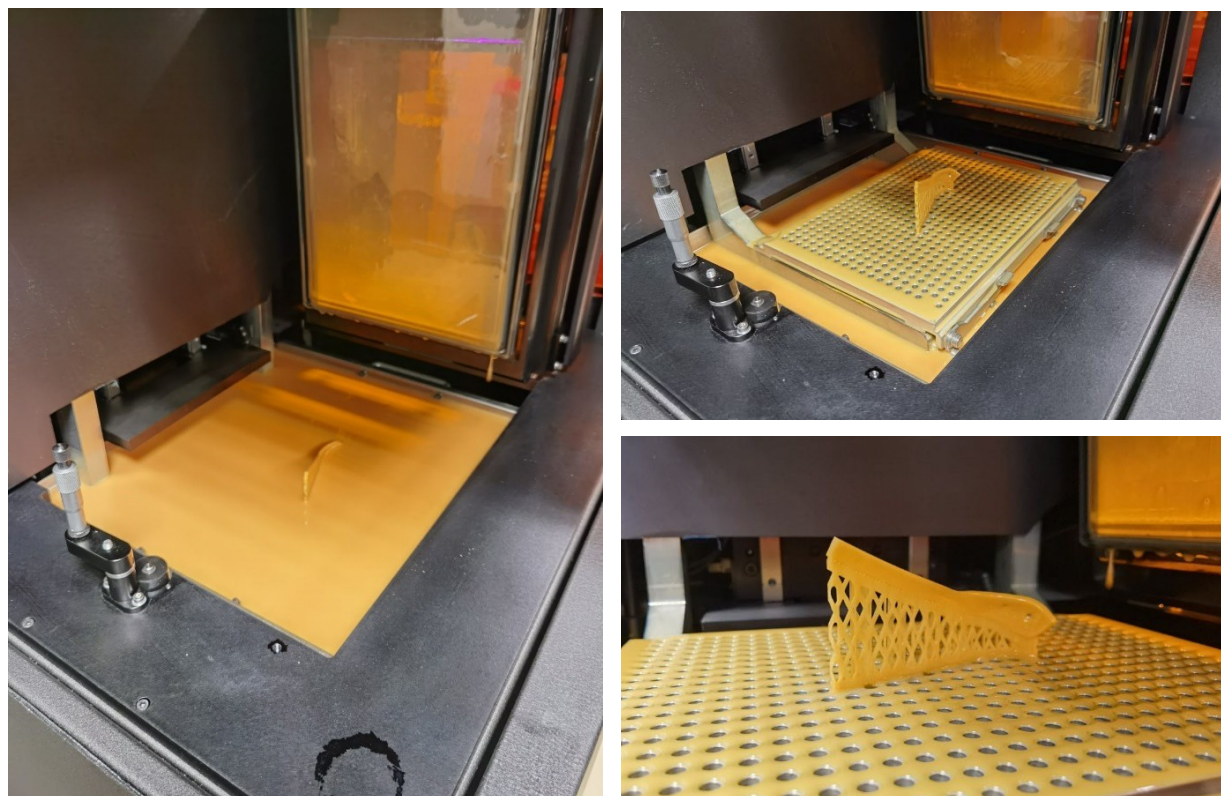


Figure 5.50 Finishing of printing of the part

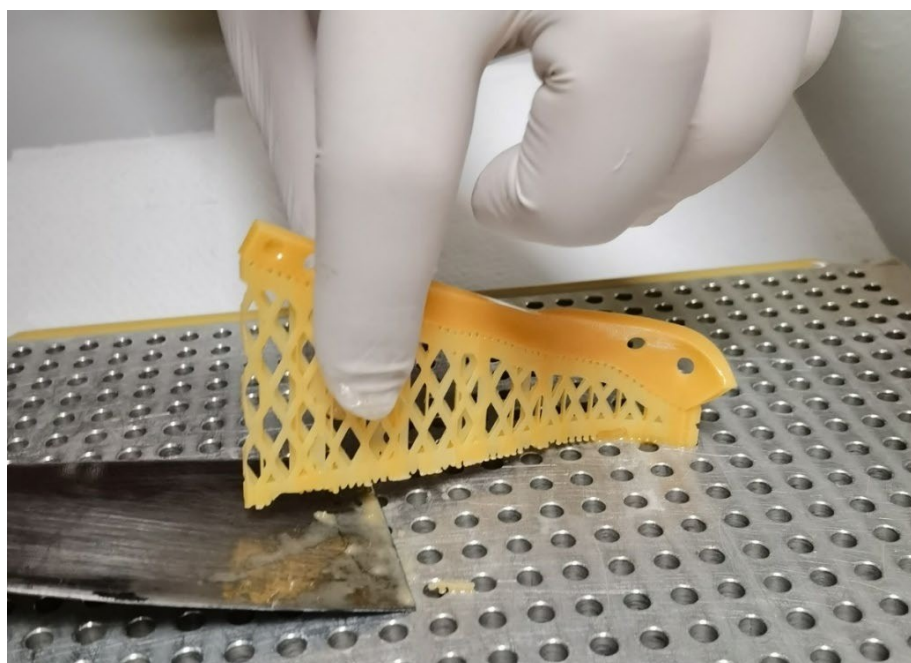


Figure 5.51. Separation of printed part from platform

This project has been funded with support from the European Commission. This publication [communication] reflects the views only of the authors, and the Commission cannot be held responsible for any use which may be made of the information contained therein.

In Figure 5.51 is shown removing of part with support structure from platform by using a spatula. After the part is removed it is necessary to wash it with isopropyl alcohol and it is advised it to put it in some bowl filled with isopropyl alcohol and to wash it and clean with brush.



Figure 5.52. Washing of part in isopropyl alcohol

This project has been funded with support from the European Commission. This publication [communication] reflects the views only of the authors, and the Commission cannot be held responsible for any use which may be made of the information contained therein.

6. Postprocessing

In the Figure 6.53 is shown process of separating support structure from part. If the machine settings are good introduced as it is shown in part 4 this is not going to be problem and there is no dangerous to damage printing part.

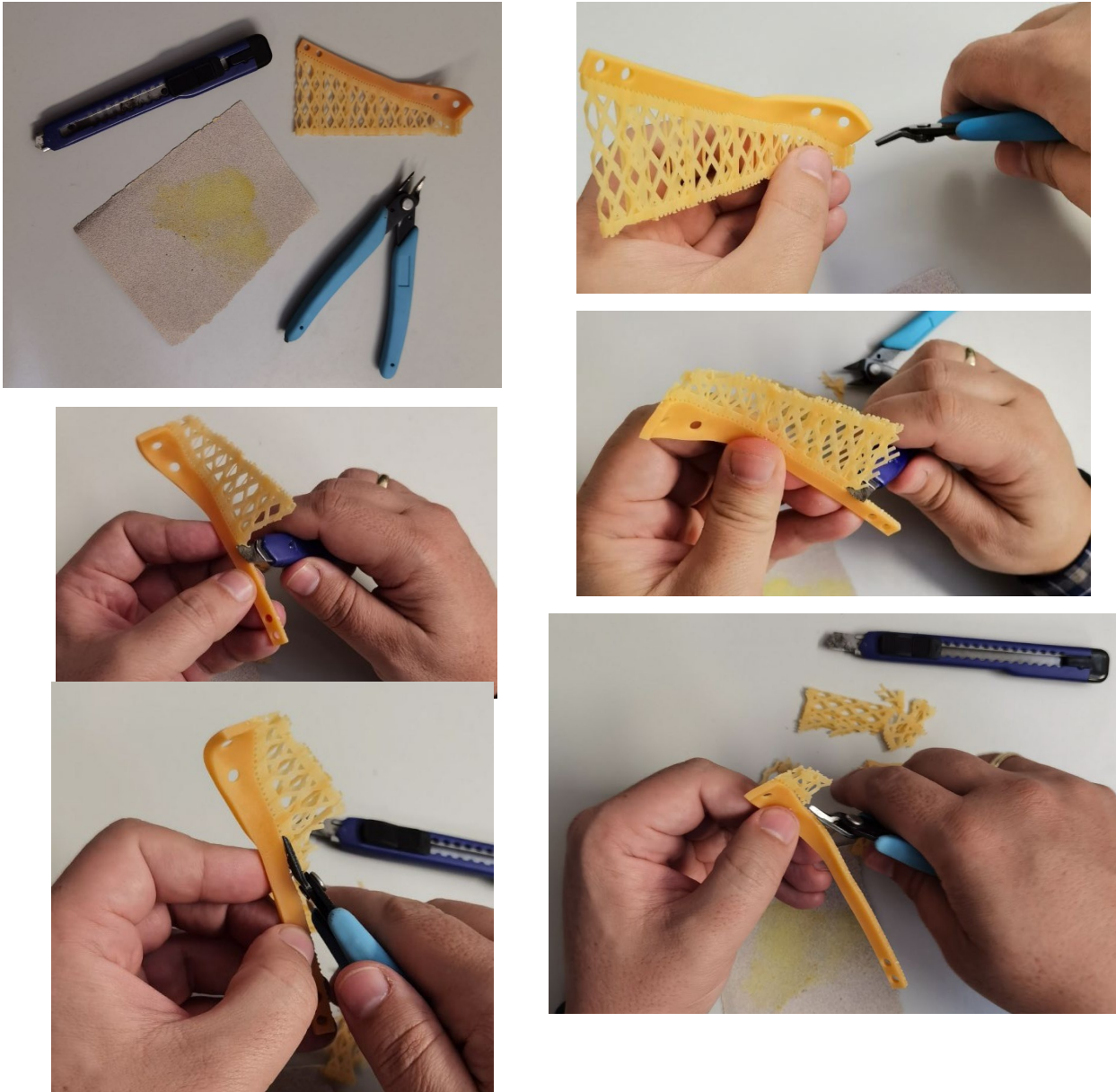


Figure 6.53. Postprocessing of 3D printed part

This project has been funded with support from the European Commission. This publication [communication] reflects the views only of the authors, and the Commission cannot be held responsible for any use which may be made of the information contained therein.



Figure 6.54. Postprocessing of 3D printed part

After separating part from support need to be used sandpaper to make smooth surface where it was connected to the support structure (Figure 6.54).

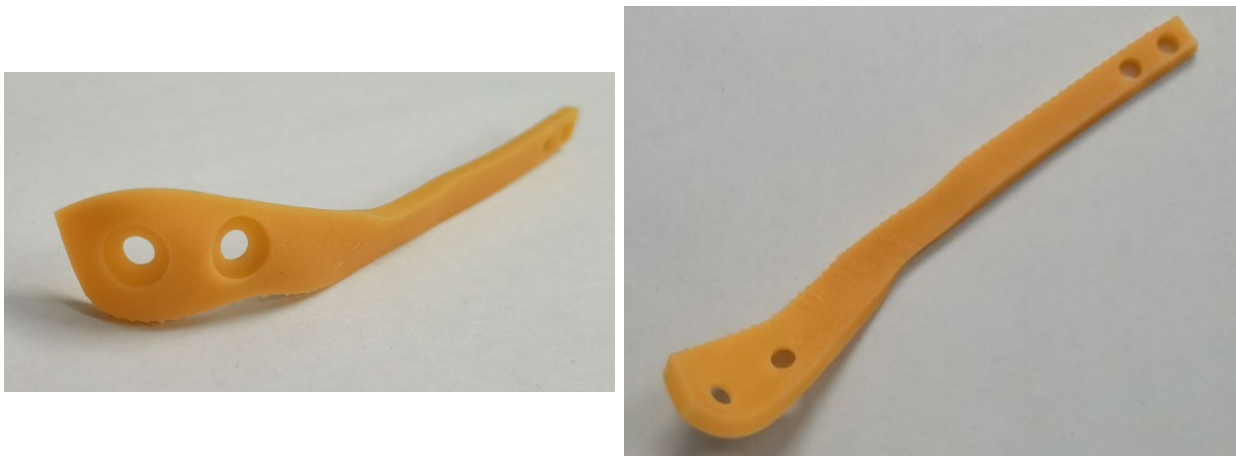


Figure 6.55. Printed part

This project has been funded with support from the European Commission. This publication [communication] reflects the views only of the authors, and the Commission cannot be held responsible for any use which may be made of the information contained therein.

In the Figures 6.55 is shown finished and postprocessed printed part. In Figure .56 is given SLA and FDM printed parts for comparison. Surfaces of SLA printed parts are much finer.



Figure 6.56. Printed part by FDM (up) and Stereolithography (down)

7. Conclusions

In this toolkit is presented printing process with all necessary pre- and postprocessing step as well as machine settings for successful printing of the part – Locking Compression Plates which is used in surgery.

The printing process was done with Envisiontec Ultra 3SP. For the slicer is used Materialise Magics. In this software need to be imported STL file that can be done in almost any CAD software. For Materialise Magics was shown the whole process of machine setting that is important for fine printing and especially for the creating good support structure. In Materialise Magics is done slicing of the part and choosing the support structure as well as positioning the part on the platform.

After the printing process is finished is important to have smooth separation of part from the printing platform as well as support structure from the printed part.

This project has been funded with support from the European Commission. This publication [communication] reflects the views only of the authors, and the Commission cannot be held responsible for any use which may be made of the information contained therein.

Erasmus+ strategic partnership for Higher Education

**BOOSTING THE SCIENTIFIC EXCELLENCE AND
INNOVATION CAPACITY OF 3D PRINTING METHODS
IN PANDEMIC PERIOD**

TOOLKIT 4

METHODOLOGY OF DESIGN AND RAPID MANUFACTURING OF MID-SURGERY SUPPLIES IN OTOLARYNGOLOGY (Fused Filament Fabrication and Vacuum Casting)

Project Title	Boosting the scientific excellence and innovation capacity of 3D printing methods in pandemic period 2020-1-RO01-KA226-HE-095517
Output	IO2 – BRIGHT e-toolkit manual for digital learning in producing medical parts by 3D printing methods in the context of the pandemic
Toolkit	Toolkit 4 Methodology of design and rapid manufacturing of mid-surgery supplies in otolaryngology (Fused Filament Fabrication and Vacuum Casting)
Date of Delivery	November 2021
Authors	Filip Górski, Remigiusz Łabudzki, Magdalena Żukowska, Mate Babic
Version	Final Variant

This project has been funded with support from the European Commission. This publication [communication] reflects the views only of the author, and the Commission cannot be held responsible for any use which may be made of the information contained therein.

Content

1.	Introduction	101
2.	Theoretical background.....	103
2.1.	Otolaryngology.....	103
2.1.1.	Oral tongue anatomy.....	103
2.1.2.	Cancer of the tongue	104
2.1.3.	Diagnostics.....	105
2.1.4.	Tumor removal surgery.....	105
2.2.	Medical imaging.....	106
2.2.1.	CT imaging	106
2.2.2.	MRI imaging.....	108
2.3.	3D printing in preoperative planning	109
3.	Work methodology	113
3.1.	Design methodology.....	113
3.2.	Manufacturing methodology	115
3.3.	DICOM medical imaging.....	116
3.4.	Segmentation of anatomical structures.....	116
3.5.	Processing the 3D mesh	118
3.6.	Design of matrices.....	119
3.7.	3D printing	123
3.8.	Casting of models.....	125
3.9.	Clinical evaluation.....	131
4.	Conclusions	134
	Acknowledgements	134
	References	134

This project has been funded with support from the European Commission. This publication [communication] reflects the views only of the author, and the Commission cannot be held responsible for any use which may be made of the information contained therein.

1. Introduction

Otolaryngology is one of the branches of medicine dealing with the diagnosis and treatment of disease problems arising within the head and neck. This range also includes ailments related to the tongue and salivary glands [1]. Cancer of the tongue is one of the most common malignancies in the oral cavity. A tongue tumor can grow relatively quickly and spread deep into the muscles of the tongue [2]. It is recommended that the resulting lesions undergo tumor resection [3]. This procedure involves radical removal of the tumor, and the operation is highly demanding due to the difficulty of accessing the tumor, it may lead to trismus or massive bleeding.

After tumor resection, a cavity remains, which must be reconstructed using the patient's tissues. Failure to accurately reconstruct the language is associated with the following problems such as difficulty swallowing, problems with articulation, which can lead to psychological problems.

Proper preoperative planning is essential for successful tumor resection and tongue tissue reconstruction. Exercises on an individualized language model can significantly improve the work of medical personnel in preoperative planning.

The answer to the need for thorough preoperative planning is to create a personalized object that reflects the shape, size and mechanical properties of anatomical structures. One-to-one creation of an individualized model is possible and cost-effective thanks to the additive manufacturing technique. It is a modern technology that allows for accurate reproduction, lowcosts, even of small objects.

The subject of the work is to present the methodology of designing and rapid production of intraoperative aids in otolaryngology. This paper presents the analysis and selection of medical data processing tools, programs for their design, and a comparison of the manufactured intraoperative tools using various methods of additive technology or the use of different materials. One of the initial assumptions of the work is the analysis and selection of medical data processing methods as well as the analysis of design tools and techniques for the rapid production of intraoperative aids. After the compilation of data, a project of intraoperative aids will be carried out with the use of various techniques of rapid production. The obtained models will be analyzed and assessed with the participation of medical personnel. On the

This project has been funded with support from the European Commission. This publication [communication] reflects the views only of the author, and the Commission cannot be held responsible for any use which may be made of the information contained therein.

basis of the above-mentioned activities, the last step will be to develop a standardized methodology of conduct and recommendations for further development.

The forms of individual goals include:

- theoretical part, this chapter is devoted to the description of the most important terms mentioned in this work and to the presentation of the achievements so far in the field of intraoperative planning with the use of incremental techniques,
- a methodological part to present the concept of the project and to present the action plan in a descriptive and graphic manner,
- a validation part, containing the general assessment of the produced models, presenting the results of a survey conducted with the participation of medical personnel and comparing the data from 3D scanning of the resulting models with their virtual designs in order to capture shape change errors.

The input data used in this study were medical imaging performed by magnetic resonance imaging of a patient referred for a tongue tumor resection.

This toolkit is based on cooperation between engineers from Poznan University of Technology and doctors from Poznan University of Medical Sciences. It has been presented with great detail in a master's thesis cited in the acknowledgement section.

This project has been funded with support from the European Commission. This publication [communication] reflects the views only of the authors, and the Commission cannot be held responsible for any use which may be made of the information contained therein.

2. Theoretical background

2.1. Otolaryngology

Otolaryngology, also known as otorhinolaryngology, is a science dealing with the diagnosis and treatment of diseases of the ears, nose and nasal sinuses, larynx (voice box), oral cavity and upper pharynx (mouth and pharynx), as well as structures of the neck and face [4]. Traditionally, in medical practice, treating the ear has been equated with treating the eye. With the development of ENT at the end of the 19th century, the relationship between the ear and throat was known, and otologists became involved with ENT specialists [5].

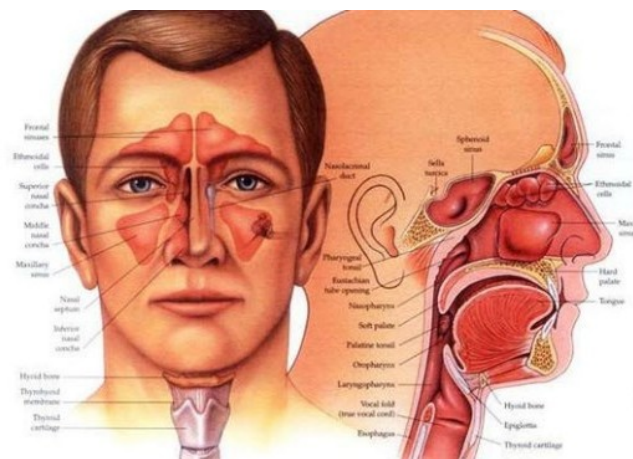


Fig. 2.1 Anatomical representation of otolaryngology [4]

2.1.1. Oral tongue anatomy

The tongue (Latin lingua) is a muscular organ in the mouth of vertebrates. Language is the organ of communication, speech, and articulation, and is the main structure that shapes and controls food during chewing and swallowing. It is a complex muscular structure covered with a specialized layer of mucosa, anatomically composed of twin structures such as muscles, veins, arteries and nerve supplies that connect to each other in the lingual septum [6]. The tongue is covered with moist pink tissue called the mucosa. Small bumps called papillae give the tongue a rough texture. Thousands of taste buds cover the surfaces of the papillae. The taste buds are a collection of nerve-like cells that connect to the nerves that go to the brain [7].

This project has been funded with support from the European Commission. This publication [communication] reflects the views only of the authors, and the Commission cannot be held responsible for any use which may be made of the information contained therein.

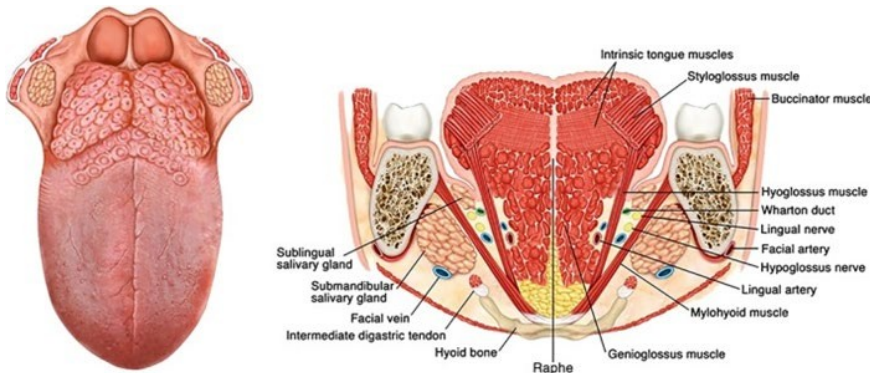


Fig. 2.2 Graphical representation of the anatomy of the tongue [8]

The tongue is anchored in the mouth with a net of hard tissue and mucosa. The loop that holds the front of the tongue down is called the frenulum. At the back of the mouth, the tongue is anchored to the hyoid bone [9].

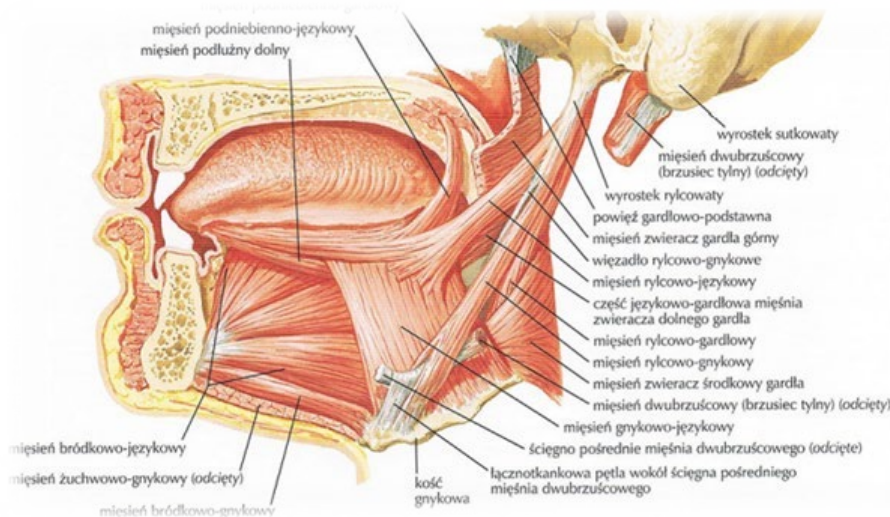


Fig. 2.3 Anatomical representation of the lateral side of the tongue

2.1.2. Cancer of the tongue

Oral cancer appears as a growth or pain in the mouth that does not go away [10]. Oral cancer, which includes cancers of the lips, tongue, cheeks, floor of the mouth, hard and soft palate, sinuses, and pharynx (pharynx) can be life-threatening if not diagnosed and treated early on.

This project has been funded with support from the European Commission. This publication [communication] reflects the views only of the authors, and the Commission cannot be held responsible for any use which may be made of the information contained therein.

Oral cancer is treated in the same way as many other cancers - with surgery to remove cancerous growths, followed by radiation therapy and / or chemotherapy (medications) to destroy any remaining cancer cells [11].

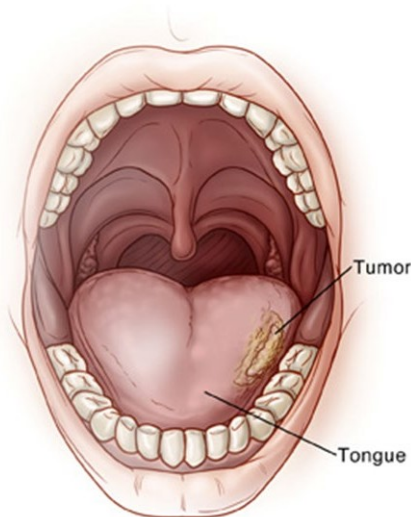


Fig. 2.4 Oral cavity with cancer of the tongue [11]

2.1.3. Diagnostics

The diagnostic test begins with an interview with the patient and an otolaryngological examination, i.e. an examination performed by an ENT doctor. Diagnosing a tumor in a person with tongue cancer is very difficult as pain, drooling and tongue immobilization are common. It is also difficult to detect metastases and determine the resection area [12]. In order to accurately diagnose the patient, modern imaging methods such as MRI or CT should be performed [13].

2.1.4. Tumor removal surgery

The term "glossectomy" is used to describe various surgical procedures for resection of tumors in the tongue [14].

Over time, the technical methods of tongue cancer resection have evolved. In the last century, most early and intermediate stage cancers of the tongue have been treated by partial glossectomy with a margin of approximately 0.5-1 cm from the macroscopic borders of the tumor [15]. At the beginning of this century, the more common approach was a broad resection with a larger free margin of macroscopic (1.5–2 cm) [16].

Today we can better plan the removal of tumors from the tongue thanks to a better understanding of the superficial and deeper local spread of the tumor along muscles, nerves

This project has been funded with support from the European Commission. This publication [communication] reflects the views only of the authors, and the Commission cannot be held responsible for any use which may be made of the information contained therein.

and vessels. Improving imaging techniques that allow surgeons to assess the involvement of each muscle, nerve, and veins in the tongue.

Complete tumor resection is an axiom of oncological surgery. Oral cancer ablation is difficult due to its anatomical, functional and aesthetic nature. Anatomical surgical planning plays an important role in achieving complete resection. The use of cross-sectional imaging, anatomical features and spatial awareness of the tumor is extremely important in planning oral cancer resection.

Usually, an indispensable step in removing a tongue tumor is also excision of the muscles and mucosa. After the procedure, a cavity remains, which is reconstructed with the patient's own tissues. A flap is collected in the form of a skin fragment with vessels from the neck, forearm or thigh. Once the wounds have healed and the rehabilitation process is complete, the patient can move his tongue, swallow, and communicate properly [3].

2.2. Medical imaging

2.2.1. CT imaging

Computed tomography scan is a medical imaging technique used in radiology for the non-invasive acquisition of detailed body images for diagnostic purposes. Personnel performing computed tomography are called radiologists or radiology technologists [17, 18].

CT scanners use a rotating X-ray tube and a row of detectors placed in a gantry (peri) to measure the attenuation of X-rays by various tissues inside the body. Multiple X-ray measurements taken from different angles are then processed on a computer using reconstruction algorithms to produce tomographic (cross-sectional) images of the body. The use of ionizing radiation sometimes limits its use due to its adverse effects. However, CT can be used in patients with metal implants or pacemakers for whom MRI is contraindicated [19].

This project has been funded with support from the European Commission. This publication [communication] reflects the views only of the authors, and the Commission cannot be held responsible for any use which may be made of the information contained therein.



Fig. 2.5 The course of the CT examination [20]

During the test, data is entered into the computer's hard drive. The information obtained from the x-rays is processed by computer to obtain an easy-to-read image. With the help of a complex analysis, taking into account the amount of radiation absorbed during the irradiation of the object from a given side, black and white images are generated showing the cross- sections of the examined organ. Moreover, computer processing is possible to obtain a spatial reconstruction of given organs. Each of the sections is divided into small parts - voxels, representing a fragment of the imaged volume. Each voxel is assigned numerical values proportional to its absorption of radiation [21].

This project has been funded with support from the European Commission. This publication [communication] reflects the views only of the authors, and the Commission cannot be held responsible for any use which may be made of the information contained therein.

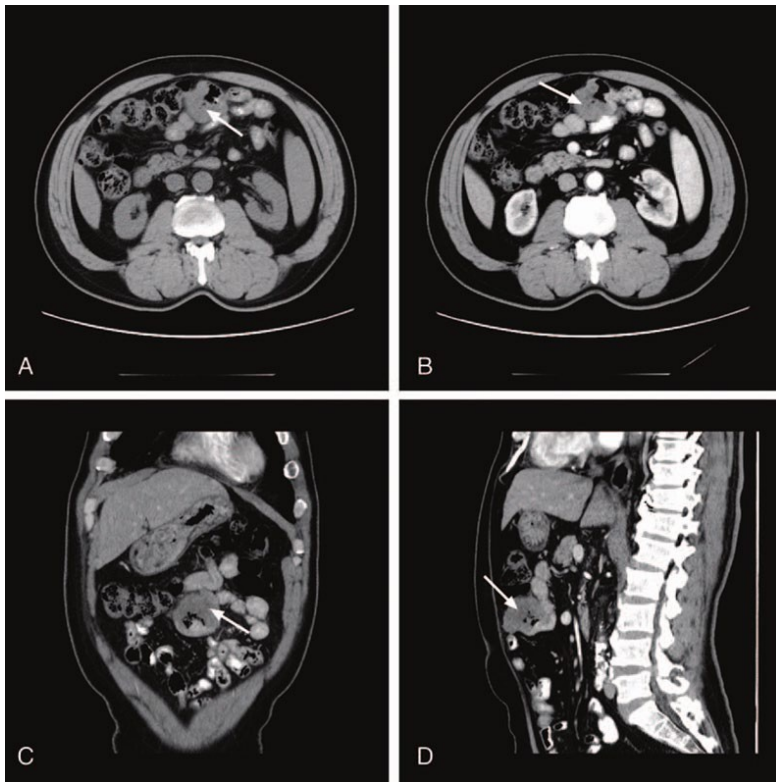


Fig. 2.6 Example of CT imaging result [22]

2.2.2. MRI imaging

Magnetic resonance imaging is a technique used in radiology to create images of the anatomy and physiological processes of the body. MRI scanners use strong magnetic fields, magnetic field gradients, and radio waves to generate images of organs in the body. During this imaging, no harmful X-rays or ionizing rays are produced, which distinguishes them from CT and PET scans [23].

MRI imaging enables excellent soft tissue differentiation, contrast, high spatial resolution and does not use harmful radiation. These features make MRI a valuable tool in the clinical and surgical environment, particularly useful in the diagnosis of neoplastic lesions [24].

This project has been funded with support from the European Commission. This publication [communication] reflects the views only of the authors, and the Commission cannot be held responsible for any use which may be made of the information contained therein.

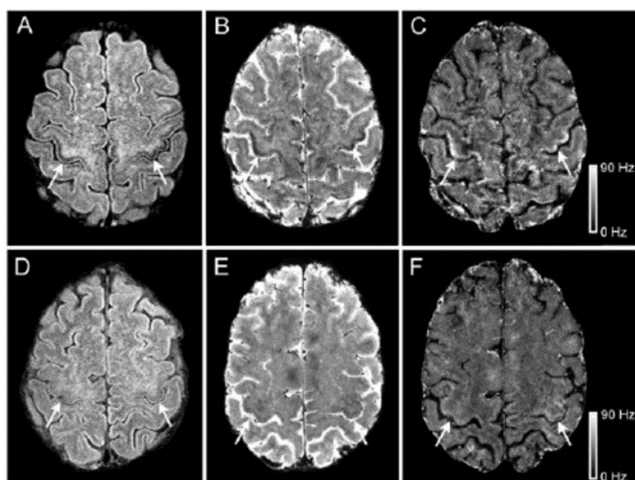


Fig. 2.7 Result of MRI of the brain [25]

2.3. 3D printing in preoperative planning

At the Greenberg Women's Health Center in the Ottawa Hospital, Maureen was treated. She had nearly 50 fibroids and did not want to undergo a hysterectomy, a complete removal of the uterus, so that she could become pregnant in the future. To this end, doctors contacted the hospital's 3D printing laboratory. Based on medical imaging data, a model was printed using acrylic and plastic. Multiple fibroids in the uterine cavity made printing very difficult and each had to be identified to recreate the exact anatomy on a 3D-printed model. Doctors commented that having the 3D model was tremendously helpful and provided a good visual aspect. The model and images from the imaging were also used during the operation itself, as the doctors could rotate the image of the uterus at any angle and degree so that they could see the object from different perspectives, which was helpful during the operation. The 3D-printed models not only help surgeons, but also help patients like Maureen understand their disease and prepare for surgery. For patients, seeing a 3D model of the problem inside their body makes it tangible and real. The operation was a success and the hospital is already working on similar projects to provide women with alternatives for complicated surgeries [26].

This project has been funded with support from the European Commission. This publication [communication] reflects the views only of the authors, and the Commission cannot be held responsible for any use which may be made of the information contained therein.



Fig. 2.8 3D model of the uterus with myomas [27]

In India, a patient with a tumor of the tongue was cured at the HCG Cancer Hospital, which specializes in the treatment of malignant tumors, thanks to the use of 3D printing. A 53-year-old woman had an extensive malignant tumor of the tongue, which was much larger than expected prior to the medical imaging analysis. As the team had difficulties in planning the operation, it was decided to use the Anatomiz 3D software to design a model and then print it.

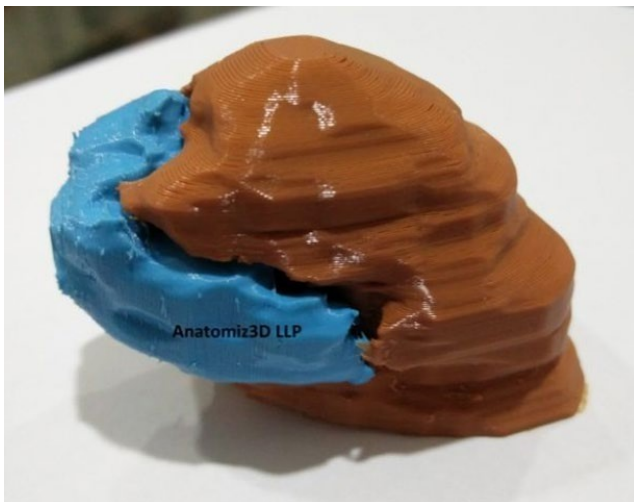


Fig. 2.9 Printed model of the tongue with its tumor [28]

For this, flexible materials were used and two separate, matching parts in different colors were printed and folded together. The model helped to understand the anatomy, depth, size and position of the tumor compared to the tongue. As a result, the staff was better prepared,

This project has been funded with support from the European Commission. This publication [communication] reflects the views only of the authors, and the Commission cannot be held responsible for any use which may be made of the information contained therein.

and the patient himself was properly acquainted with the course of the surgery thanks to the presentation of the printed models [29].

At the Poznań University of Technology, in order to create an appropriate intraoperative aid, an anatomical model of the kidney was designed, together with its tumor and blood vessels, which were then produced using rapid prototyping techniques. Models were also designed on the basis of medical imaging and then processed in dedicated programs. However, in this case the final model was not completely printed, here a mold, tumor and blood vessels were produced by rapid prototyping techniques. The printed parts were attached to a matrix and then covered with a silicone material resembling the structure of the kidney after solidification. The model reflects the personalized nature of the organs and tumor of a given patient [30].

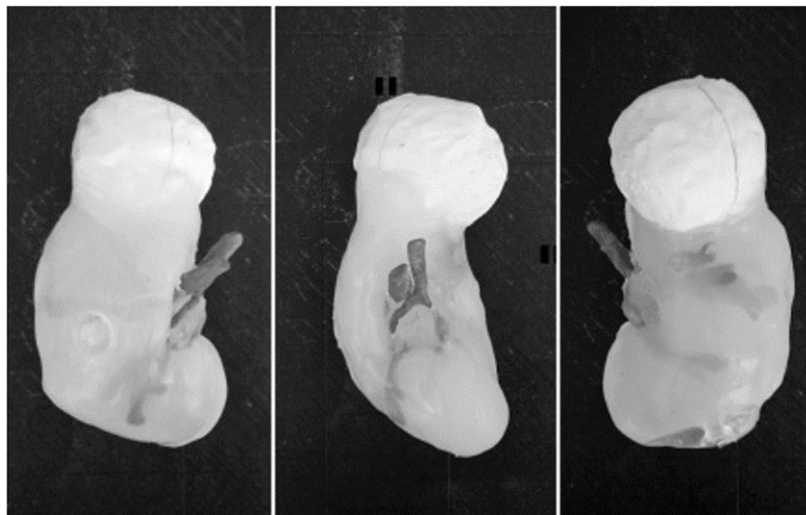


Fig. 2.10 Finished kidney model [30]

In the Małopolska Ultrasound Workshop, models are used to diagnose fetal heart defects developed by Dr. n. med. Marcin Wiecheć and the company GRID in Krakow. Examination of the fetal heart is very difficult because the organ contracts with a high frequency, which is difficult to interpret only by ultrasound, and the fetus often changes its position, making it difficult to diagnose any heart defects. Initially, during the first training trials, the doctors used only 2D and 3D images made with the use of ultrasound. However, this message was found not to influence doctors sufficiently. To stimulate the imagination of gynecologists, it was decided to create 3D models that can be further unfolded thanks to the introduced magnets. It should be added that these models not only have a positive impact on the education of

This project has been funded with support from the European Commission. This publication [communication] reflects the views only of the authors, and the Commission cannot be held responsible for any use which may be made of the information contained therein.

doctors, but also patients, and in this case parents are able to understand the problem in a much better way, which was not easy only when presenting 2D diagrams or images [31].



Fig. 2.11 3D model of the fetal heart [32]

This project has been funded with support from the European Commission. This publication [communication] reflects the views only of the authors, and the Commission cannot be held responsible for any use which may be made of the information contained therein.

3. Work methodology

3.1. Design methodology

MIMICS is a medical engineering software based on 3D images that converts an image into a 3D model and allows you to scale objects. Opportunities for participation in this program range from research and development to major clinical operations [33].

3D Slicer is computer software designed to solve advanced problems related to image processing, with an emphasis on clinical and biomedical applications. Development platform for rapidly building and implementing custom solutions for research and commercial products using free and open source software [34].

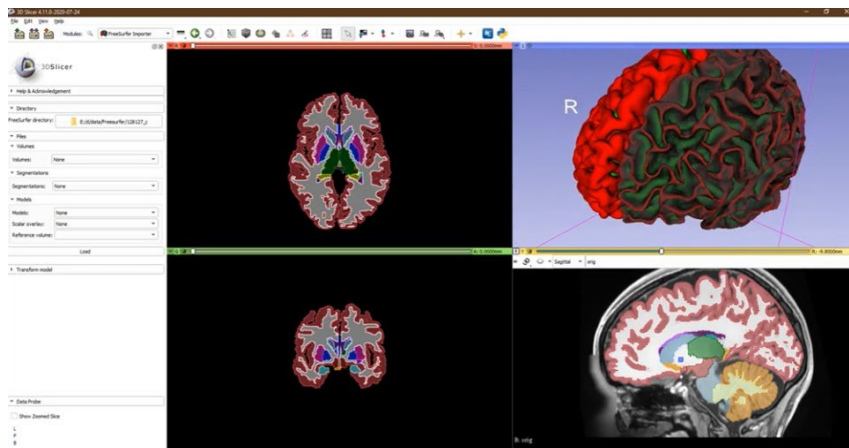


Fig. 3.1 Introduction to the 3D Slicer program [34]

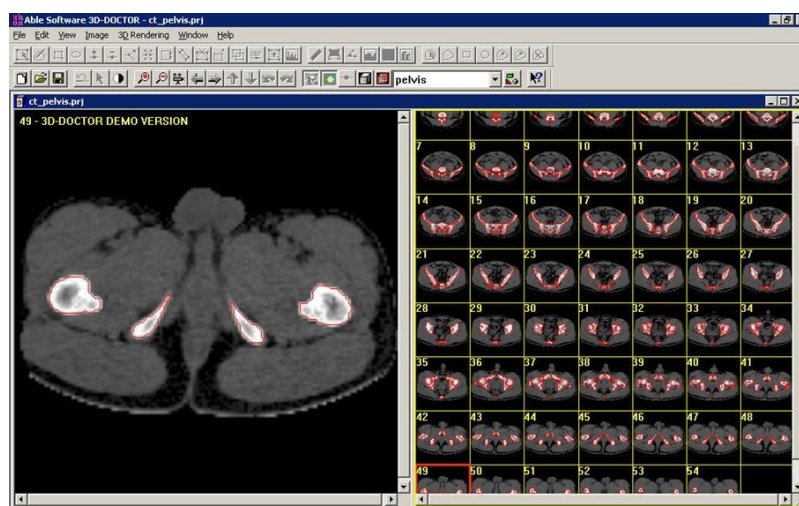


Fig. 3.2 Presentation of the program in the demo version of 3D-Doctor [35]

This project has been funded with support from the European Commission. This publication [communication] reflects the views only of the authors, and the Commission cannot be held responsible for any use which may be made of the information contained therein.

InVesalius is a free medical software for generating virtual reconstruction of structures in the human body. Based on two-dimensional images obtained with computed tomography or MRI equipment, the software generates virtual three-dimensional models corresponding to the anatomical parts of the human body. After building 3D DICOM images, the software allows you to generate STL files. These files can be used for rapid prototyping [36].

For research purposes, the InVesalius program was used in this work. It meets all the requirements needed for the research, allows you to change the format and segment the structure in 3D. The program is available in a free version and its use is very intuitive.

Meshmixer is a prototype design tool based on high-resolution dynamic triangle meshes. We are exploring new possibilities for this surface representation for interactive design and manufacturing in the context of a practical system that we make available to the public.

Blender is a free and open source 3D computer graphics toolkit used to create animated movies, visual effects, art, 3D printed models, motion graphics, interactive 3D applications, virtual reality, and computer games. Blender features include 3D modeling, UV unwinding, texturing, raster graphics editing, rigging, and skinning, fluid and smoke simulation, particle simulation, soft body simulation, sculpting, animation, match moving, rendering, motion graphics, video editing and composing [37].

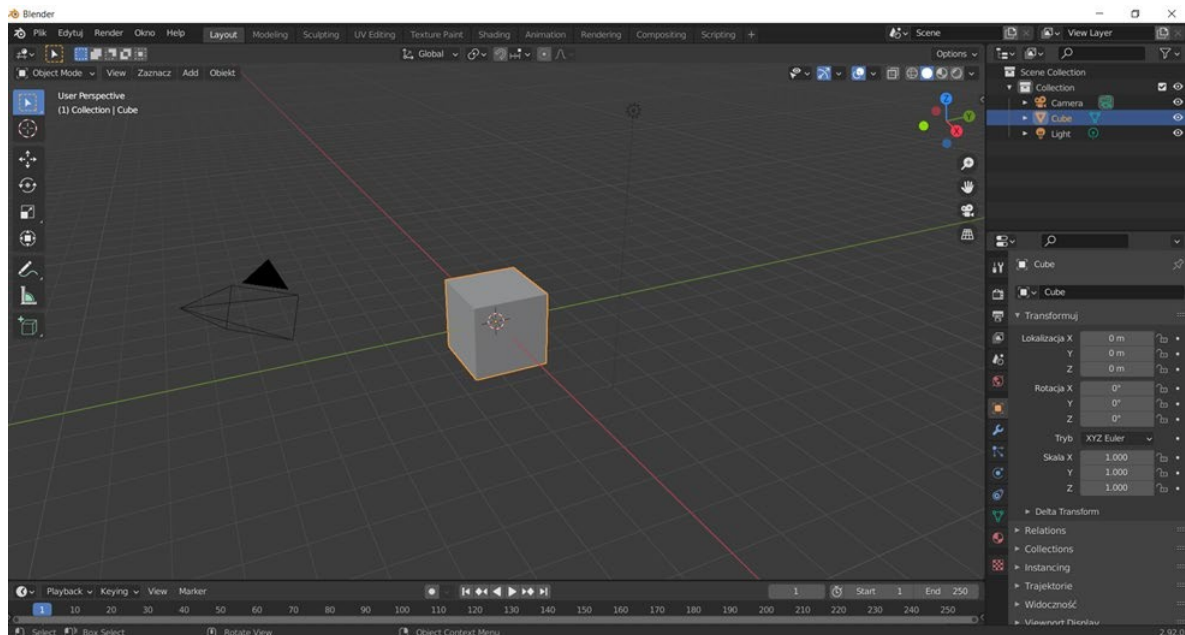


Fig. 3.3 Blender software window view

Due to the ease of use, the Meshmixer system was selected for the purposes of the study.

This project has been funded with support from the European Commission. This publication [communication] reflects the views only of the authors, and the Commission cannot be held responsible for any use which may be made of the information contained therein.

3.2. Manufacturing methodology

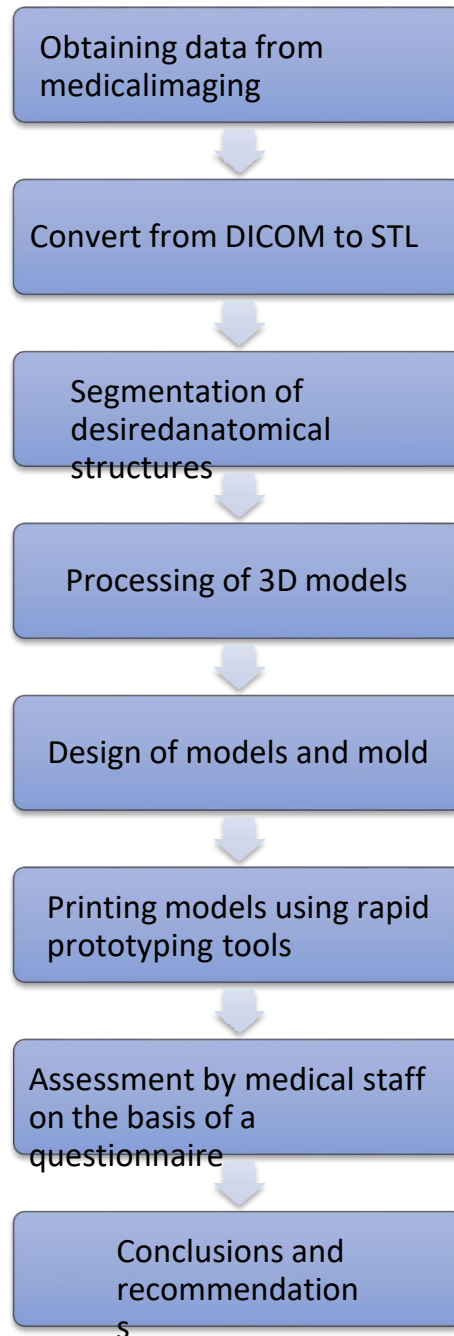


Fig. 3.4 Diagram of the organization of the conducted research

This project has been funded with support from the European Commission. This publication [communication] reflects the views only of the authors, and the Commission cannot be held responsible for any use which may be made of the information contained therein.

3.3. DICOM medical imaging

On the basis of cooperation between the Poznań University of Technology and the Clinical Hospital of Heliodor Święcicki of the Medical University of Karola Marcinkowski in Poznań, the data provided in the form of DICOM from MRI imaging for the conducted research was one of the patients. These photos show an MRI of the head, and the area of interest is the tongue and the tumor of the tongue. One of the first steps was to import data from imaging to InVesalius 3.1. It enabled the conversion of the file from the DICOM standard to the STL format and setting the parameters, the thickness of a single layer is 1 mm.

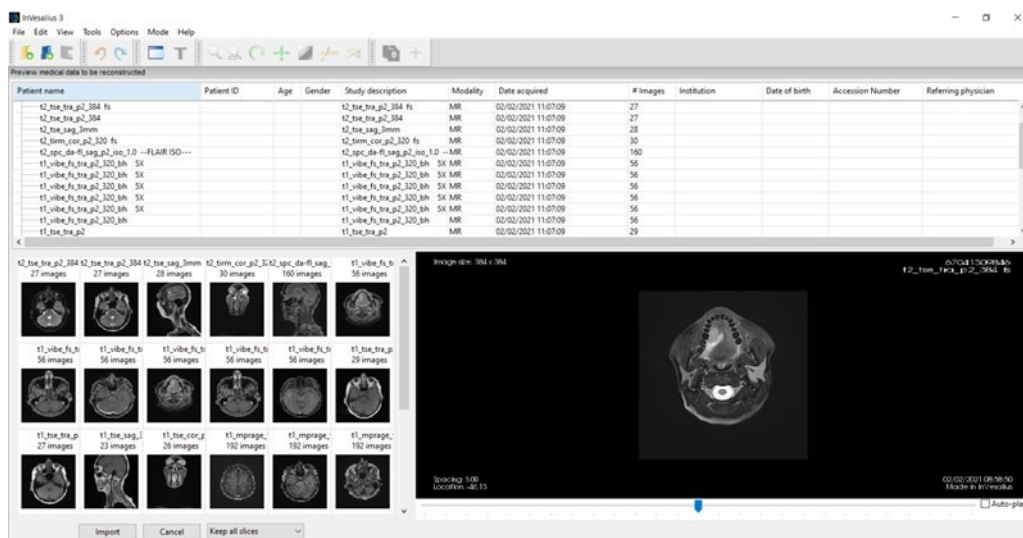


Fig. 3.5 Data import in InVesalius 3.1.

Data import to the program allowed to generate images of the skull as a 3D model, which made it easier to locate and measure the structures of the tongue and its tumor. The malignant neoplasm of a given patient is located on the right side of the tongue, however, the complete diagnosis of the lesion was relatively difficult, therefore a radiological consultation was performed for this purpose.

3.4. Segmentation of anatomical structures

Then in InVesalius 3.1. the segmentation of the structures of the tongue and its tumor was carried out. Various taskbars appear on the screen after the data is imported. On the left side you can see the image manipulation tools and on the right side there are windows showing the same three-dimensional image in 3 different planes. There are sliders next to each of the

This project has been funded with support from the European Commission. This publication [communication] reflects the views only of the authors, and the Commission cannot be held responsible for any use which may be made of the information contained therein.

windows, which are used to change the viewed cross-section. Below is a 3D image of a patient's skull with a tongue tumor.

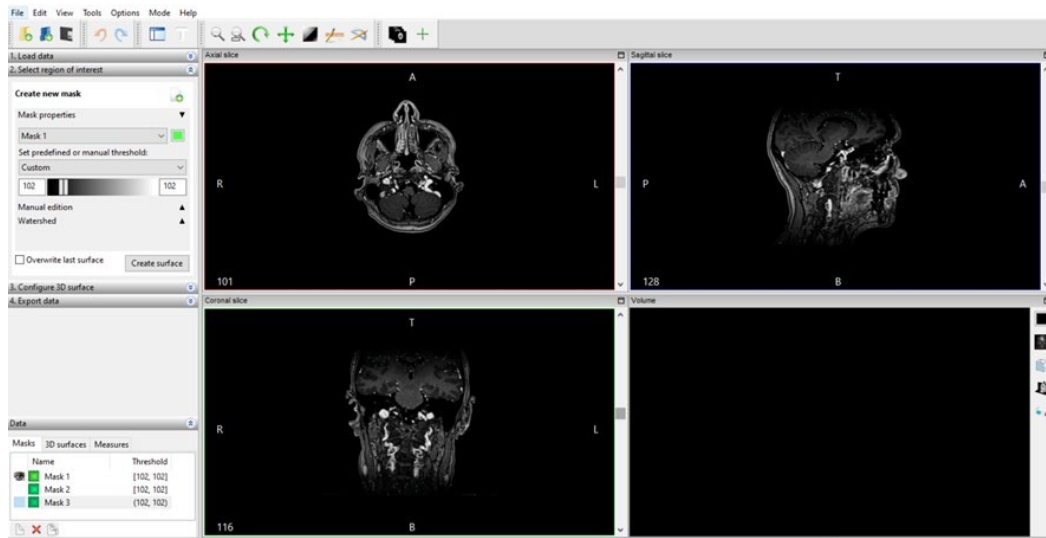


Fig. 3.6 Presentation of imported files in the InVesalius program

In order to segment the structures, it was necessary to set the appropriate mask properties, so as to manually perform the segmentation, layer by layer, of anatomical structures such as the tongue and the tumor of the tongue. For this purpose, the predefined or manual threshold has been selected as custom in the properties of the mask, so that in the further happiness of segmentation, you can only change the type and size of the brush or the erasing element.

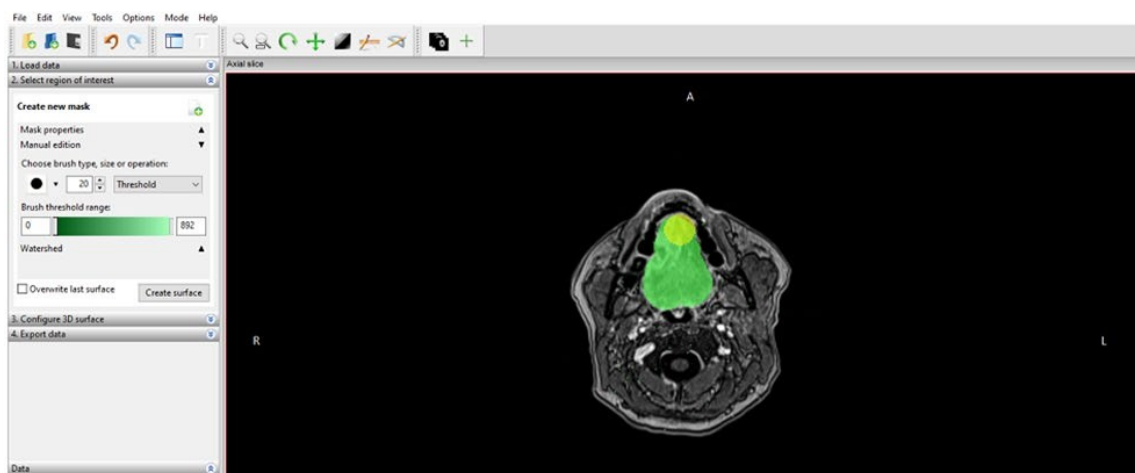


Fig. 3.7 Screenshot taken during tongue segmentation

This project has been funded with support from the European Commission. This publication [communication] reflects the views only of the authors, and the Commission cannot be held responsible for any use which may be made of the information contained therein.

The effects of the work described above are presented below:

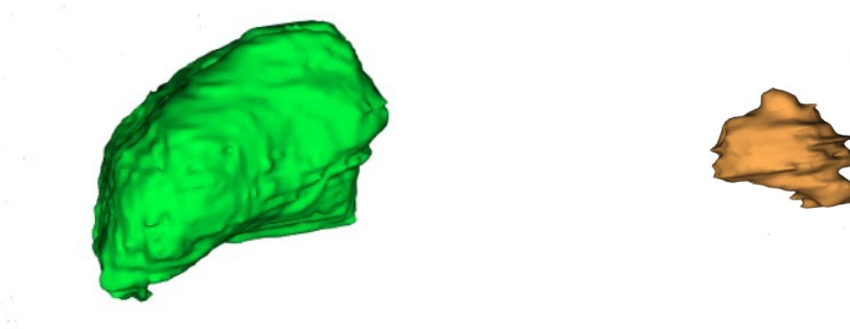


Fig. 3.8 On the left side there is a segmented model of the tongue and on the right side is its tumor

Since the segmentation was based on the isolation of structures layer by layer, the models are characterized by significant inequalities. These structures are not yet suitable for printing or for creating casting matrices, so the next step will be to process the model.

3.5. Processing the 3D mesh

In order to make the models as real as possible and to facilitate the printing of individual models, they were processed using the GOM Inspect Suite system. For this purpose, several functions were used, such as smoothing, selecting surface triangles, closing holes interactively/automatically. The most frequently used function when machining models was smoothing, you can find it by opening the operation options and going to the mesh, as shown in the figure below

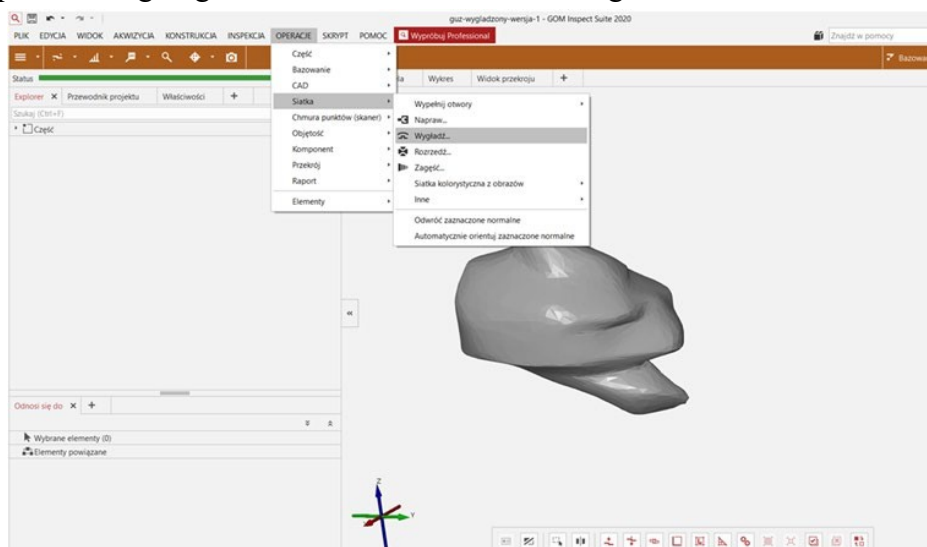


Fig. 3.9 GOM Inspect Suite

This project has been funded with support from the European Commission. This publication [communication] reflects the views only of the authors, and the Commission cannot be held responsible for any use which may be made of the information contained therein.

The results of the operations performed for both models are presented below:

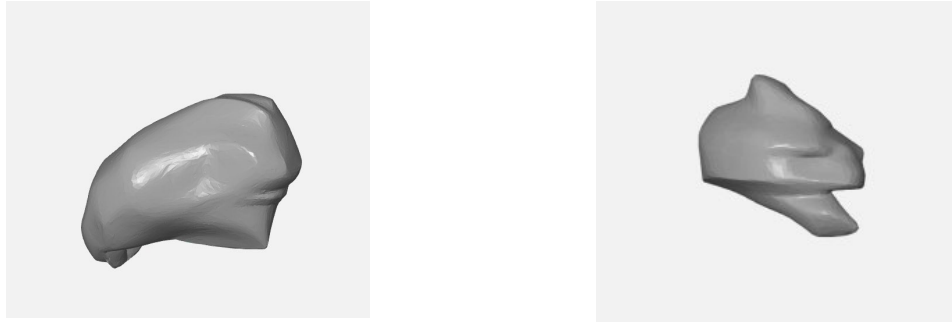


Fig. 3.10 The final effect of machining the models from the left tongue on the right tumor

3.6. Design of matrices

The last of the design elements was the preparation of molds for the tongue with the tumor and the tumor itself. For this purpose, the Meshmixer program and the STL models designed at that time were used. In both cases, the first step was to import the designed models. Then, overflow and venting channels with a diameter of 6 [mm] were added to each of the models, located in the tops of the models, and infusions placed on the side and in the center of the models for the tongue form with a tumor with a diameter of 11 [mm], for the tumor the diameter was the same dimensions every transfer, that is, it measured 6 [mm]. For this purpose, the cylinder-shaped objects already in the program were added, and then they were sized and positioned in the appropriate places using the transform function in the edit function tools.

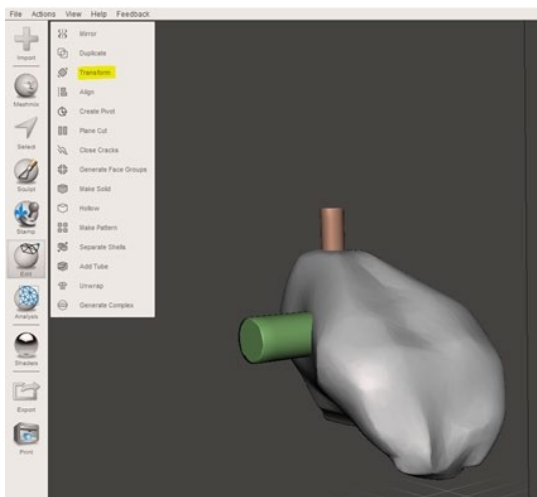


Fig. 3.11 Designing an overflow using the transform function

This project has been funded with support from the European Commission. This publication [communication] reflects the views only of the authors, and the Commission cannot be held responsible for any use which may be made of the information contained therein.

After creating the infusion and overflow, you had to select these elements together with the model, open the edit option in the taskbar again, but this time the Make Solid option was selected, setting Solid Accuracy and Mesh Density to the maximum possible values as in Figure 5.7, if the object had any kind of holes this function could be performed. Setting these functions was required so that the next operation, which will be subtracting models, could be performed correctly.

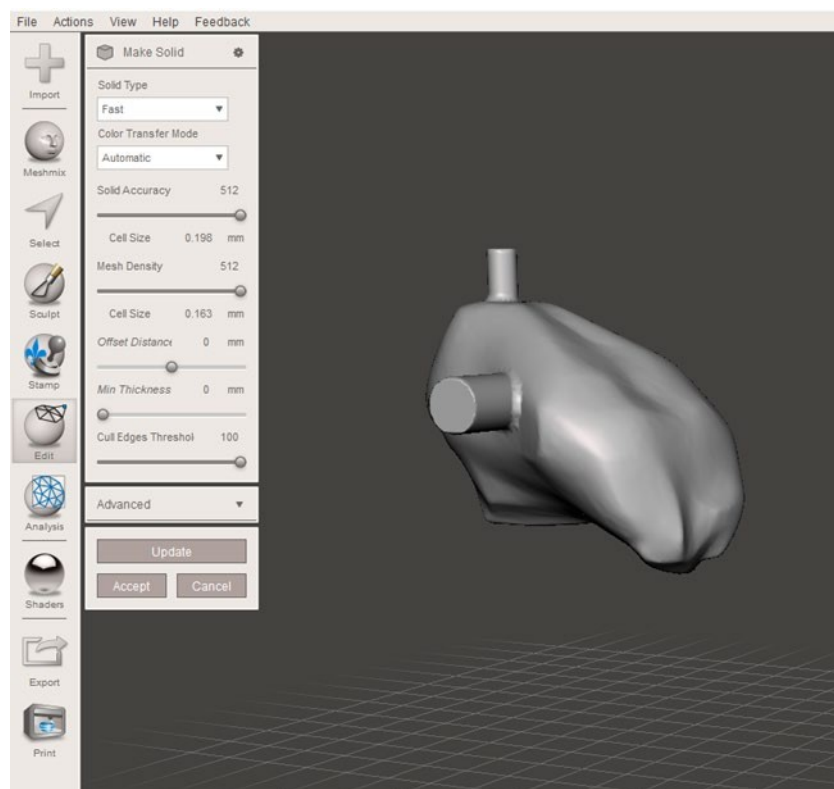


Fig. 3.12 Design of the die core

Once the die core was prepared, a casting box had to be prepared. For this purpose, the shape was again obtained from the objects proposed by the Meshmixer program, and in the Meshmix options, both the tongue and the nodule were selected as cuboids. The main goal of designing the boxes was to keep the volume as small as possible, so that the printing was not time-consuming and financially optimal. The initial dimensions of the cuboid in the case of the tongue were 57x72x70 mm, and in the case of the tumor, the dimensions of the cuboid as well as its final dimensions of the form were 25x30x35 mm. The created objects also had to be subjected to the Make Solid function and set the aforementioned parameters.

This project has been funded with support from the European Commission. This publication [communication] reflects the views only of the authors, and the Commission cannot be held responsible for any use which may be made of the information contained therein.

When two objects were created for both the tongue and the tumor - a cuboid and a form, it was time to subtract one model from another. The program enables such an operation using the Boolean Difference function. For this purpose, in the Object Browser panel, the object was first selected, from which the next selected object was to be subtracted, as shown in Figure 5.8.

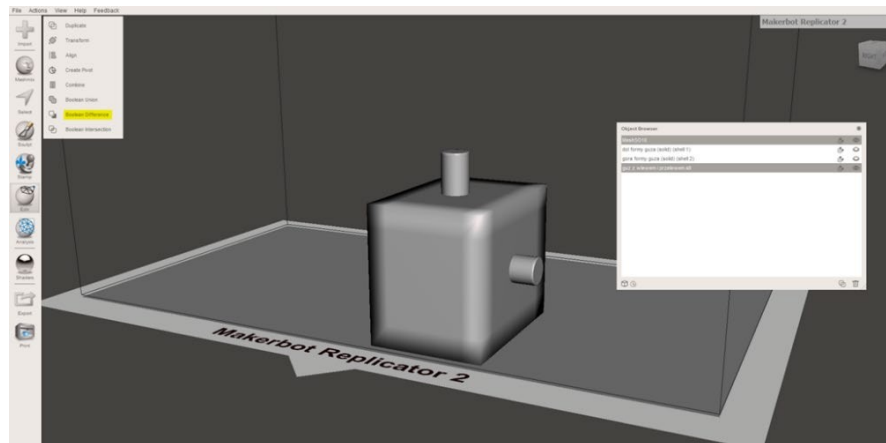


Fig. 3.13 Using the Boolean Difference function to obtain the form of a tumor

In the case of the tumor matrix, the cuboid had too much unsuitable volume, so it was transformed. With the plane cut operation available in the edit functions, the volume of the mold was reduced as shown in the figure below.

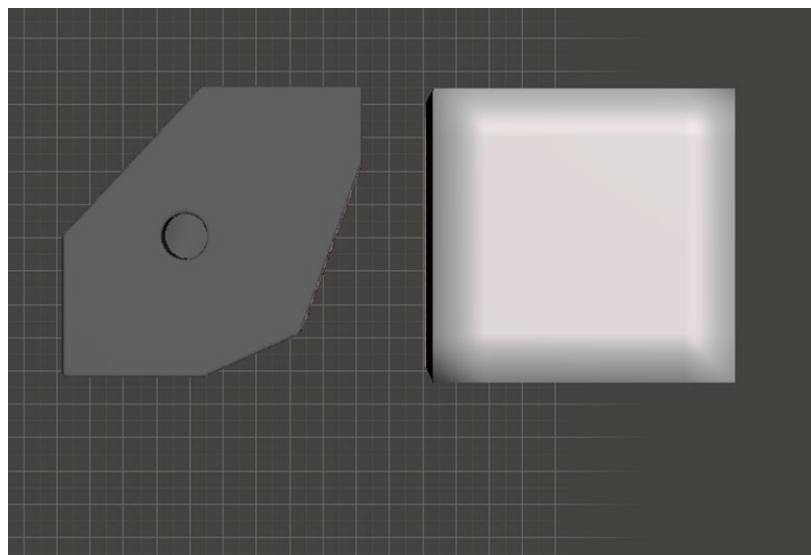


Fig. 3.14 Comparison of the optimized object with its initial version

This project has been funded with support from the European Commission. This publication [communication] reflects the views only of the authors, and the Commission cannot be held responsible for any use which may be made of the information contained therein.

The final step was to use the plane cut function again to separate the molds into two parts so that the resulting castings could be easily removed. For this purpose, the division of the facilities was carried out through the overflow and venting channel.

This is how the designed and ready-to-print casting models look like for a tongue with a bump:

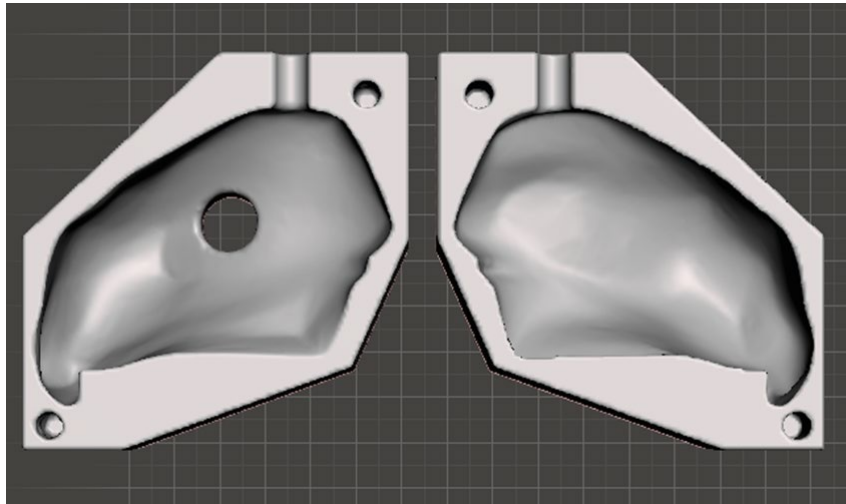


Fig. 3.15 Casting form of a tongue with a tumor

Below are casting molds designed to cast a tongue tumor:

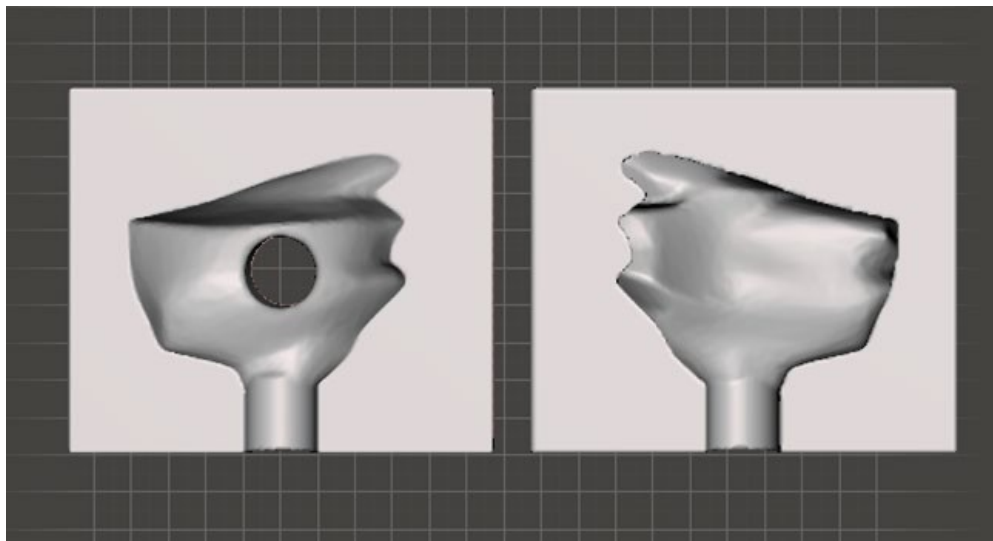


Fig. 3.16 Tongue tumor matrix

This project has been funded with support from the European Commission. This publication [communication] reflects the views only of the authors, and the Commission cannot be held responsible for any use which may be made of the information contained therein.

3.7. 3D printing

In order to print the previously described models, the objects were imported into PrusaSlicer 2.3.3. Formerly known as Slic3r Prusa Edition and Slic3r PE, the program is an open source, feature-rich, frequently updated tool that gives you the ability to export printfiles for Original Prusa 3D printer [38].

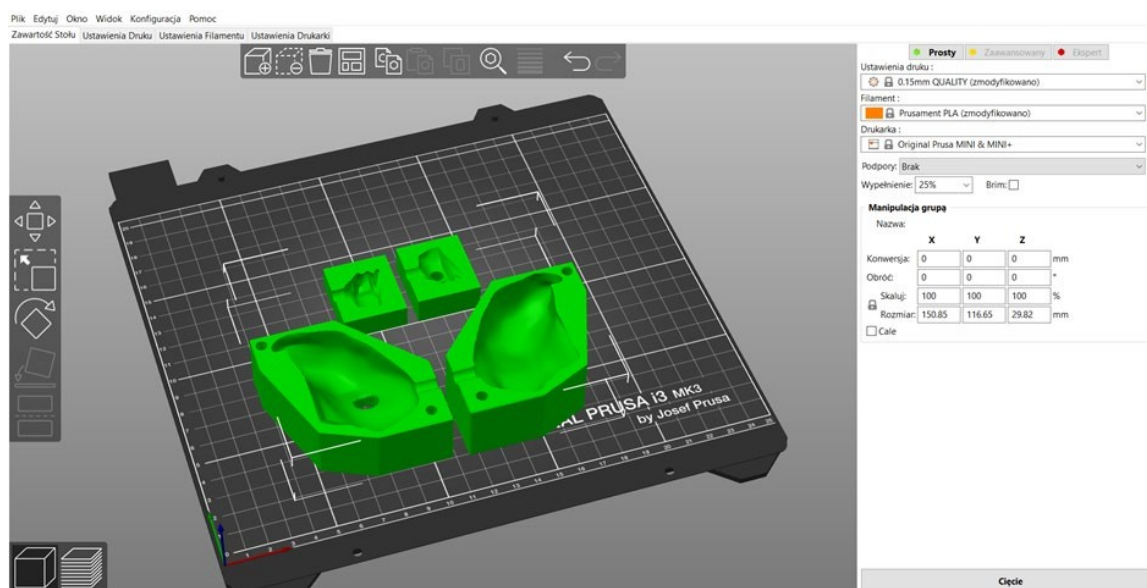


Fig. 3.17 Screenshot of PrusaSlicer with casting molds [38]

The table with the printing parameters of the above-illustrated forms is presented below:

Parameters	Values
Material	PLA
Filling	25%
Thickness	0,15 [mm]
Printing time	9 [h]
Volume	524,73 [cm ³]

This project has been funded with support from the European Commission. This publication [communication] reflects the views only of the authors, and the Commission cannot be held responsible for any use which may be made of the information contained therein.

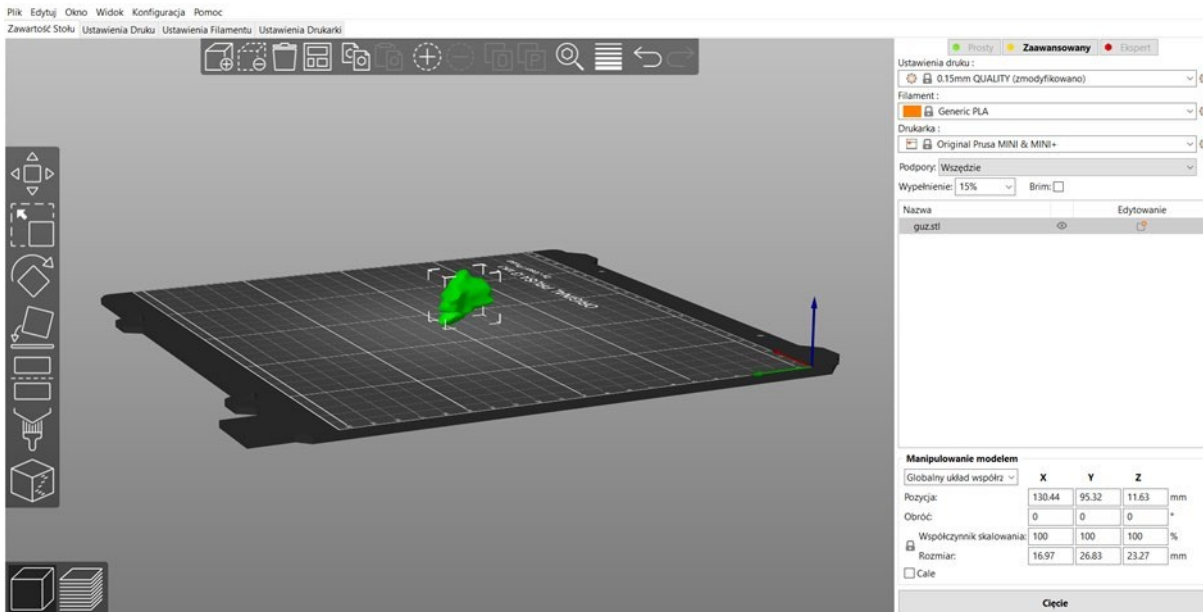


Fig. 3.18 A screenshot of the PrusaSlicer program with a bump

In the screenshot above, in preparation for printing, there was a lump of the tongue. The object has irregular shapes and does not contain any element that could be considered as the basis for printing. In order for the printing process to run correctly, the model had to be printed with supports. The supports were made of the same material as the object itself - Fiberlogy.

Parameters	Values
Material	Fiberlogy PLA
Filling	15%
Thickness	0,15 [mm]
Printing time	27 [min]
Volume	10,59 [cm ³]

All models were printed with the Prusa i3 MK3S printer in the 3D printing laboratory at the Poznań University of Technology.

Below is a photo of the 3D printed models, in the upper part of the picture you can see a mold of the tongue with a tumor, and in the lower part of the picture a form of a tumor of the tongue.

This project has been funded with support from the European Commission. This publication [communication] reflects the views only of the authors, and the Commission cannot be held responsible for any use which may be made of the information contained therein.

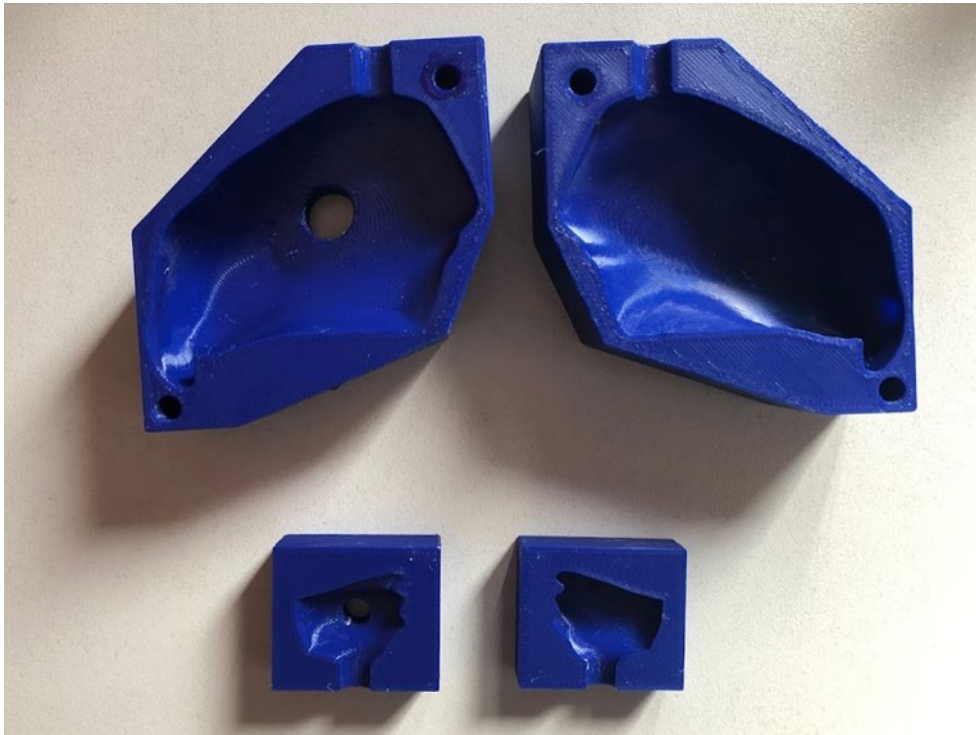


Fig. 3.19 Casting forms of the tongue and its tumor

In the next photo, a printout of a nodule made of flexible material (Fiberflex) will be shown:



Fig. 3.20 Tumor printout

3.8. Casting of models

After printing the casting molds of the tongue and the tongue tumor, the next step was to cast the models. The goal was to obtain three models of the tongue with their tumors, where

This project has been funded with support from the European Commission. This publication [communication] reflects the views only of the authors, and the Commission cannot be held responsible for any use which may be made of the information contained therein.

each tumor was made of different materials. In this section, we will describe the course of the foundry processes and show how various parameters can affect the final result.

The first step in all the operations was to locate the tumor of the tongue in the cast mold. As the tumor is inside the tissue, its location was arbitrary, selected on the basis of photos taken during the design. The location of the tumors in a casting mold is shown below.



Fig. 3.21 Location of the tumor

In each case, the molds had to be carefully secured with tape, then drain and inlet channels were installed, which were also secured against material spilling with tape. The mold, covered with an insulating layer, was placed in a vice as shown in Fig. 3.22.



Fig. 3.22 A mold prepared for the casting process

This project has been funded with support from the European Commission. This publication [communication] reflects the views only of the authors, and the Commission cannot be held responsible for any use which may be made of the information contained therein.

Ultimately, three different models of the tongue will be created along with its tumor. The materials were selected in consultation with the medical staff, based on the presentation of samples of various materials. The semi-finished product intended for the casting of the tongue in all cases was - Sorta Clear 12. However, the bumps will be successively made of materials such as Fiberflex (printed), Dragon Skin 10 and XTX 45 DRY (cast). A table with the properties of the given materials is presented below.

List of materials used						
Technology	Type	Trade name	Hardness [Shore A]	Colour	Additional information	
					Time life [min]	Setting time [h]
FDM	Mod. TPE	Fiberflex	90 (40D)	Black	Printing temp. 200-220°C	
VC	Silikon	Dragon Skin 10 Very Fast	10	Milk	4	0,5
VC	Silikon	Sorta Clear 12	12	Transparent	40	12
VC	Silikon	XTX 45 DRY	43	Transparent	90	12

Sorta Clear 12 is a transparent silicone rubber material that cures within 12 hours at room temperature. It cures with negligible shrinkage (0.1%) at room temperature. The manufacturer sells a material split into two substances, A as a catalyst and B as a base. Part B should be shaken thoroughly before use, and then both substances should be measured in a ratio of 1:1. The mixing process should take about three minutes and be carried out intensively. In each case, the material deaeration was referred to differently, which will be presented in more detail in the description of the given example models.

This project has been funded with support from the European Commission. This publication [communication] reflects the views only of the authors, and the Commission cannot be held responsible for any use which may be made of the information contained therein.



Fig. 3.23 SORTA-Clear silicone rubber 12 [39]

In the case of the first model, the then printed tumor was attached to a casting mold with a mounting compound. It was made of Fiberflex material, without the internal filling of the model, which was to ensure greater flexibility. Then the form with the inflow and venting system was secured and mounted in a vice. Parts A and B of Sorta Clear 12 were measured and mixed as recommended by the manufacturer, however, this model did not vent under vacuum. The next day, the casting was removed from the mold and the unnecessary hardened silicone parts were removed. The result of the actions is shown in Figure 3.24.



Fig. 3.24 First model

The structure of the model was cast correctly; however many air bubbles are visible. Their presence does not significantly affect the quality of the model, but its aesthetic value.

On the same day as the casting of the first model was prepared, a model of the tongue tumor itself was also created so that it could be used the next day to prepare the second model. The tumor casting mold was secured with tape, an infusion / venting system was added and then installed in a smaller vice similar to the tongue mold. The cast material was Dragon Skin

This project has been funded with support from the European Commission. This publication [communication] reflects the views only of the authors, and the Commission cannot be held responsible for any use which may be made of the information contained therein.

10, as with Sorta clear, the manufacturer sells the base and catalyst separately, but in this case the ratio is 10:1. The substances were thoroughly mixed, the liquid was not deaerated, and after mixing, poured into a syringe, with which the material was placed in the mold and allowed to solidify. Pictures of the tumor of the tongue are presented below.



Fig. 3.25 Tongue tumor made from Dragon Skin 10

Once the tumor model described above was ready, it had been attached to the larger mold using a different silicone, the material was otherwise difficult to attach because silicone does not show adhesion to other materials. Then the form with the inflow and venting system was secured and it was mounted in a vice. Parts A and B of Sorta Clear 12 were measured and the red dye was added to the liquid, then mixed thoroughly until the ingredients were combined. The difference in this case was that the material already in the form was placed in a vacuum chamber to vent it.



Fig. 3.26 Bleeding the material

This project has been funded with support from the European Commission. This publication [communication] reflects the views only of the authors, and the Commission cannot be held responsible for any use which may be made of the information contained therein.

After the material was deaerated, the mold was allowed to stand until it reached the concentration of silicone. The next day, the model was taken out of the mold. The material did not have as many air bubbles as the previous one, but unfortunately there were significant shortcomings. However, the side with the tumor was cast correctly, which allowed for a simulated operation to proceed.



Fig. 3.27 Secondary model

On the same day as the casting of the second model was prepared, a model of the tongue tumor itself was also created so that it could be used the next day to prepare the third model. The process of making the tumor cast was exactly the same as before, the only difference was in the casting material. Here, the semi-finished product was Dragon Skin 10, and its preparation was similar to Sorta Clear 12. Also, the base and the catalyst had to be mixed intensively in a 1: 1 ratio for about 3 minutes. The material was then transferred to the syringe and from there to the already sealed mold. After pouring, the material was allowed to solidify in the mold.

The next day, the tumor model (Dragon Skin 10) was removed and, with the help of another silicone, attached to the tongue mold in the appropriate place. Then, as a standard, a casting mold was prepared for pouring the material. In the latter case, the base with the catalyst was mixed, then a special mixing package was prepared in order to put it into the vacuum chamber. The liquid was deaerated, then poured into a syringe and placed in a casting mold. The next day, the model was pulled out and properly processed. When pouring the material, the syringe contained air which was forced into the mold along with the material, which resulted in a slight discomfort at the top of the last model.

This project has been funded with support from the European Commission. This publication [communication] reflects the views only of the authors, and the Commission cannot be held responsible for any use which may be made of the information contained therein.

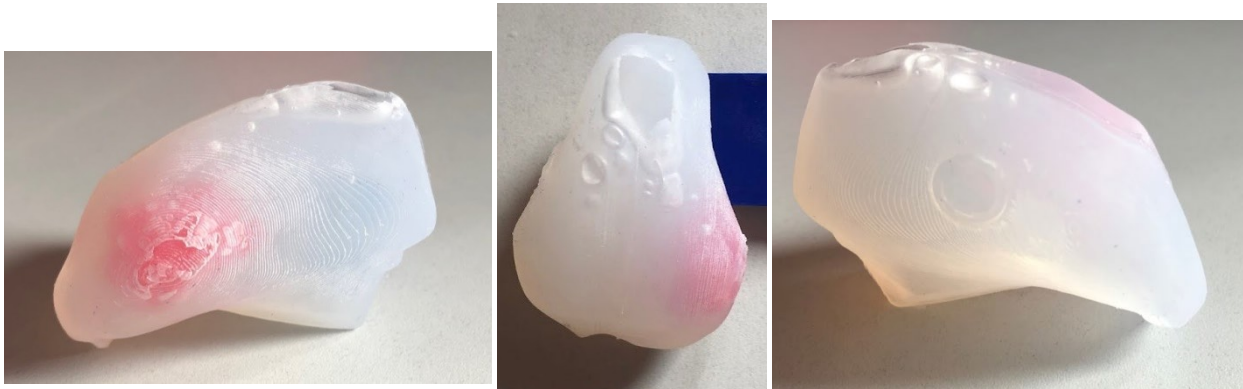


Fig. 3.28 The third model

3.9. Clinical evaluation

As part of the planned clinical evaluation, a simulated surgery process was performed followed by a survey. The clinical evaluation was attended by two surgeons working every day at the Clinical Hospital. Heliodor Świącicki of the Medical University of Karol Marcinkowski and a medical student from the Medical University of Karol Marcinkowski.

One of the first stages of the simulated operation was the preparation of surgical instruments, which included a surgical vice, surgical tweezers, and surgical knives. Then the models were inspected and the selected area was marked with a marker, as it is usually done in the operating theater.



Fig. 3.29 Operation simulation - marking

This project has been funded with support from the European Commission. This publication [communication] reflects the views only of the authors, and the Commission cannot be held responsible for any use which may be made of the information contained therein.

The next step was to incision the area marked at that time and then excise the tumor model(Fig. 3.30). The operation was performed jointly by two surgeons on the tongue with the tumor cast from Dragon Skin 10 silicone material and the tumor cast from XTX 45 DRY silicone material (dyed).



Fig. 3.30 Operation simulation – next steps

People who performed a simulated operation confirmed that the miseries are not a problem if they are not in the desired location, in this case within the tumor and its margin. The color of the silicone models turned out to be a very important factor during the planning and during the simulated operation. The transparency of the tongue model together with its colored tumor allowed a better view of the tumor visibility and its correct excision. These types of models were assessed as very good in terms of didactic value, intended for students and less experienced doctors. However, the simulated operation on the transparent model is not very realistic. The operation carried out on the colored model was closer to the actual operation, it reflects the difficulty of the operation. In this case, the tumor was excised with too small a margin and part of it remained in the tongue.



Fig. 3.31 The tongue model together with its colored tumor

his project has been funded with support from the European Commission. This publication [communication] reflects the views only of the authors, and the Commission cannot be held responsible for any use which may be made of the information contained therein.

Remnant of a tumor model in the tongue for the stained form of the tongue (Fig 3.32).

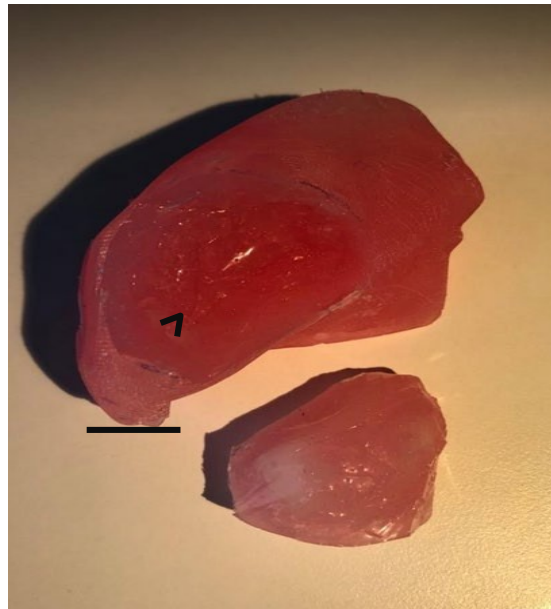


Fig. 3.32 Tumor model in the tongue

To sum up, according to the doctors' assessment, the models have greater use in didactic, not entirely imaging, applications. The language banner model is perfect for exercises, and the color model is more realistic, but a less useful application will be to test the skills of a young doctor. For an experienced physician for imaging purposes, preparation for surgery and assistance during the procedure, a hard model, printed from plastic, is sufficient.

This project has been funded with support from the European Commission. This publication [communication] reflects the views only of the authors, and the Commission cannot be held responsible for any use which may be made of the information contained therein.

4. Conclusions

The module presents the role of rapid prototyping techniques in otolaryngology with the use of 3D Printing and Vacuum Casting techniques. As part of this procedure, anthropometric measurements of the patient tongue were carried out using a 3D scanner. The data provided in the form of DICOM from MRI imaging for the conducted research was one of the patients, then executed segmentation of desired anatomical structures, processing of 3D models, design of models and mold, printing models using rapid prototyping tools, assessment by medical staff on the basis of a questionnaire.

Acknowledgements

The realization of the project was possible thanks to the financing of the Polish Ministry of Education and Science. The results were obtained as a result of cooperation with surgeons from Poznan University of Medical Sciences – dr. Jacek Banaszewski and dr Agata Andruszko-Buczowska.

The study and toolkit descriptions were based on the thesis written by MSc. Renata JEZIŃSKA, entitled “Methodology of design and rapid manufacturing of mid-surgery supplies in otolaryngology”.

The publishing of this project toolkit has been financially supported by the ERASMUS KA226 project entitled “Boosting the scientific excellence and innovation capacity of 3D printing methods in pandemic period”, the implementation of the project being supervised by the National Agency for Community Programmes in the Fields of Education and Vocational Training (project reference: 2020-1-RO01-KA226-HE-095517).

References

- [1] <https://www.cmpromed.pl/otolaryngologia-czym-sie-zajmuje>
- [2] https://www.gcm.pl/index.php/baza_uslug-uslug-a-56-operacje_nowotworow_jezyka.html
- [3] <https://drrysz.pl/rak-jezyka/>
- [4] <http://medical.padishahtravel.com/ent-treatment/>
- [5] <https://www.britannica.com/science/otolaryngology>
- [6] https://www.researchgate.net/publication/330088942_Classification_of_GLOSSECTOMIE_S_a_proposal_for_tongue_cancer_resections
- [7] <https://www.webmd.com/oral-health/picture-of-the-tongue>
- [8] <https://www.ncbi.nlm.nih.gov/pmc/articles/PMC6590454/figure/hed25466-fig-0001/>

- [9] <https://www.webmd.com/oral-health/picture-of-the-tongue>
- [10] <https://pubmed.ncbi.nlm.nih.gov/28244479/>
- [11] <https://www.webmd.com/oral-health/guide/oral-cancer>
- [12] https://pl.wikipedia.org/wiki/Rak_j%C4%99zyka
https://www.researchgate.net/publication/325070365_Aktualne_metody_diagnostyki_obrazowej_raka_jamy_ustnej_-_badanie_TK_MRI_DWI-MRI_oraz_PETTK
- [13] Sigal R, Zagdanski AM, Schwaab G, et al. CT and MR imaging of squamous cell carcinoma of the tongue and floor of the mouth. *Radiographics*. 1996;16:787-810
- [14] Royster HP, Lehr HB, Raventos A, Demuth WE. Management of patients with squamous cell carcinoma of the tongue. *Ann Surg*. 1961;154:563-572
- [15] Calabrese L, Tagliabue M, Maffini F, Massaro MA, Santoro L. From wide excision to a compartmental approach in tongue tumors: what is going on? *Curr Opin Otolaryngol Head Neck Surg*. 2013;21:112-117
- [16] <https://www.mayoclinic.org/tests-procedures/ct-scan/about/pac-20393675>
- [17] <https://web.archive.org/web/20141109192141/https://www.arrt.org/Patient-Public/Patient-Page>
- [18] https://en.wikipedia.org/wiki/CT_scan
- [19] <https://www.mayoclinic.org/tests-procedures/ct-scan/about/pac-20393675#dialogId7648275>
- [20] https://pl.wikipedia.org/wiki/Tomografia_komputerowa
- [21] https://www.researchgate.net/publication/319247119_Metastatic_spread_of_solid_subtype_lung_adenocarcinoma_to_the_small_intestine_with_anemia_and_melena_A_case_report/figures?lo=1
- [22] https://en.wikipedia.org/wiki/Magnetic_resonance_imaging
- [23] https://www.researchgate.net/publication/323147635_Brain_MR_CT_Images_Feature_Extraction_to_Enhance_Abnormalities_Quantification
- [24] https://www.researchgate.net/publication/224822138_Iron_Accumulation_in_Deep_Cortical_Layers_Accounts_for_MRI_Signal_Abnormalities_in_ALS_Correlating_7_Tesla_MRI_and_Pathology
- [25] <https://ohfoundation.ca/be-inspired/3d-printing-helps-complex-surgery-to-remove-50-tumours-saves-uterus/>
- [26] <https://ohfoundation.ca/be-inspired/3d-printing-helps-complex-surgery-to-remove-50-tumours-saves-uterus/>
- [27] <https://3dprintingindustry.com/news/tongue-cancer-patient-receives-best-treatment-thanks-3d-printing-tech-94699/>
- [28] <https://3dprintingindustry.com/news/tongue-cancer-patient-receives-best-treatment-thanks-3d-printing-tech-94699/>

thanks-3d-printing-tech-94699/

[29] http://www.ptzp.org.pl/files/konferencje/kzz/artyk_pdf_2018/T1/2018_t1_634.pdf

[30] <https://pulsmedycyny.pl/polscy-lekarze-stworzyli-modele-serca-plodu-3d-892323>

[31] http://dydaktyka.fizyka.umk.pl/Wystawy_archiwum/z_omegi/serce%203D.htm

[32] <https://www.materialise.com/en/medical/mimics-innovation-suite/mimics>

[33] <https://www.slicer.org/>

[34] <https://www.3d-doctor.com/>

[35] <https://en.wikipedia.org/wiki/InVesalius>

[36] [https://en.wikipedia.org/wiki/Blender_\(software\)](https://en.wikipedia.org/wiki/Blender_(software))

[37] <https://www.prusa3d.com/prusaslicer/>

[38] <https://www.kaupo.de/shop/en/SILICONE-RUBBER-Platinum-Cure/SORTA-CLEAR-SERIES/SORTA-Clear-12/SORTA-Clear-12-1-Silicone-Rubber.html>

BRIGHT

Erasmus+ strategic partnership for Higher Education

BOOSTING THE SCIENTIFIC EXCELLENCE AND INNOVATION CAPACITY
OF 3D PRINTING METHODS IN PANDEMIC PERIOD

TOOLKIT 5 PRODUCTION OF MEDICAL PARTS WITH USE OF FUSED DEPOSITION MODELLING AND REPRAP TECHNOLOGIES

Project Title	Boosting the scientific excellence and innovation capacity of 3D printing methods in pandemic period 2020-1-RO01-KA226-HE-095517
Output	IO2 – BRIGHT e-toolkit manual for digital learning in producing medical parts by 3D printing methods in the context of the pandemic
Toolkit	Toolkit 5 Production of medical parts with use of Fused Deposition Modelling and Reprap technologies
Date of Delivery	November 2021
Authors	Filip Górski, Filip Sarbinowski, Sven Maričić
Version	Final variant

Content

1.	Introduction	139
2.	Case description	140
3.	Design	142
3.1.3D Scanning		142
3.2.CAD modeling		144
4.	Manufacturing	149
4.1.	Additive manufacturing by Fused Deposition Modeling technology	149
4.2.	Post processing, assembly and fitting	154
5.	Conclusions	155
	Acknowledgements	155
	References	156



Co-funded by the
Erasmus+ Programme
of the European Union

1. Introduction

This toolkit presents methods of production of medical products by use of additive manufacturing.

A case of a customized product, which must be produced solely by 3D printing (based on 3D scanning of patient's anatomy) is presented in a step by step manner. Issues related to design and manufacturing are presented in more detail in the further chapters.

This project has been funded with support from the European Commission. This publication [communication] reflects the views only of the author, and the Commission cannot be held responsible for any use which may be made of the information contained therein.



2. Case description

Hundreds of thousands of people every day experience injuries that require the stabilization of specific parts of the body to heal. Until recently, one of the most commonly used methods of stiffening were gypsum dressings (Fig 2.1), which are in fact bandages impregnated with an aqueous gypsum solution applied to the area of the body to be stabilized. This solution is characterized by a large number of disadvantages, including high weight, low durability, X ray impermeability and difficulty in maintaining the hygiene of the plastered area. Moreover, if it is inserted incorrectly, it can cause serious complications, such as necrosis, nerve paresis or weakening of muscles and tendons.



Fig 2.1. Gypsum dressing [www 01].



Fig 2.2. Universal orthosis [www 02].

Currently, one of the most popular alternatives to plaster are universal orthoses (Fig 2.2). There is no doubt that these types of stabilizers are much more user-friendly, if only because they can be removed without destroying them or because they are lighter, but due to their universal size, it is easy to make a mistake when fitting them, which in turn can lead to abrasions and a limited stabilization effect, and thus longer convalescence. One can also distinguish individualized orthoses, the shape of which is adapted to the body of a specific patient, which reduces the problems resulting from incorrect fit, but the need to carry out precise measurements around the stiffened area and the manual manufacturing process of each piece result in a high cost of the orthosis. This problem is particularly acute in the case

This project has been funded with support from the European Commission. This publication [communication] reflects the views only of the author, and the Commission cannot be held responsible for any use which may be made of the information contained therein.

of orthoses for children, because - in the case of long-term use - it often turns out that the patient has already outgrown his orthosis and it is necessary to buy a new one.

Rapid Manufacturing technologies turn out to be a way to reduce the above drawbacks. Thanks to the use of 3D scanning and 3D printing with the FDM method, it is possible to quickly design and manufacture cheap and light orthoses for the upper limbs, lower limbs (Fig 2.3), neck or back braces (Fig 4) perfectly suited to the body of a particular patient. The growing popularity of such a solution is evidenced not only by the rapidly growing number of scientific studies on this subject [DOM14, GUI19, KUO19, TEL17], but also by the existence of commercial companies offering the production of personalized orthoses [www 03 – 06].



Fig 2.3. Individualized orthosis printed with FDM technology [www 07].



Fig 2.4. Individualized back brace printed with FDM technology [www 08].

Social awareness of these new opportunities is also growing. Patients realized the numerous drawbacks and limitations of standard stabilization techniques, thus they are looking for help in finding alternatives in additive manufacturing sector. This was also the case with nine-year-old boy named Jan, who suffered a double fracture of his left arm as a result of an accident on a playground. Doctors decided to insert Kirschner wires, which are an auxiliary and temporary element in fracture stabilization. As Jan is an extremely mobile boy, it was not decided to put on a plaster, but the hand had to be somehow immobilized. Looking for a good solution, the parents turned to the AutoMedPrint team operating

at the Department of Production Engineering of the Poznań University of Technology. The following paper describes the procedure which allowed Jan to enjoy his new orthosis two days after his arrival in the team's laboratory. The case, as well as the system itself, was presented at the website of the AutoMedPrint project [www 09]. The methodology of creating custom wrist hand orthoses and their manufacturing by 3D printing was presented in a scientific paper [GOR20].

3. Design

3.1. 3D Scanning

During consultations with a physiotherapist, it was determined that the patient needed an orthosis that would position his forearm at right angles to the arm. Moreover, details of the orthosis division planes and the method of connecting them were also specified. Then, geometric measurements of the patient's limb were carried out.

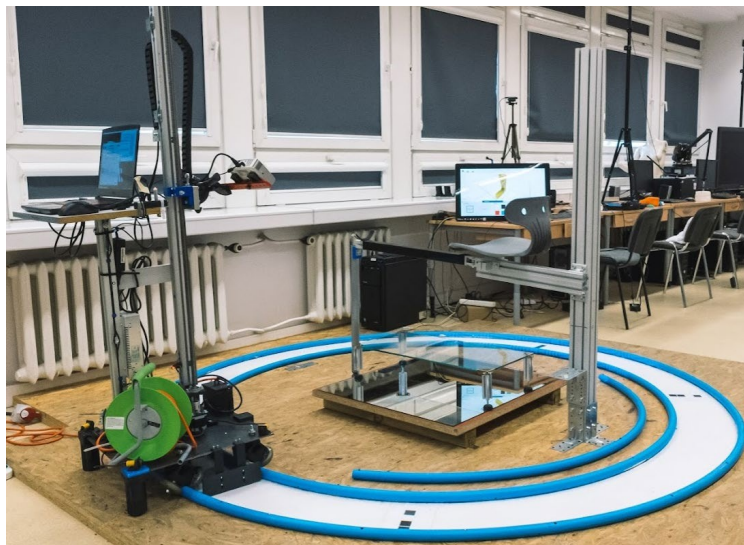


Fig 3.5. Measurement stand [www 09]

During this process, a series of images of the patient's limb in its various positions were taken, which were then combined on the basis of common points. For this purpose the custom automatic trolley with stationary structured light scanner David SLS-3 coupled with MeshLab software were used (Fig 3.5).

The data processing is shortly presented in (Fig 3.6) and illustrated in (Fig 3.7). In general, it focuses on obtaining a clean representation of a selected fragment of a given limb, of which data can be extracted for further design in a CAD system.

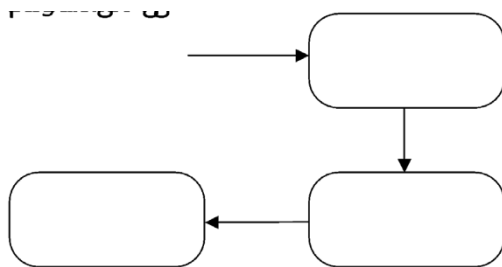


Fig 3.6. Scan data processing scheme.

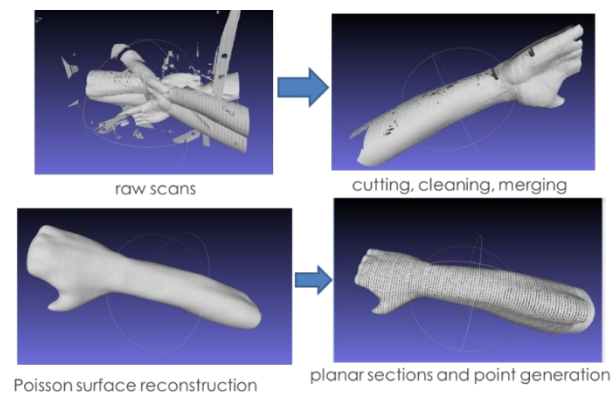


Fig 3.7. Mesh cleaning process.

The process consists of the following stages:

1. Combining scans

- background cleaning,
- geometric transformations (rotations, translations, mirror),
- best fit.

2. Cleaning and processing the resulting scan

- deleting unnecessary data,
- closing holes,
- smoothing,
- removing artifacts, repairing,
- triangle reduction, reconstruction (optional).

3. Data extraction

- automated measurements,
- creating sections,

- save to txt and workbooks (Excel).

The first two stages are done mostly automatically by scanners' software, however some manual adjustments (cleaning and closing holes etc.) were also required.

During the third stage, the point data has been extracted to create a parametric limb representation in CAD. External algorithms of MeshLab and Excel software (automation scripts) extracted points from a 3D scan of a limb by making a series of cross-sections, and then filtered and selected them on the basis of appropriate mathematical criteria.

3.2. CAD modeling

The basis for creating the outline of the orthosis is the so-called multi-section solid, i.e. the 3D solid spread over a group of spline curves (spline), placed on planes parallel to each other (Fig 3.8). These curves are made of points whose coordinates come directly from the measurement data, i.e. the 3D scan of the patient, processed with the MeshLab software and the automated Excel spreadsheet.

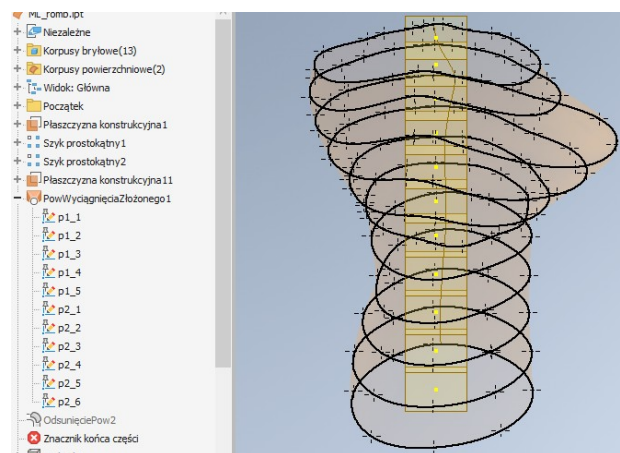


Fig 3.8. Wireframe curves.

Cross-sections made in the MeshLab software are created at a distance of 2 mm. From all the sections, 15 representative sections are then selected – 4 representing arm with elbow joint, 5 representing forearm and 6 - the wrist and hand. Sections are selected based

on manual measurements entered into the software (Scan Assistant) during the 3D scan or later to the patient data file or directly to the Excel spreadsheet. The measurements of forearm and hand are made in accordance with the diagram shown in Figure 3.9.

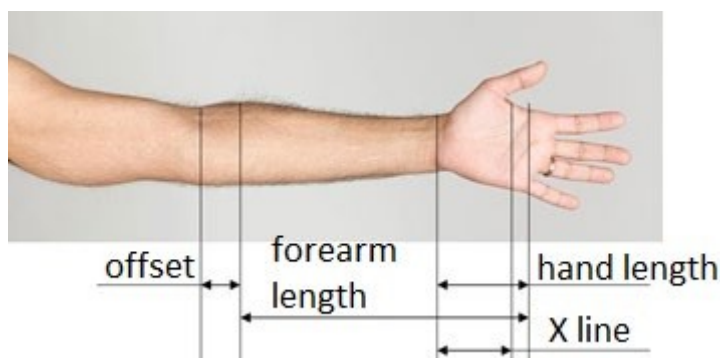


Fig 3.9. Forearm and hand measurements diagram.

For the 9 sections representing the forearm and arm, curves consisting of 8 points are created, and for the remaining 6 sections - curves consisting of 18 points, as shown in the examples in Figure 3.10.

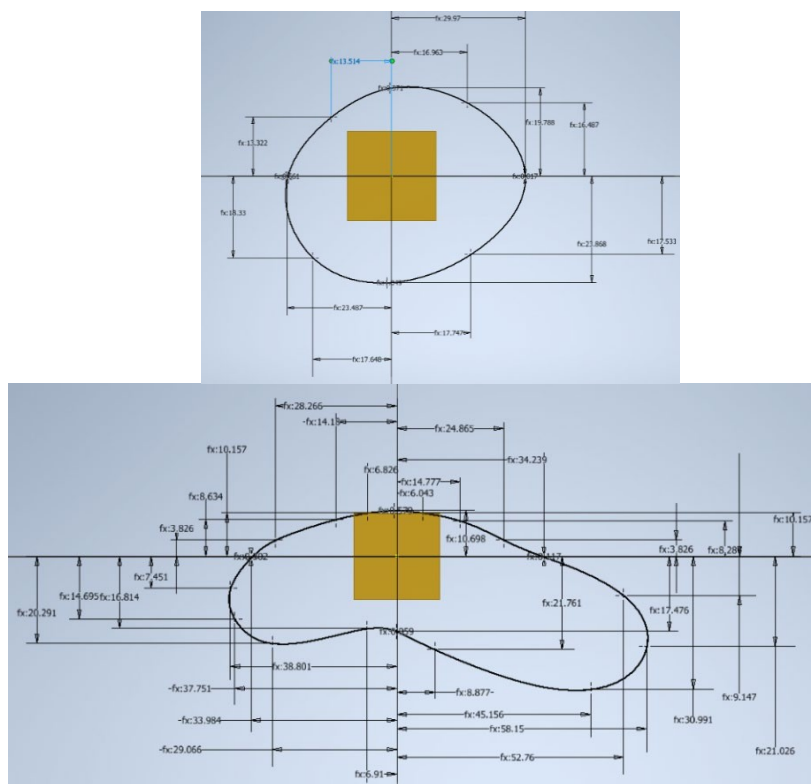
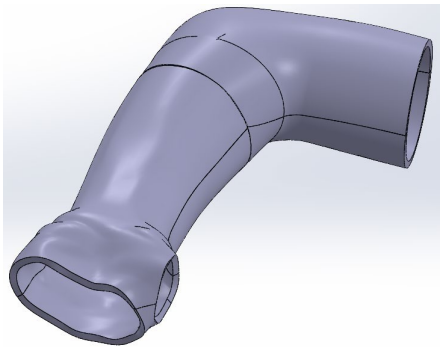


Fig 3.10. Wireframe sketches of a) wrist part and b) hand part.

On the basis of the base body, the orthosis shell was created - the contour moved away from the base body by the distance (clearance) of 3 mm. The shell is cut with planes to create a full contour of the orthosis (Fig 3.11). The standard thickness of the orthosis is 4



mm.

Fig 3.11. Orthosis shell.

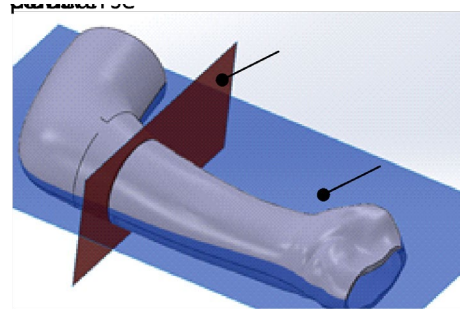


Fig 3.12. Planes of division.

The outline of the orthosis was divided into four parts – one of the dividing planes was oriented by the center of the thumb hole and the forearm axis, so that the orthosis can be easily put on (coronal division), while the other was defined in such a way that it was perpendicular to the fracture axis and offsetted from the top of the orthosis by 192 mm (Fig 3.12), which was dictated by anatomical reasons (transverse division).



Fig 3.13. Orthosis with different types of openwork.

The openwork is parametric and can take one of three forms: standard curvilinear,

rhomboid and hexagonal (Figure 3.13). In special situations, the openwork may be not implemented, and a monolithic orthosis is obtained (e.g. for therapeutic purposes, if it is

made of a flexible material, such as TPU). In this case, to meet the patient's request, hexagonal openwork was used.

Segments resulting from the transverse division should be combined after manufacturing. For this purpose, connection manifolds has been manually added (Fig 3.14), that allow them to be connected with screws. The two halves were joined by a formfit – a groove is generated in one of the halves, and a projection in the other with the same course as shown in Figure 3.15. In addition, the halves of the orthosis have holes that allow them to be attached to the patient's hands with disposable polymer clips.

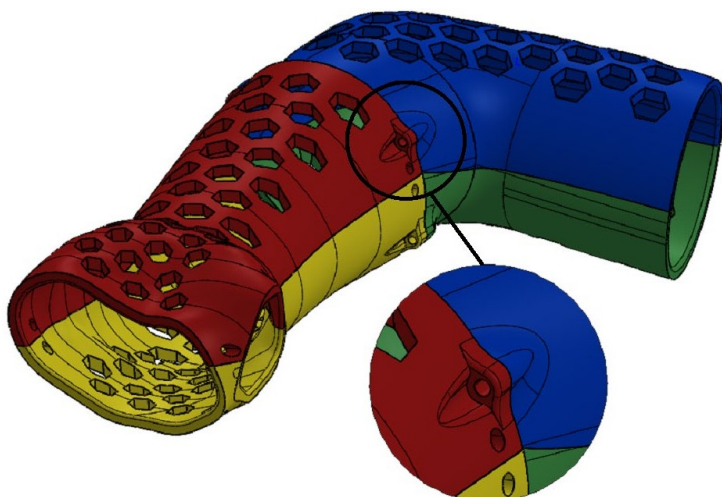


Fig 3.14. Connection manifolds.

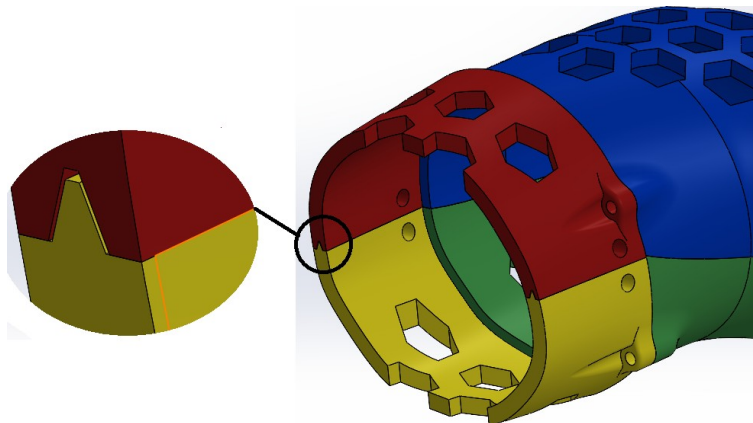


Fig 3.15. positioning groove.

The edges of the model have been rounded to eliminate uncomfortable sharp edges in use (especially in the area of the thumb).

All parameters of the auto-generating model are saved in a dedicated Excel sheet (Fig 3.16). In addition to the coordinates of the points of individual curves, it also contains parameters such as offset (clearance), orthosis thickness or openwork parameters. The sheet is linked to the orthosis model saved in a single file in .ipt (Inventor Part) format.

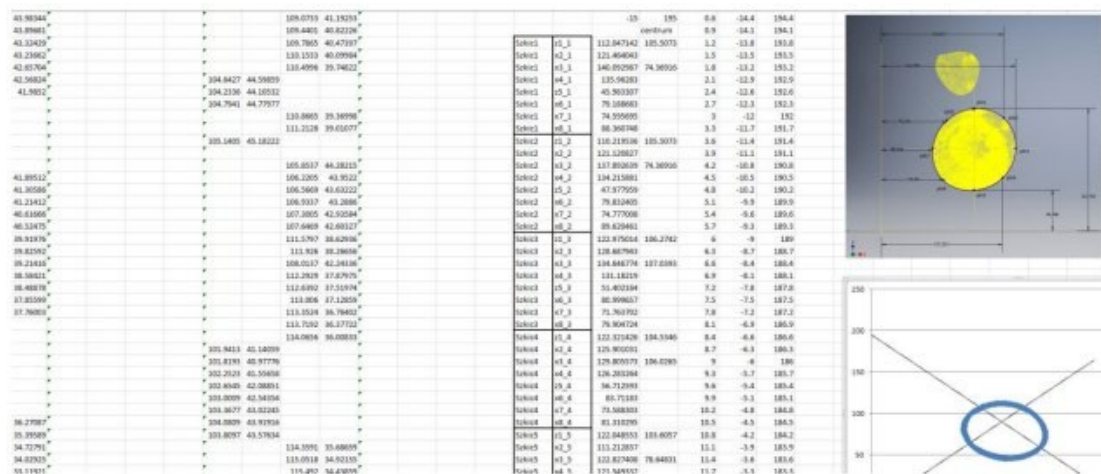


Fig 3.16. Sheet with model parameters.

After a successful update, files with the parts of the orthosis were generated in the triangle mesh (STL) format to be printed on an additive manufacturing device. After generating

This project has been funded with support from the European Commission. This publication [communication] reflects the views only of the author, and the Commission cannot be held responsible for any use which may be made of the information contained therein.

the files for printing, the information is transferred to the software controlling the operation of the additive manufacturing device. The end result is shown in the Figure 3.17. The orthosis consists of 4 parts – two halves of the wrist-forearm part and two halves of the elbow part.

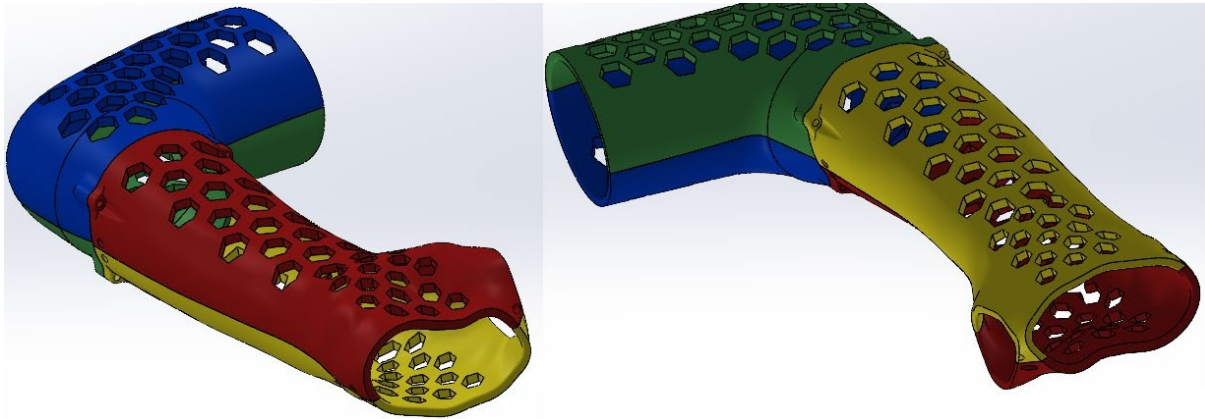


Fig 3.17. Model of the orthosis.

4. Manufacturing

4.1. Additive manufacturing by Fused Deposition Modeling technology

The FDM technology uses thermoplastics in the manufacturing process, i.e. plastics used to form geometry at high temperatures. Models printed in this technology are created by applying successive layers of semi-liquid material, which is extruded from a heated nozzle. The material, called filament has the form of a line with a constant diameter (1.75 mm or 2.85 mm) wound on the spool.

It is important to deliver the filament to the extruder and the print head of the device in the continuous and uninterrupted way. To facilitate this, the filament is usually guided through the tube. The print head is heated to the temperature needed to only plasticize the given material - filament shouldn't be melted. Plastic that is extruded to the worktable solidifies almost immediately and thus, forms a desired structure. The diagram of an exemplary FDM printer is presented in the figure 3.18.

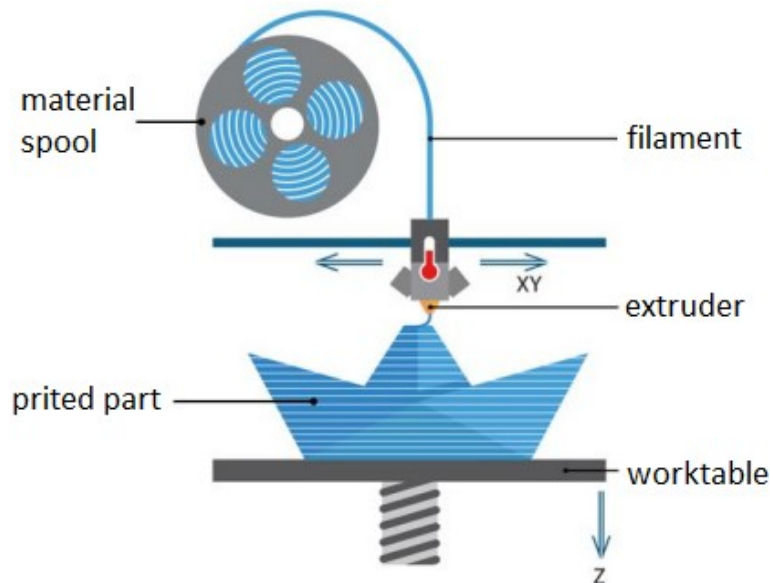


Fig 3.18. FDM printer [www 09].

The first stage of the process of additive manufacturing of the orthosis in the FDM technology was the import of 3D models of its parts in the form of STL files to the 3D printer software in order to create instructions for the device in the form of a G-code file. Each of the models was oriented in the virtual workspace of the Simplify3D software in such way that the largest dimension was perpendicular to the table. It was also decided that the orthosis would be produced of two different materials: PLA and PA12 (nylon). The PLA orthosis was produced in two colors (blue and red), while the nylon orthosis was completely white.

Various machines were used for printing of different parts and materials. The list is presented below:

- PLA, elbow parts – FlashForge Creator Pro
- PLA, forearm orthosis – Creality CR-10V
- PA12, elbow parts – Zortrax M200+
- PA12, forearm orthosis – Zortrax M300 Dual

The machines were selected for material and build size. The parameters were selected by the authors' best knowledge, some of them were impossible to change (Zortrax machines – speeds and some other parameters can't be changed in the machine software).

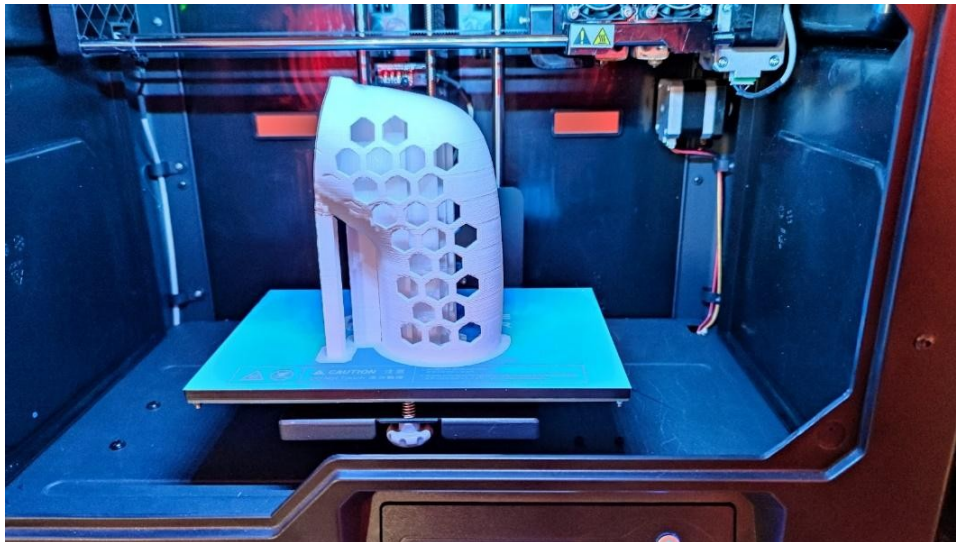


Fig 3.19. Manufactured orthosis part in the printer.

After setting the parameters, the solids were divided into layers, automatic supports and raft were added (Fig 3.20), and then the control program was generated. The FlashForge Creator Pro device does not allow to import G code directly from a PC, so it was first saved on

an SD card, and then placed in the device's reader. In case of other machines, they were linked by USB. The next step was to print the part.

Before starting the printing process, it was necessary to check the condition of the build plate and remove any dirt and filament residues. The printing process was monitored in the event of possible errors. If an error occurred, printing was interrupted. During this step, the printing time of each part was measured. After printing was finished and the heatbed had cooled down, the model was torn off the platform and removed from the device (Fig 3.21).

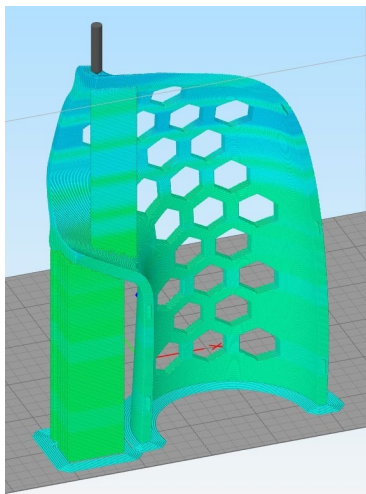


Fig 3.20. Part with supports.



Fig 3.21. Manufactured orthosis parts – nylon

Table 3.1 presents summary of all prints – used machines, materials, manufacturing parameters and results (time and mass).

Table 3.1. Summary of printed parts of the orthosis

No.	Part ID	Material	Machine	Parameters	Outcome
1.	Elbow 1	PLA	FlashForge Creator Pro	nozzle=0,4 mm l. thickness=0,2 mm top bottom 3/3	time = 5 h material = 66 g
2.	Elbow 2			perimeters 3 infill=15% support on temp 200° / 60° C	time = 7,5 h material = 114 g

				speed 50 mm/s	
3.	Forearm1		Creality CR-10 V3	nozzle=0,6 mm l. thickness=0,2 mm top bottom 3/3 perimeters 3	time = 3,5 h material = 54 g
4.	Forearm2			infill=15% support on temp 210° / 60° C speed 52 mm/s	time = 3,5 h material = 55 g
5.	Elbow 1	PA12 (nylon)	Zortrax M200+	nozzle=0,4 mm l. thick=0,19 mm top bottom 5/5 perimeters 3	time = 12 h material = 57 g
6.	Elbow 2			infill=30% support on temp 260° / 85° C speed 40 mm/s	time = 13,5 h material = 41 g
7.	Forearm1		Zortrax M300 Dual	nozzle=0,4 mm l. thickness=0,2 mm top bottom 5/4 perimeters 3	time = 9,5 h material = 90 g
8.	Forearm2			infill=20% support on temp 260° / 95° C speed 30 mm/s	time = 9,5 h material = 92 g

4.2. Post processing, assembly and fitting

The parts of the orthosis are not ready for use right after manufacturing – it is necessary to subject them to finishing.

The first step was to carefully remove the supports and the raft so as not to damage the printed element. It was also necessary to sand the parts by hand with sandpaper - there were imperfections on their outer surfaces that negatively affected the aesthetics of the orthosis. In order to reduce the risk of abrasions and increase the overall comfort of use, the inner surface of the orthosis has been padded with soft EVA (Ethylene- vinyl acetate) foam (Fig 3.22), certified for skin contact.

The final stage of the work was to join the parts by nuts and bolts. The final effect of the work, already in use, is shown in Figure 3.23.

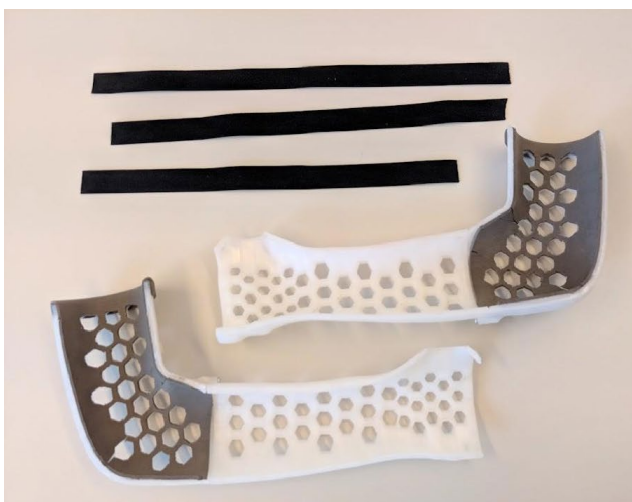


Fig 3.22. Ready-to-use parts of the orthosis (nylon).



Fig 3.23. Manufactured orthosis (PLA) during use.

5. Conclusions

The module describes the process of creating an individualized, incrementally manufactured upper limb orthosis for a fractured patient. As part of this procedure, anthropometric measurements of the patient's limb were carried out using a 3D scanner. The data obtained during the scanning was loaded into the proprietary software, which, in a way that did not require the user's participation, processed them into geometric information describing the appropriate dimensions of the parametric model of the orthosis. The automatically generated model was manufactured additively from PLA material using the FDM technology.

The orthosis produced in this way is equal to, and in many respects even surpassed, classical solutions.

The key aspect here is individualization - in contrast to universal orthoses, the one described in this paper is precisely adapted to the human body, which increases its rehabilitation effectiveness.

Another important feature is the very short production time - only two days passed from the start of measurements to the handover of the device to the user, which means not only a short waiting time but also a significant cost reduction - their sum, including the cost of machine operation and the cost of the material, is about EUR 70.

The ease of assembly and disassembly will also be a great comfort for the user, which translates into easy hygiene. It is also worth noting that further development of the described technology may make it possible to implement it in medical clinics.

Acknowledgements

The realization of the studies on individualized product design was possible thanks to the financing of the Polish National Center of Science and Development, programme "LIDER VIII".

The publishing of this project toolkit has been financially supported by the ERASMUS KA226 project entitled "Boosting the scientific excellence and innovation capacity of 3D printing methods in pandemic period", the implementation of the project being supervised by the National Agency for Community Programmes in the Fields of Education and Vocational Training (project reference: 2020-1-RO01-KA226-HE-095517).

References

- [DOM14] Dombroski C.E., Balsdon M.E., Froats A., The use of a low cost 3D scanning and printing tool in the manufacture of custom-made foot orthoses: a preliminary study, *BMC Res Notes*, Vol 60 (2014), 443. <https://doi.org/10.1186/1756-0500-7-443>
- [GUI19] Guida P., Casaburi A., Busiello T., et al. An alternative to plaster cast treatment in a pediatric trauma center using the CAD/CAM technology to manufacture customized three-dimensional- printed orthoses in a totally hospital context: a feasibility study. *J Pediatr Orthop B.*, Vol 28 (2019), pp. 248-255. <https://doi.org/10.1097/BPB.0000000000000589>
- [GOR20] Górski F., Wichniarek R., Kuczko W., Żukowska M., Lulkiewicz M. (2020), Experimental Studies on 3D Printing of Automatically Designed Customized Wrist-Hand Orthoses, *Materials*, 13(18), 4091.
- [KUO19] Kuo Y.R., Fang J.J., Wu C.T., et al. Analysis of a customized cervical collar to improve neck posture during smartphone usage: a comparative study in healthy subjects. *Eur Spine J*, Vol 29 (2019), pp. 1793-1803. <https://doi.org/10.1007/s00586-019-06022-0>;
- [TEL17] Telfer S., Woodburn J., Collier A., et al. Virtually optimized insoles for offloading the diabetic foot: A randomized crossover study, *J Biomech*, Vol 60 (2017), pp. 157-161. <https://doi.org/10.1016/j.jbiomech.2017.06.028>;
- [www 01] Ten materiał zastąpi w przyszłości gips - <https://geekweek.interia.pl/raporty/raport-medycyna-przyszlosci/medycyna/news-ten-material-zastapi-w-przyszlosci-gips,nld,940794>; accessing date: 14.11.2021
- [www 02] https://www.orteo.pl/ortezy-kostki-i-stopy/orteza-na-stope-i-golen-but-marszowy-krotki-walker-fixed-walk?gclid=CjwKCAiAm7OMBhAQEiwArvGi3AeUOjtYjW9RQawhHEe3GFV0Fp7-w0jQtEaBwXYatM6V5btEbxMmfRoCY4gQAvD_BwE; accessing date: 14.11.2021
- [www 03] iSun 3D – <https://www.isun3d.com/en/>; accessing date: 14.11.2021
- [www 04] EOS – <https://www.eos.info>; accessing date: 14.11.2021
- [www 05] Korthotics – <https://www.korthotics.com.au/>; accessing date: 14.11.2021
- [www 06] Ortheo 3D – <https://ortheo3d.com/>; accessing date: 14.11.2021
- [www 07] 3D Print Innovations – <https://www.biotechnc.com/posts/3d-print-innovations/383>; accessing date: 14.11.2021
- [www 08] <https://massportal.com/back-brace/>; accessing date: 14.11.2021
- [www 09] Scopri la stampa 3D – <https://www.superficialab.com/scopri-la-stampa-3d/>; accessing date: 14.11.2021

BRIGHT

Erasmus+ strategic partnership for Higher Education

BOOSTING THE SCIENTIFIC EXCELLENCE AND INNOVATION CAPACITY
OF 3D PRINTING METHODS IN PANDEMIC PERIOD

TOOLKIT 6 RAPID TOOLING

Project Title	Boosting the scientific excellence and innovation capacity of 3D printing methods in pandemic period 2020-1-RO01-KA226-HE-095517
Output	IO2 – BRIGHT e-toolkit manual for digital learning in producing medical parts by 3D printing methods in the context of the pandemic
Toolkit	Toolkit 6 Rapid tooling
Date of Delivery	November 2021
Authors	Peter Košťál, Erika Hrušková, Branislav Rabara
Version	Final variant

Content

1 Introduction	159
2 CAD model preparation for silicone molding.....	161
3 Realization of casting into a silicone mold	166
4 Conclusion.....	181

1 Introduction.

Throughout history, artisans have used molds to make everything from Bronze Age weaponry to modern-day consumer products. While early molds were commonly shaped in stone, modern science has developed materials that are far easier to work with, such as silicone.

Today, a various industries rely on silicone molding. Product developers i.e., engineers, DIY makers, and even chefs all make silicone molds to create one-off or smaller runs of parts.

This practical guide referring to silicone mold-making will describe everything you need to know before getting started, provide a list of items you need, and give you a step-by-step guide for incorporating silicone molds into any type of project.

Silicone is a good choice for mold-making because it offers several benefits. You can easily create custom designs using silicone molding. The molds themselves are also quite durable, so you can use them repeatedly without the fear of breakage. Silicone's inorganic makeup—compared to rubber, its organic counterpart—makes it highly resilient to heat and cold, chemical exposure, and even fungi. Some of the benefits of silicone molds include the following ones:

Flexibility

Silicone's flexibility makes it easy to work with. Silicone molds are pliable and lightweight compared to stiffer substances like plastic and they are also easier to remove once a part is fully formed. Thanks to silicone's high level of flexibility, both the mold and the manufactured part are less likely to break. You can use custom silicone molds to shape everything from complex engineering components to holiday-themed ice cubes or confections.

Stability

Silicone withstands temperatures from -65° to 400° degrees Celsius. Additionally, it can have an elongation of 700%, depending on the formulation. Highly stable under a broad range of conditions, you can put silicone molds in the oven, freeze them, and stretch them during removal.

Durability

In most cases, you will get many runs out of a silicone mold. However, it is important to note that the life span of molds can vary greatly. The more frequently you cast, and the more complex or detailed your design is, the faster your mold might degrade. To maximize the life of your silicone molds, clean them with mild soap and water, dry them thoroughly, and store them individually without stacking.

Common Applications for Silicone Molds

Hobbyists and professionals alike rely on silicone molds because of their versatility and ease of use. Here are a few examples of industries and applications that make silicone molds to produce prototypes, jewelry, food and beverage, consumer goods, medicine, etc.

2 CAD model preparation for silicone molding

The purpose of this manual is to define and illustrate in detail the process of casting into a silicone mold. The joint of an orthosis reinforcement is used for exemplification. The joint consists of a pair of arms (parts R1 and R2) connected by a pin. These arms are currently made from metallic materials (Fig. 2.1). The purpose is to replace them with plastic ones so that they are lighter and more usable in healthcare.



Fig. 2.1 Real orthosis

In our case of orthosis arms, 3D CAD models of the components must be developed at first.

These models will be two, first part (R1) and the other part (R2). The NX software from Siemens is used for designing the 3D models.

The first step in creating a 3D CAD model is to select a suitable sketch plane. One of the three basic planes of the coordinate system, any planar surface of the existing body, or a newly defined plane can be used for sketching. A sketch of the base body is drawn in this plane (Fig. 2.2). This sketch needs to be fully constrained. The constraints can be geometric (concentricity, perpendicularity, parallelism, symmetry, etc.) or dimensional (linear or angular dimensions). Geometric constraints are always preferable, so that the number of dimensions is minimized.

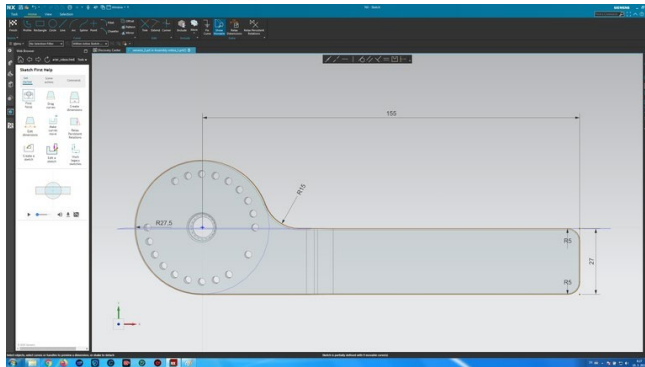


Fig.2. 2 Sketch of the part R1

Subsequently, various 3D operations can be applied to the sketch (rotation, extrusion, etc.) In our case, the extrusion is used to obtain the basic 3D part R1 (Fig. 2.3).

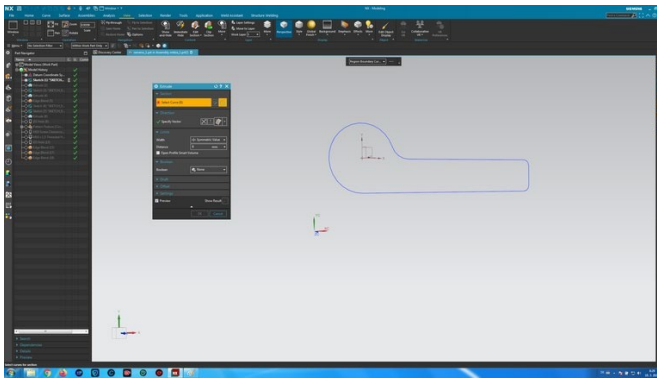


Fig. 2.3 Base body extrusion of part R1

Additional geometric elements will be created on this body. The appropriate sketch plane is selected again, the sketch is drawn and bound, then a suitable 3D operation is applied to the sketch (Fig. 2.4).

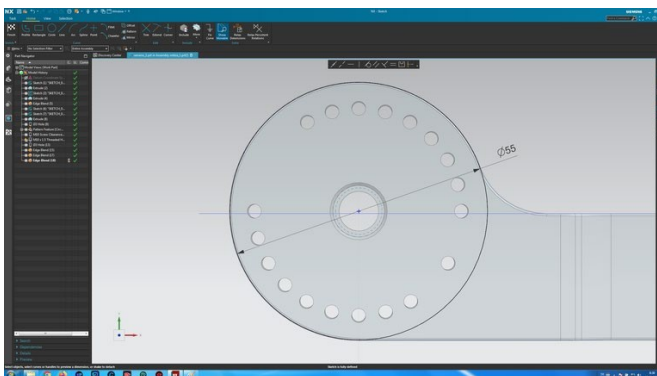


Fig. 2.4 Creating of another sketch

Subsequently, the material is pulled out and a joint is created. It is necessary to create several identical holes, which will be distributed along a circle. A pair of such holes is created at first (Fig. 2.5).

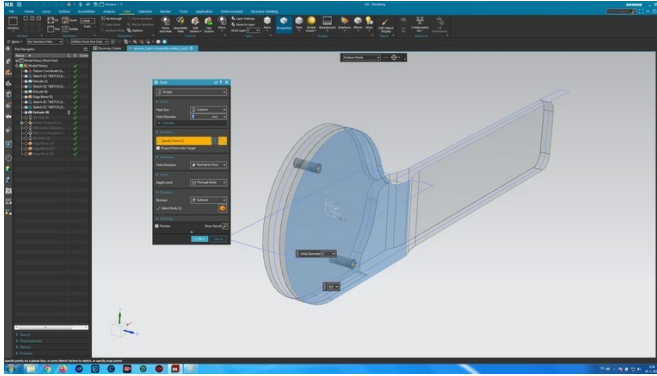


Fig. 2.5 Creating a pair of holes on the circle

Subsequently, using this pair of holes, an array of holes is generated as needed (Fig. 2.6).

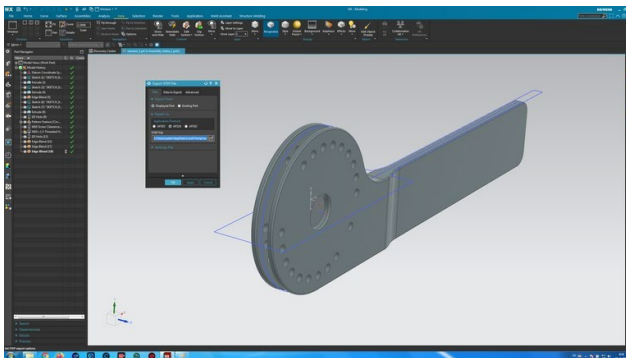


Fig. 2.6 Hole pattern generation

The next step consists in creating an axial hole for the joint (Fig. 2.7).

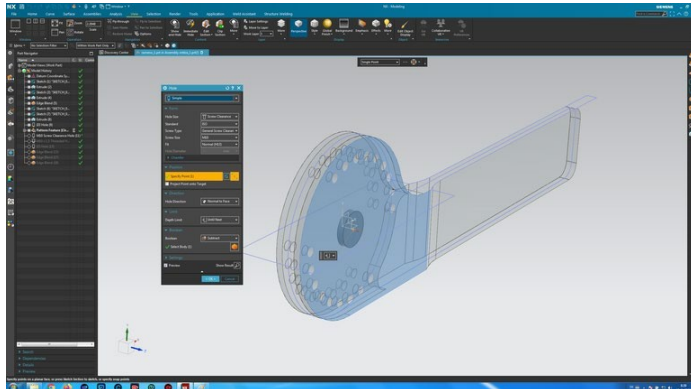


Fig. 2.7 Definition of the central hole

It is necessary to chamfer or fillet the resulting edges (Fig. 2.8).

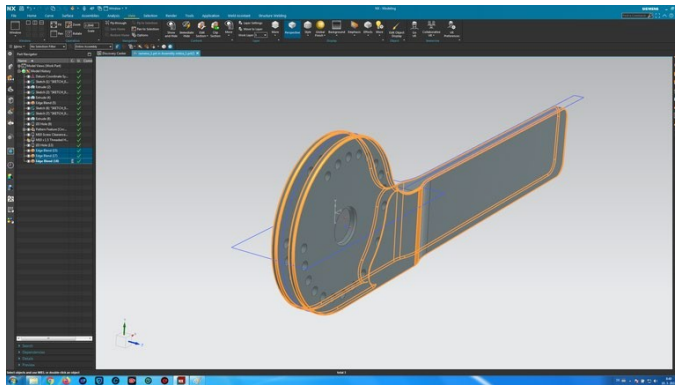


Fig. 2.8 Edge blending

This whole procedure is repeated until the required 3D CAD model is obtained (Fig. 2.9). The last operation is to export the 3D CAD model to STEP format for further processing.

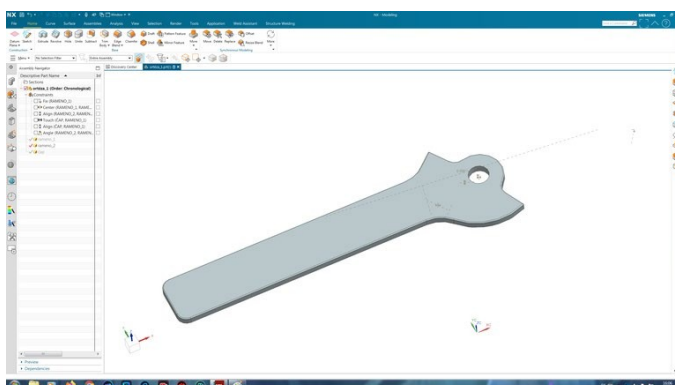


Fig. 2.9 3D model of part R1

The 3D CAD model of the R2 arm will be generated in the same way. In the next stage, an assembly is created to verify the correct dimensions and shapes of the R1 and R2 arms. Figure 210 shows the assembly of the orthosis arms. The individual arms are connected in a joint using a pin.

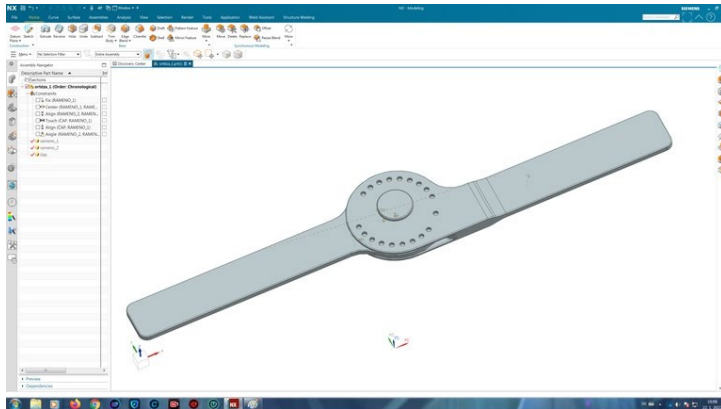


Fig. 2.10 Assembly of both parts R1 and R2

The 3D models of the individual arms are transformed into STEP files to be processed and printed on a 3D printer. The finished 3D arms serve as master physical models for producing silicone molds.

3 Realization of casting into a silicone mold

MOLD PRODUCTION

The mold was produced for the parts R1 and R2, which were designed using the NX Siemens software and subsequently obtained by 3D printing (Fig. 3.11).

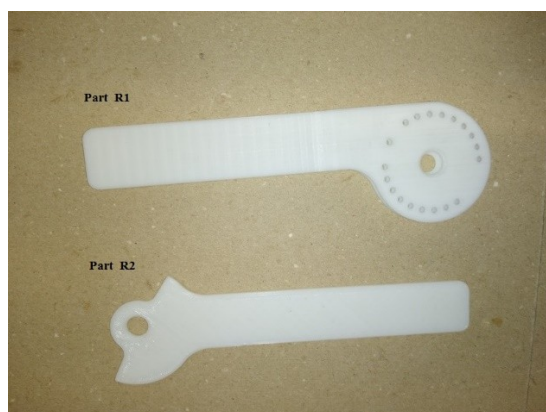


Fig. 3.11 Physical models of parts R1 and R2

The following aspects must be clarified before starting the production of the mold: appropriate production method, specific possibilities of fixing the mold, location of the separator to be used, and type of silicone to be used. Subsequently, the edges of the physical models R1 and R2 are cleaned, degreased, and trimmed. There is a notch on part R1 that needs casting. To ensure the shape of the notch, it is necessary to insert plexiglass, which also must be trimmed (Fig.3.12).



Fig. 3.12 Insertion of plexiglass to the R1 model

Double-sided tape is used to fix the R1 model onto plexiglass (Fig. 3.13).

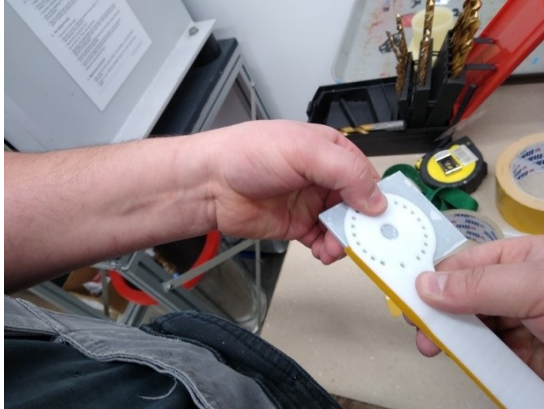


Fig. 3.13 Using double-sided tape to fix the R1 model onto the plexiglass

In order to achieve the shape of the part, the minimum wall thickness of the silicone mold must be 20 mm. Two cases are made of plexiglass plates. The dimensions of the cases are 10x22x10cm and 5x22x10cm, respectively. The individual parts of the cases are glued together (Fig. 3.14). In the company BIZZCOM it is advantageous to use plexiglass for producing the molds, because they use it as a waste material.



Fig. 14 Production of mold casing

The duct plane is used as a separation surface of the casting mold (Fig. 3.15). This strategy is used for both parts (R1 and R2).



Fig. 3.15 Duct tape used for materializing the separation surface on the R2 model

The amount of silicone needed for producing the mold is determined in accordance with the exact dimensions of the cases. After re-evaluating the silicone preparation process, it is more advantageous to mix the entire silicone quantity at once than for individual parts. The silicone mixing vessel must be carefully cleaned. A mixing ratio of hardener and base component of 1:10 is recommended. The individual quantities of mixture quantities are as follows: 200 g of hardening agent and 2000 g of silicone. Before using it, the mixture must be freed of air bubbles and other gaseous impurities in a vacuum chamber for approximately 10 minutes (see Fig. 3.16 and Fig. 3.17).



Fig. 3.16 Weighing the hardening agent

T



Fig. 3.17 Removing air bubbles and other gaseous impurities from the mixture of silicone and hardening agent in a vacuum chamber

The processing time of the silicone mixture is 60 minutes. This mixture of silicone has a long workability and low shrinkage (about 1%). So, it is possible to use it for producing accurate molds.

The silicone mixture is then poured into the case (Fig. 3.18). The aim is to determine a unique casting point and to pour the silicone slowly in the vicinity of the casing wall. The air bubbles remained in the silicone volume are simply removed by heating with a hot air gun or blowing warm air with a hair dryer.



Fig. 3.18 Pouring the silicone mixture into the case

The molds containing the physical models R1 and R2 are then allowed to harden (preferably for 24 hours). Unwanted air bubbles remained in the molds are removed in an MK-Mini vacuum chamber (Fig. 3.19).

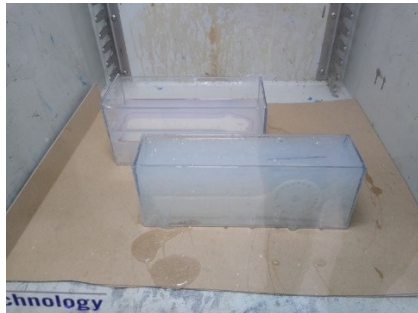


Fig. 3.19 Silicone molds for R1 and R2 parts placed in the vacuum chamber

REMOVING THE R1 PHYSICAL MODEL FROM THE MOLD

After the silicone has hardened, the mold must be removed from the casing and its edges must be trimmed. In the next stage, the embedded model must be also extracted. In order to do that, the silicone mold must be cut with a scalpel, but only so that the silicone can be open to remove the physical model (Fig. 3.20). The aim is to avoid the complete separation of the mold in two pieces (i.e., avoid any difficulties caused by joining and fitting the two parts of the mold). The plexiglass must be also extracted from the mold. R1 weight is the 25g.



Fig. 3.20 Removing the R1 physical model from the mold

Their mutual position is indicated on the mold and on the plexiglass with a marker (Fig. 3.21), to identify the exact position where the plexiglass is inserted into the mold before casting. Before inserting the plexiglass, its surface must be covered with a separator spray. The mold cavity must also be sprayed with the same substance. The separator will facilitate the separation of the casting from the silicone mold. The R1 physical model weighs 25 g.



Fig. 3.21 Marking of mutual position

REMOVING THE R2 PHYSICAL MODEL FROM THE MOLD

While cutting the mold with a scalpel along the separation surface, the tip of the scalpel must be guided along the red line indicating the edge of the adhesive tape which will form the parting surface. In order to ensure the exact position of the two parts of the mold during the casting process, several protrusions must be made on the parting surface of the silicone mold. These protrusions will serve as a lock when assembling the mold.

The R2 physical model weighs 10 g. Five vent holes are created in the molds. These vents will allow the air to escape when the resin is poured into the mold (Fig. 3.22).



Fig. 3.22 Creation of five vent holes in the mold

CASTING INTO THE SILICONE MOLD

The plexiglass must be inserted before casting in the position individualized with the marker. As already mentioned, the surface of the plexiglass must be sprayed with a separator before the insertion into the mold (Fig. 3.23). The mold cavity must be also sprayed. The separator will facilitate the separation of the casting from the silicone mold. In our case, the mold cavity does not need to be sprayed with a separator because the resin used has no affinity, compatibility with the silicone mold material. In the case of epoxy casting, it is necessary to use a separator.



Fig. 3.23 Application of separator on the plexiglass

The mixing ratio is 100:45 (45 Polyol and 100 Isocyanate), the silicone form is heated to 70°C. The processing time is 8 minutes (after this time the resin is hardened). The time of mixing the components is 1 min -1.5 min. The mixing process takes place in a vacuum chamber at a pressure of -0.1 MPa. After mixing, the compound is poured into a nylon mold which is prepared in a vacuum chamber. After pouring the compound, the mold degassed for about 1 minute. After its removal from the vacuum chamber, the mold with the casting is placed in a heated oven for 90 minutes at a temperature of 70°C.

CASTING

Prior to casting, the plexiglass must be inserted into the silicone mold in the position indicated with the marker. Then the resin is prepared for the weight of part R1 (25 g).

In the case of part R2, about 20% of resin must be added for the inlet. This allowance is calculated to compensate the loss on the walls of the vessel, the loss on the stirrer and the like. A funnel is inserted in the mold placed in the vacuum chamber to be used for pouring the resin.

CASTING INTO THE SILICONE MOLD (1)

While mixing, a few drops of red dye should be added to the resin to better see the flow of the resin in the mold during casting (Fig. 3.24).



Fig. 3.24 Red dye added to the resin

After casting, the resin is hardened in the furnace. The casting is then removed from the mold. At first, the adhesive tape that holds the mold together is removed (Fig. 3.25).



Fig. 3.25 Removing the adhesive tape

This tape is cut with a trimmer. In our case, the product cracked when the part R1 was removed from the mold during the break-off of the inlet (Fig 3.26, 3.27 and 3.28).

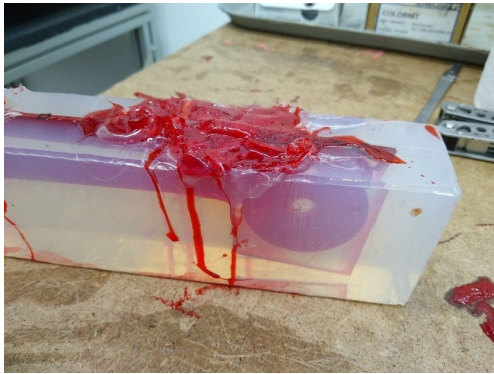


Fig. 3.26 Casting of R1 after breaking the inlet system

There were also a lot of small air bubbles captured in the arm (Fig. 3.29). This means that this part is unusable and therefore it is necessary to cast it again.



Fig. 3.27 Removing the R1 casting from the mold



Fig. 3.28 Taking away of plexiglass

Plexiglass is like the core of the mold and creates a slit in the joint part of R1.



Fig. 3.29 Unexpected bubbles in the casting R1

It was probably a mistake that both parts are cast together in a vacuum chamber. After filling the first mold (part R2), the vacuum chamber had to be vented in order to be able to move the molds and pouring the mixture into the R1 mold. An unnecessarily massive inlet and a hole were formed on the R1 model, while the longitudinal narrow side of the R1 part was free. That was the place where unwanted air bubbles occurred.

Part R2 was removed from the mold without any difficulty. It was also free of defects. Even though it was usable, this part was cast again (Fig. 3.30).



Fig. 3.30 Removing the R2 casting from the mold

Although this set of parts R1 and R2 was damaged, they were cleaned (Fig. 3.31).

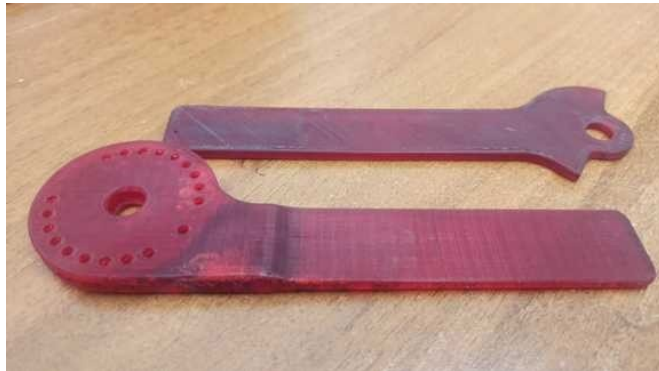


Fig. 3.31 Set of red arms after cleaning the castings (defective air bubbles can be noticed in the R1 part)

As both parts were manufactured again, the material from which they were cast was also changed. This time the material used was similar to ABS after curing.

CASTING INTO THE SILICONE MOLD (2)

Fig. 3.32 shows the data sheet of the material used in the second casting attempt.

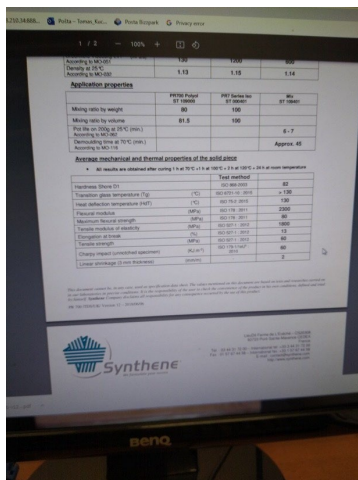


Fig. 3.32 Data sheet of the material used in the second casting attempt

The molds had to be cleaned before further casting. First, they were cleaned mechanically, the remnants in the vent channels were removed, and the mold was blown with compressed air.

Subsequently, the mold was chemically cleaned with the help of technical alcohol. The cavity of the mold thus cleaned was then sprayed with a separator. The plexiglass was also cleaned and sprayed with a separator. As previously mentioned, the plexiglass serves as a core of the mold and creates a gap on the R1 part at the joint.

The molds treated in this way were bound together with adhesive tape. The plexiglass was added to the mold for part R1 so that the part of the arm where the bubbles occurred in the previous case was not in contact with vacuum. The inlet and vent of the mold were also created (Fig. 3.33).



Fig. 3.33 Mold of R1 with plexiglass placed at the top

The molds were then placed in an oven and heated at 70°C.

While the molds were heating up, the resin for casting was prepared. According to the resin data sheet, the ingredients were mixed in a ratio of 80: 100. The workability of the compound was achieved after mixing it for about 6 minutes. The individual components were weighed before placing them in the vacuum chamber (Fig. 3.34).

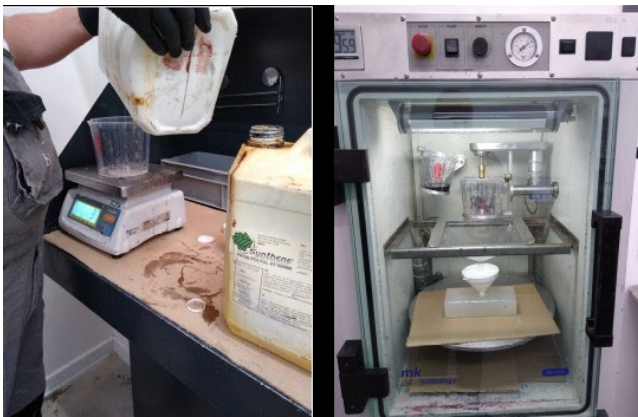


Fig. 3.34 Weighing the individual components of the mixture and their insertion in the vacuum chamber

After heating, each mold was placed in the vacuum chamber. When the vacuum value has reached the value -1, the individual prepared components of the resin were mixed. After perfect mixing (about 2 minutes), the mixture was poured into the mold (Fig. 3.35).



Fig. 3.35 Preparing the mixture and pouring it into the mold placed in a vacuum chamber

The filled mold was left in the vacuum chamber for about 4 minutes to fill reliably and to remove all the gaseous bubbles formed in the chemical reaction of the mixture from the casting by vacuum (Fig. 3.36).



Fig.3. 36 Vacuum degassing of the R1 mold

After degassing, the filled mold was transferred to the furnace after removing the second mold from it (Fig. 3.37). The method used for casting into the second mold was the same.



Fig. 3.37 Filled molds stored in the oven for resin curing

Both filled molds were allowed to cure in an oven at 70°C for about an hour (the manufacturer recommends at least 45 minutes). After curing the mixture, the molds were removed from the oven. The molds are then allowed to cool on the table at the roomtemperature. After cooling, the molds were disassembled, and the castings extracted in the same way as in the previous case (Fig. 3.38). After extraction from the mold, the raw castings did not show any defects or other damages.



Fig. 3.38 Raw castings extracted from the molds

The raw castings were then put back into the furnace for heat treatment according to manufacturer's recommendations: 1 hour at 70°C , 1 hour at 100°C , 2 hours at 120°C , and 24 hours at room temperature. After removing the inlets and venting, the finished castings were lightly sanded using fine sandpaper and the edges were trimmed (Fig. 3.39 and Fig.3. 40).



Fig. 3.39 Grinding of castings after removing the inlet and vent



Fig.3.40 A set of black R1 and R2 parts after cleaning the castings, without noticeable defects

Fig. 3.41 shows all R1 and R2 parts placed next to each other.



Fig. 3.41 Cast parts R1 and R2

The parts R1 and R2 manufactured from different materials are as follows: concrete - WHITE - 3D printing - master model, RED - casting in silicone - failed, BLACK cast in silicone –correct and final version.

4 Conclusion

Silicone casting can be used in various domains. As part of this project, an effort was made to point out and highlight its use in medicine. As an example, an orthosis was used to support the elbow part of the hand. Casting into a silicone mold was carried out in the company Bizzcom sr.o. in Bučany, Slovak Republic. In the original version, the orthosis is made of metal, but the purpose was to make it as simple as possible so that it was strong, weight-wise, and usable in the rehabilitation of the human body limb. From the realized CAD model, a real 3D model was created by means of a 3D printer as a physical model used for the creation of a silicone mold. Subsequently, two casting experiments were carried out, as in the first one the quality of a part was affected by air bubbles (red version). The second attempt was successful, and the quality of the castings was quite satisfactory (black version). At the same time, the effort to use the separator on individual parts, thanks to which the silicone mold is removed, and the effort in obtaining the silicone mold was that its minimum wall thickness must always be 20 mm in order for the silicone to preserve the shape of the part.

FINAL CONCLUSIONS

As it was mentioned in the introductory chapter, the BRIGHT toolkit manual which has been prepared by the BRIGHT consortium in relation with 3D printing technologies for producing specific parts (applications) made for the medical sector consisting in 6 laboratory toolkit modules.

The BRIGHT toolkit manual is related not just to the basics knowledge about 3D printing processes that could be used for certain application in close correlation to the CAD particularities of the parts and specific technology of 3D printing selected for the realizing of these applications, and also to the other preliminary steps that are required to be followed for pre-validation steps of the needed to be performed for the setup of the 3D printing equipment (pre-processing steps), setup of the 3D printing orienting and parameters specific that are used for 3D printing process itself and post-processing steps that are needed to be realized in the end.

Acknowledgement:

The publishing of this project e-toolkit manual has been financially supported by the ERASMUS KA226 project entitled “Boosting the scientific excellence and innovation capacity of 3D printing methods in pandemic period”, the implementation of the project being supervised by the National Agency for Community Programmes in the Fields of Education and Vocational Training (project reference: 2020-1-RO01-KA226-HE-095517).